

Mariana Gomes Gonçalves Arêlo Manso

Designing and preparation of new BACE1 inhibitors for Alzheimer's disease treatment

Dissertação de Mestrado em Química Farmacêutica Industrial, orientada pelo Professor Doutor Jorge António Ribeiro Salvador e pela Professora Doutora Armanda Emanuela Castro e Santos e apresentada à Faculdade de Farmácia da Universidade de Coimbra

Janeiro 2017



UNIVERSIDADE DE COIMBRA

Mariana Gomes Gonçalves Arêlo Manso

Designing and preparation of new BACE1 inhibitors for Alzheimer's disease treatment

Dissertação de Mestrado em Química Farmacêutica Industrial, orientada pelo Professor Doutor Jorge António Ribeiro Salvador e pela Professora Doutora Armanda Emanuela Castro e Santos e apresentada à Faculdade de Farmácia da Universidade de Coimbra

Janeiro 2017



UNIVERSIDADE DE COIMBRA

Cover image description:

The chemical structures of asiatic acid, triacetate asiatic acid, amide derivatives and fluorinated derivatives are represented in the image with the atom of fluorine highlighted. In the center of the image is represented a brain.

“Excessive reservations and paralyzing despondency have not helped the sciences to advance nor are they helping them to advance, but a healthy optimism that cheerfully searches for new ways to understand, as it is convinced that it will be possible to find them.”

Alois Alzheimer

Aos meus pais e irmão,
os meus maiores pilares.

Aos meus colegas do laboratório de Química Farmacêutica
pelo apoio e ajuda essenciais.

Em memória do meu tio Manuel Manso,
a minha maior referência.

Acknowledgments

Todo o caminho percorrido ao longo deste trabalho permitiu-me evoluir não só cientificamente, mas também pessoalmente e nada disto seria possível sem o contributo de algumas pessoas a quem deixo aqui o meu pessoal reconhecimento e sincero agradecimento.

Em primeiro lugar, ao Professor Doutor Jorge Salvador e à Professora Doutora Armada Santos, orientadores deste trabalho, agradeço todo o conhecimento e competências científicas e profissionais que me transmitiram. Agradeço também toda a partilha de saber, apoio, disponibilidade e perseverança revelada ao longo deste trabalho.

A todos os docentes e funcionários do Laboratório de Química Farmacêutica da Faculdade de Farmácia da Universidade de Coimbra, em particular à D. Graça e à D. Anabela, agradeço por todo o carinho, disponibilidade, apoio e boa disposição.

Ao Pedro, do Laboratório de RMN da Universidade de Coimbra, por toda a disponibilidade e paciência que sempre teve comigo e com as minhas amostras.

À Marisa, à Rosa Resende e a todas as pessoas do CNC por me terem acolhido tão bem e me terem ensinado tantas competências novas.

Às minhas colegas de laboratório, Mónica e Patrícia, por terem percorrido este caminho comigo. Sem vocês eu não teria conseguido.

Ao Doutor Bruno Gonçalves, por ter sempre razão e me ter dado todas as ferramentas necessárias para a realização deste trabalho. Obrigada por teres tentado passar-me um pouco da tua paixão por esta área e por estares sempre disponível para mim.

À Doutora Vanessa Mendes, por toda a ajuda, motivação e paciência que teve comigo.

Às minhas amigas do coração, Susana e Rita por estarem sempre lá e nunca me falharem.

À Salete pelas palavras certas no momento certo.

Ao Emanuel e ao Bryan pela amizade e paciência na ajuda do inglês.

À D. Elisa, Sr. Manuel, Manuela, Filipe e Filipa, por serem como família e me terem apoiado em todos os momentos.

À família Silva por todo o carinho e amizade que tiveram comigo nestes cinco anos.

Ao Núcleo de Explicações Voluntárias, NExT, e a toda a sua equipa por me terem mostrado o quanto se ganha em dar.

Acknowledgements

Aos meus amigos de Celorico da Beira por me mostrarem que não é a distância que afasta as pessoas.

A todas as pessoas que conheci na Cidade dos Estudantes que me acompanharam de uma forma ou de outra neste percurso académico e sem as quais esta experiência não teria sido a mesma coisa.

E por último, e o mais importante, um profundo obrigada a toda a minha família, em particular aos meus pais e ao meu irmão. Obrigada pela confiança que sempre tiveram nas minhas escolhas, por todas as oportunidades que me proporcionaram e por me terem dado todas as ferramentas necessárias para eu ser a mulher que sou hoje.

General Contents

| | |
|-----------------------|------|
| Resumo | V |
| Abstract | VII |
| List of Abbreviations | IX |
| List of Figures | XI |
| List of Tables | XIII |
| List of Schemes | XV |

Chapter I

| | |
|--|----|
| I. General Introduction | 3 |
| I.1 Alzheimer's Disease | 3 |
| I.1.1 The amyloid cascade hypothesis | 4 |
| I.1.2 Amyloid- β production | 7 |
| I.1.3 BACE1 as therapeutic target for Alzheimer's Disease | 11 |
| I.1.4 BACE1 inhibitors development | 13 |
| I.1.5 Limits of BACE1 inhibitors | 16 |
| I.2 Fluorine atom in medicinal chemistry | 18 |
| I.2.1 Incorporation of fluorine atoms in BACE1 inhibitors | 18 |
| I.2.1.1 General fluorine properties | 19 |
| I.2.1.2 Impact of fluorine in lipophilicity of new potential BACE1 inhibitors | 20 |
| I.2.1.3 Impact of fluorine in pK_a of new potential BACE1 inhibitors | 22 |
| I.2.1.4 Increasing brain penetration through the incorporation of fluorine atoms in new potential BACE1 inhibitors | 24 |
| I.2.1.5 Impact of fluorine on hERG activity of new potential BACE1 inhibitors | 25 |
| I.2.1.6 Impact of fluorine in metabolism | 26 |

| | | |
|---------|---|----|
| 1.2.1.7 | Influence of fluorine in the conformation of new potential BACE1 inhibitors | 27 |
| 1.1.2 | Strategies of fluorination | 29 |
| 1.1.2.1 | Monofluorination techniques | 29 |
| 1.1.2.2 | Difluoromethylation techniques | 31 |
| 1.1.2.3 | Trifluoromethylation techniques | 31 |
| 1.1.2.4 | The use of fluorinated synthons | 34 |

Chapter II

| | | |
|-----|-----------------------|----|
| 2. | Scientific objectives | 37 |
| 2.1 | General objectives | 37 |
| 2.2 | Specific objectives | 37 |

Chapter III

| | | |
|---------|---|----|
| 3. | Synthesis of new potential BACE1 inhibitors | 39 |
| 3.1 | Asiatic acid in Alzheimer's disease | 41 |
| 3.2 | Preparation and structural elucidation of asiatic acid derivatives | 43 |
| 3.2.1 | Preparation and structural elucidation of compound AA_2 | 44 |
| 3.2.2 | Preparation and structural elucidation of amide derivatives | 44 |
| 3.2.2.1 | Compound AA_3 | 45 |
| 3.2.2.2 | Compound AA_4 | 48 |
| 3.2.2.3 | Compound AA_5 | 51 |
| 3.2.3 | Preparation and structural elucidation of the fluorinated amide derivatives | 54 |
| 3.2.3.1 | Compound AA_6 | 55 |
| 3.2.3.2 | Compound AA_7 | 58 |
| 3.2.3.3 | Compound AA_8 | 61 |

| | |
|--|----|
| 3.2.4 Preparation and structural elucidation of the hydrolyzed derivatives | 64 |
| 3.2.4.1 Compound AA_9 | 65 |
| 3.2.4.2 Compound AA_10 | 68 |
| 3.3 Experimental section | 72 |
| 3.3.1 Chemical | 72 |
| 3.3.2 Experimental procedure | 72 |

Chapter IV

| | |
|--|----|
| 4. Concluding Remarks and future prospects | 83 |
|--|----|

Chapter V

| | |
|-----------------------------|----|
| 5. Bibliographic references | 87 |
|-----------------------------|----|

Resumo

A doença de Alzheimer (DA) é uma patologia neuro-degenerativa progressiva caracterizada por uma disfunção sináptica e perda de neurónios em algumas áreas subcorticais o que conduz subsequentemente à demência. Isto ocorre, sobretudo, devido à excessiva acumulação e deposição do peptídeo β -amiloide ($A\beta$) na forma de placas amiloides, e à formação de tranças neurofibrilares.

O facto de alguns estudos sugerirem que o aparecimento de placas amiloides ocorre antes da formação das tranças neurofibrilares e, sabendo que a forma familiar da DA (FAD) está associada, entre outras, a uma mutação do gene da APP que causa a superprodução de $A\beta$, faz da inibição da produção de $A\beta$ uma abordagem terapêutica a esta patologia com potencial para alterar o curso da doença. Assim, a BACE1, ou β -secretase, tem sido considerada o alvo principal no desenvolvimento de novas terapias para a doença de Alzheimer.

Várias tentativas têm sido feitas de modo a desenvolver pequenas moléculas inibidoras da BACE1. Vários inibidores têm sido descritos, contudo poucos contêm o equilíbrio entre a potencia *in vitro* e as propriedades farmacocinéticas necessárias de modo a obter eficácia *in vivo*.

O ácido asiático é um composto bem estudado com potencial terapêutico em diferentes patologias incluindo doenças neuro-degenerativas. Um estudo recente mostrou que o efeito protetor deste composto está associado com a inibição dos níveis de BACE1 fazendo desta molécula um candidato promissor ao desenvolvimento de novos inibidores da β -secretase.

Assim, este trabalho focou-se na síntese de novos derivados fluorados do ácido asiático sendo as suas estruturas elucidadas recorrendo a análise espectral.

Com o objetivo de preparar novos potenciais inibidores da BACE1, este trabalho focou-se na síntese de novos derivados fluorados do ácido asiático, bem como na sua elucidação estrutural através de análise espectral.

Palavras - chave: neuro-degeneração, Alzheimer, $A\beta$, BACE1, β -secretase, ácido asiático, fluoração.

Abstract

Alzheimer's disease (AD) is a progressive neurodegenerative pathology characterized by synaptic impairment and the loss of neurons in some subcortical areas, which afterwards leads to dementia. This occurs primarily due the excessive accumulation and deposition of β -amyloid peptide ($A\beta$) in the form of plaques, and the generation of neurofibrillary tangles.

Considering the studies suggesting the appearance of amyloid plaques occurs before neurofibrillary tangles and taking into account that the familiar form of AD (FAD) is associated, among others, with an APP gene mutation leading to the overproduction of $A\beta$, the inhibition of $A\beta$ production as the potential to be a disease-modifying therapy. Based in this hypothesis, BACE1, or β -secretase, has been considered a prime target in the development of new therapies to Alzheimer's disease.

Many efforts have been made to develop small BACE1 inhibitors as drugs for AD and, although various inhibitors have been described, few had presented a balance between the *in vitro* potency and the necessary pharmaco-kinetic properties to achieve *in vivo* effectiveness.

Asiatic acid is a well-studied compound with therapeutic potential in many different pathologies including neurodegenerative diseases. A recent study showed that the neuroprotective effect of this compound is associated with the down-regulation of BACE1 protein levels making this molecule a good candidate to study in this work.

In order to prepare BACE1 inhibitor candidates, this work focused on the synthesis of new fluorinated asiatic acid derivatives, as well as their structural elucidation by spectral analysis.

Key words: neurodegeneration, Alzheimer, $A\beta$, BACE1, β -secretase, asiatic acid, fluorination.

List of Abbreviations

- AA – asiatic acid
AD – Alzheimer’s disease
ADAM – a disintegrin and metalloprotease
AICD – APP intracellular domain
APOE4 – apolipoprotein E4
APP – Amyloid precursor protein
Asp2 – aspartyl protease 2
A β – β -amyloid peptide
BACE1 – β -secretase 1
BACE2 – β -secretase 2
CatD – cathepsin D
CNS – Central nervous system
CSF – Cerebrospinal fluid
DAST – Diethylaminosulfur trifluoride
DEPT – distortionless enhancement by polarization transfer
DMAP – 4-dimethylpyridine
dq – double quartet
dt – double triplet
FAD – familiar form of Alzheimer’s disease
hERG – human Ether-à-go-go-Related Gene
HIV – human immunodeficiency virus
Hz – hertz
J – coupling constant
kD – kilo Dalton
log D – partition coefficient
MAPT – microtubule association protein tau
NFT’s – neurofibrillary tangles
NMR – mononuclear magnetic resonance
Pgp – P-glycoprotein
pKa – logarithmic acid dissociation constant
pKb – logarithmic basic dissociation constant

List of Abbreviations

ppm – part per million

PS1 – presenilin 1

PS2 – presenilin 2

PSEN – γ - secretase

sAAP α – shorter APP- α fragment

sAAP β – shorter APP- β fragment

SAD – sporadic form of Alzheimer's disease

TFMS – trifluoromethanesulphinate

THF – Tetrahydrofuran

TLC – thin layer chromatography

δ – chemical shift

List of Figures

| | | |
|--------------------|---|----|
| Figure 1 - | Non-amyloidogenic and amyloidogenic pathways in APP cleavage | 8 |
| Figure 2 - | Conformation of mature BACE1. Represented in red is the open flap and in blue the closed flap | 11 |
| Figure 3 - | Most common transition-states isosteres used to design new BACE1 inhibitors | 13 |
| Figure 4 - | Fluorine chemotypes in marketed drugs | 18 |
| Figure 5 - | Influence of fluorine atoms addition to the log D of BACE1 inhibitors | 21 |
| Figure 6 - | Effects of fluorine atom in the preferential conformation of Indinavir | 28 |
| Figure 7 - | Some reagents used for nucleophilic monofluorination | 30 |
| Figure 8 - | Some reagents used for electrophilic monofluorination | 30 |
| Figure 9 - | Some reagents used for difluoromethylation reactions | 31 |
| Figure 10 - | Some reagents used in nucleophilic trifluoromethylation reactions | 32 |
| Figure 11 - | Some reagents used in radical trifluoromethylation reactions | 32 |
| Figure 12 - | Some reagents used in electrophilic trifluoromethylation reactions | 33 |
| Figure 13 - | Chemical structure of asiatic acid with the carbons numbered | 42 |
| Figure 14 - | Chemical structure of compound AA_3 | 45 |
| Figure 15 - | ¹ H NMR spectrum of compound AA_3 | 46 |
| Figure 16 - | ¹³ C NMR spectrum of compound AA_3 | 47 |
| Figure 17 - | ¹³⁵ DEPT spectrum of compound AA_3 | 48 |
| Figure 18 - | Chemical structure of compound AA_4 | 48 |
| Figure 19 - | ¹ H NMR spectrum of compound AA_4 | 49 |
| Figure 20 - | ¹³ C NMR spectrum of compound AA_4 | 50 |
| Figure 21 - | ¹³⁵ DEPT spectrum of compound AA_4 | 51 |
| Figure 22 - | Chemical structure of compound AA_5 | 51 |
| Figure 23 - | ¹ H NMR spectrum of compound AA_5 | 52 |
| Figure 24 - | ¹³ C NMR spectrum of compound AA_5 | 53 |
| Figure 25 - | ¹³⁵ DEPT spectrum of compound AA_5 | 54 |
| Figure 26 - | Chemical structure of compound AA_6 | 55 |
| Figure 27 - | ¹ H NMR spectrum of compound AA_6 | 56 |
| Figure 28 - | ¹³ C NMR spectrum of compound AA_6 | 57 |

List of Figures

| | |
|---|----|
| Figure 29 - $^{135}\text{DEPT}$ spectrum of compound AA_6 | 58 |
| Figure 30 - Chemical structure of compound AA_7 | 58 |
| Figure 31 - ^1H NMR spectrum of compound AA_7 | 59 |
| Figure 32 - ^{13}C NMR spectrum of compound AA_7 | 60 |
| Figure 33 - $^{135}\text{DEPT}$ spectrum of compound AA_7 | 61 |
| Figure 34 - Chemical structure of compound AA_8 | 61 |
| Figure 35 - ^1H NMR spectrum of compound AA_8 | 62 |
| Figure 36 - ^{13}C NMR spectrum of compound AA_8 | 63 |
| Figure 37 - $^{135}\text{DEPT}$ spectrum of compound AA_8 | 64 |
| Figure 38 - Chemical structure of compound AA_9 | 65 |
| Figure 39 - ^1H NMR spectrum of compound AA_9 | 66 |
| Figure 40 - ^{13}C NMR spectrum of compound AA_9 | 67 |
| Figure 41 - $^{135}\text{DEPT}$ spectrum of compound AA_9 | 68 |
| Figure 42 - Chemical structure of compound AA_10 | 68 |
| Figure 43 - ^1H NMR spectrum of compound AA_10 | 69 |
| Figure 44 - ^{13}C NMR spectrum of compound AA_10 | 70 |
| Figure 45 - $^{135}\text{DEPT}$ spectrum of compound AA_10 | 71 |

List of Tables

| | | |
|------------------|---|----|
| Table 1 - | Strengths and weakness of the amyloid cascade | 6 |
| Table 2 - | BACEI inhibitors currently in clinical trials | 15 |
| Table 3 - | Most common phenotypes observed in mice BACEI ^{-/-} | 16 |
| Table 4 - | Atomic parameters of fluorine atom compared with other halogens and atoms | 19 |
| Table 5 - | Effect of fluorine substitution on pKa and pKb values | 22 |
| Table 6 - | Effects of fluorine atom addition to the properties of a BACEI inhibitor | 23 |
| Table 7 - | β -secretase (BACEI) inhibitors with high <i>in vivo</i> efficacy: effect of a trifluoromethyl group on the compound properties | 25 |
| Table 8 - | Quantitative valuation of the impact of fluorine substitution on P-gp mediated efflux permeability, lipophilicity and metabolic stability of BACEI inhibitors | 26 |

List of Schemes

| | |
|---|----|
| Scheme 1 - Cascade of events supported by the amyloid hypothesis | 5 |
| Scheme 2 - General synthetic scheme | 43 |
| Scheme 3 - Preparation of compound AA_2 | 44 |
| Scheme 4 - Preparation of compounds AA_3, AA_4 and AA_5 | 45 |
| Scheme 5 - Preparation of compounds AA_6, AA_7 and AA_8 | 55 |
| Scheme 6 - Preparation of compounds AA_9 and AA_10 | 65 |

Chapter I

Introduction

I. Introduction

I.1 Alzheimer's disease

Alzheimer's disease (AD) is a progressive neurodegenerative disorder considered to be the most common cause of irreversible dementia (Wang *et al.*, 2006). This disease is clinically characterized by a progressive decline in intellectual functions including memory loss, difficulties with language, perception and execution of movement with loss of mobility and muscle mass, visuospatial difficulties and attention problems (Forstl *et al.*, 1999). Abnormal neuropsychiatric behavior is also seen, which include depression, psychosis, anxiety and agitation (Cummings, 1995).

According to 2016 Alzheimer's Statistics, around the world nearly 44 million people have Alzheimer's or a related dementia, being this pathology most common in Western Europe. In Portugal alone it's estimated that 182 526 people had dementia in 2012 which represents 1.71% of the Portuguese population (data according to the Dementia in Europe Yearbook 2013 report). These values become more drastic when considering the global cost of Alzheimer's and dementia which is estimated to be \$605 billion, equivalent to 1% of the entire world's gross domestic product (dating according to the 2016 Alzheimer's Statistics). Therefore, there is a huge medical and economical need for the development of novel therapeutic strategies that target the pathologies of AD and slow or cease the disease progression.

Histopathologically the AD's brain presents neuron and synapse loss and it is characterized by two major pathological biomarkers: intracellular neurofibrillary tangles (NFTs), which consist of hyperphosphorylated tau protein, and extracellular amyloid plaques essentially composed by amyloid- β peptide (A β), a hydrophobic peptide (Tapiola *et al.*, 2009). Similar plaques appear in other pathologies such as some variants of Lewy body dementia, inclusion body myositis and in cerebral amyloid angiopathy. Besides these two major hallmarks, it also occurs an innate immune response with activation of inflammatory processes with complement factors like eicosanoids, chemokines and cytokines being elevated in the brain and cerebrospinal fluid of AD patients. (Heneka *et al.*, 2015).

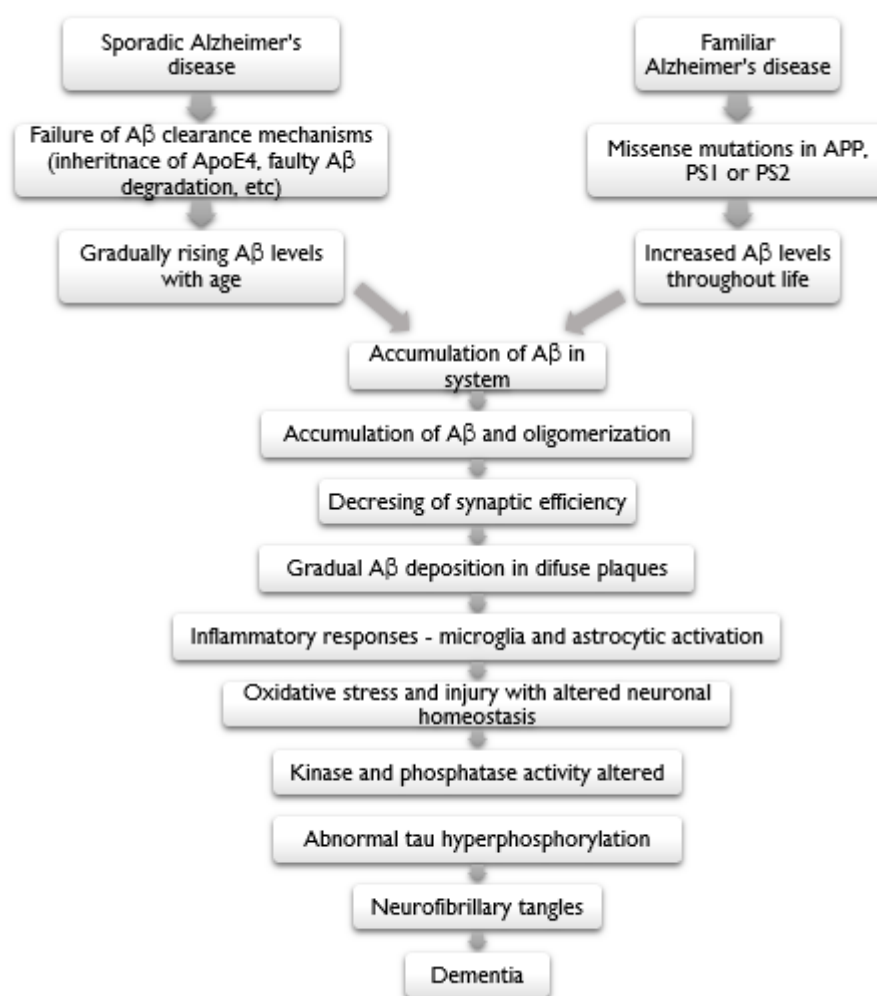
The average duration of the illness is 8-10 years but the clinical symptomatic phases are preceded by preclinical and prodromal stages that typically begin over two decades earlier

(Masters *et al.*, 2015). The majority of AD cases are sporadic (SAD) where aging, the presence of apolipoprotein E4 (*APOE4*) allele (Corder *et al.*, 1993) and vascular diseases (Soneira *et al.*, 1996) represent risk factors for this pathology. This type of AD has a mean age of onset of 80 years old and the failure to clear $A\beta$ peptide from the brain tissue is believed to be the main cause for this pathology.

A small percentage of AD cases are familial (FAD) and result from autosomal dominant mutations in either the amyloid precursor protein (APP), or the presenilin (PS1 and PS2) genes which cause overproduction or formation of an aberrant form of $A\beta$. This familial form of the disease has an early age of onset around 45 years old. Although the differences in the age of onset, both forms of AD - SAD and FAD - have the same rate of disease progression and the same biomarkers and in both forms the appearance and the increasing amount of $A\beta$ seems to be a crucial factor in this disease.

1.1.1 The amyloid cascade hypothesis

The amyloid cascade hypothesis is the dominating hypothesis to explain the mechanisms leading to Alzheimer's disease. It states that $A\beta$ plays a central role in the pathogenesis since $A\beta$ plaques begin a cascade of events that initially affect the function of the synapses and ultimately leads to neuronal loss and dementia (Hardy *et al.*, 2002). A summary of the process is shown in Scheme 1.



Scheme I - Cascade of events supported by the amyloid hypothesis.

Scheme adapted from (Selkoe, 2002)

This hypothesis is accepted by the majority of researchers. Indeed, the genetic mutations implied in familial AD, which lead to the accumulation of A β peptide, are a strong support of this theory. Also, the genetic risk conferred by the APOE gene status upkeeps the view of A β peptide accumulation as a major pathological event. Importantly, the human A673T mutation, which lowers A β production, protects against AD (Jonsson *et al.*, 2012). However, this hypothesis does not explain all the observations seeing both *in vitro* and *in vivo* more particularly the interaction of A β with protein tau. Studies show that mutations in the tau gene could cause autosomal dominant frontotemporal lobe dementia that result in tauopathy similar to that seen in AD but without the presence of A β plaques (Hutton *et al.*, 1998). So it was concluded that tau pathology alone is sufficient to cause progressive neurodegeneration but in AD its role seems to be downstream of A β pathology, i.e., A β causes tau pathology (Gotz *et al.*, 2001). In the table below – Table I - it is possible to see

some strengths and weaknesses of the amyloid cascade hypothesis.

Table 1 - Strengths and weakness of the amyloid cascade, adapted from (Herrup, 2015).

| | Strengths | Weaknesses |
|-----------------------------------|---|---|
| <i>Genetics</i> | <ul style="list-style-type: none"> • APP and PSEN genes are the only genes identified that cause FAD • APOE variants affect AD risk and also Aβ clearance in SAD cases • Rare A673T APP mutation lowers Aβ production and protects against AD | <ul style="list-style-type: none"> • No α-secretase (ADAM10) or BACE mutations yet found in FAD cases • APP, PSEN, BACE and microtubule association protein tau (MAPT) polymorphisms show little association in SAD cases • MAPT mutations are associated with frontotemporal dementia |
| <i>Biochemistry</i> | <ul style="list-style-type: none"> • Amyloid comes from APP after cleavage by γ-secretase (PSEN) • Conditions that favor γ-secretase cleavage to the longer Aβ₄₂ favor aggregation and AD • APOE4 increases risk of AD and slows clearance of Aβ | <ul style="list-style-type: none"> • Transgenic mice expressing only Aβ suggest amyloid alone is not sufficient • Other biochemical deficits are present in AD and are sufficient to create dementia |
| <i>Animal and cellular models</i> | <ul style="list-style-type: none"> • Overexpression of human APP in mouse produces plaques • Mouse transgenic for human APP show memory deficits <ul style="list-style-type: none"> • Aβ is toxic to neurons in culture • Overexpression of human APP in fruit flies produces neurodegeneration | <ul style="list-style-type: none"> • Overexpression of human APP in mouse does not produce tangles, neurodegeneration or AD-like dementia • PSEN transgenics show neither plaques, tangles or neurodegeneration |
| <i>Pathology</i> | <ul style="list-style-type: none"> • Amyloid plaques are more frequent in AD affected brains | <ul style="list-style-type: none"> • Tangles correlate better with neurodegeneration than plaques • Individuals with substantial plaque burdens can have normal cognition |
| <i>Clinical findings</i> | <ul style="list-style-type: none"> • Presence of plaques in brain associated with increased AD risk • In some subjects with amyloid burdens and early dementia, anti-amyloid therapy improves cognition | <ul style="list-style-type: none"> • After AD begins, immunoclearing of plaques does not improve cognition |
| <i>Epidemiology</i> | | <ul style="list-style-type: none"> • Certain nonsteroidal anti-inflammatory drugs reduce AD risk by half |

Based on this hypothesis six treatment strategies have been proposed. The first is the inhibition of enzymes that generate A β ; the second is the prevention of A β oligomerization or the enhancement of its clearance from the cerebral cortex. In this approach the use of active or passive A β immunization is the most common method with antibodies against A β decreasing cerebral levels of this peptide and promoting its clearance (Bard *et al.*, 2000). The third approach is an anti-inflammatory strategy. This strategy is based on the observation that a cellular inflammatory response in the cerebral cortex is provoked by the progressive accumulation of A β (Czirr *et al.*, 2012). A fourth approach is the modulation of cholesterol homeostasis. Statins (Haag *et al.*, 2009) and other cholesterol lowering drugs (Refolo *et al.*, 2001) are associated with a reduced risk of Alzheimer disease. This is due to the relationship between cholesterol and APP processing (Cheng *et al.*, 2007). The fifth approach targets the A β aggregation dependence on metallic ions Cu²⁺ and Zn²⁺ (Bush *et al.*, 1994) which chelation may prevent deposition. The sixth approach is trying to prevent the synaptotoxic and neurodegenerative effects triggered by A β using compounds with antioxidant, neuroprotective, and/or neurotrophic properties (Hardy *et al.*, 2002).

Although many of these strategies have different approaches, the main target in most of them relates to the existence of A β and its excessive formation and accumulation, the main premise of the amyloid hypothesis.

1.1.2 Amyloid- β production

A β is a short peptide with 36 - 43 amino acids responsible for the initiation of a neurotoxic cascade that leads to neuronal death and dementia (Dislich *et al.*, 2012). Although its normal function is not well understood several studies indicate that A β have numerous physiological roles which include activation of kinase enzymes (Tabaton *et al.*, 2010), protection against oxidative stress (Baruch-Suchodolsky *et al.*, 2009), regulation of cholesterol's transport (Igbavboa *et al.*, 2009) and anti-microbial activity (Kumar *et al.*, 2016, Soscia *et al.*, 2010).

A β is generated by the cleavage of amyloid precursor protein (APP), a type I integral transmembrane protein that is cleaved by several proteases called secretases (Esler *et al.*, 2001). The gene for APP is located on chromosome 21, which is associated with a significantly increased risk of early-onset Alzheimer's disease in people with Down syndrome

that carry an extra copy of this chromosome (Wiseman *et al.*, 2015). Although APP has been related with the pathology of AD, there are a lot of studies showing that APP has its own physiological functions specially in neurons, where it has a role on the regulation of synaptic function and neuronal activity. *In vitro* studies, showed that the lack of APP affected synapse formation and neurotransmission on primary cultures of mice hippocampal neuron (Priller *et al.*, 2006). Noteworthy, mice lacking APP and APP-like protein 2 presented deficits on the structure and function of synapses. (Wang *et al.*, 2005). On the other hand, mice overexpressing APP exhibit enhanced synaptic plasticity and spatial memory (Ma *et al.*, 2007).

The APP cleavage can occur via amyloidogenic (pathogenic) or non-amyloidogenic (non-pathogenic) pathway as indicated in Figure 1.

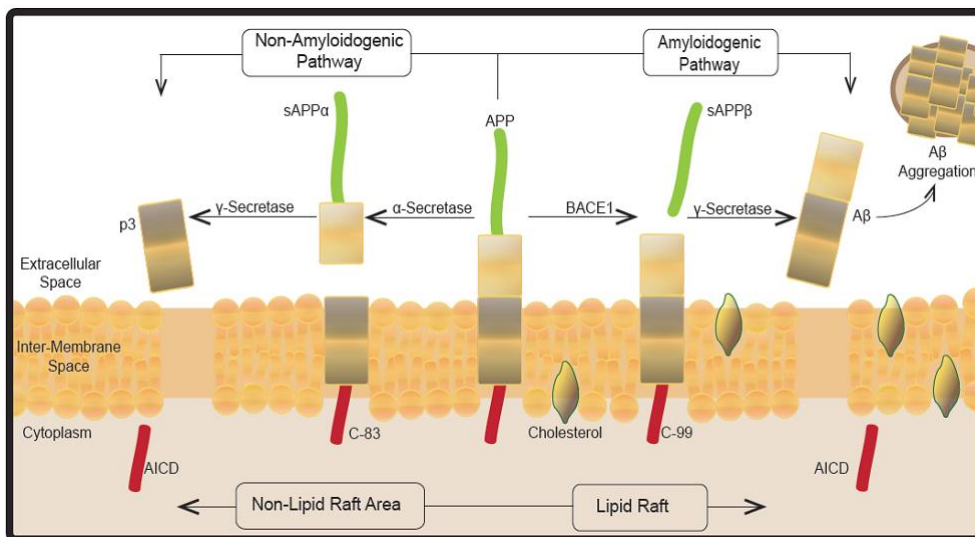


Figure 1 - Non-amyloidogenic and amyloidogenic pathways in APP cleavage (Read, 2013). The non-amyloidogenic pathway (non-pathogenic) begins with α -secretase, which releases sAPP α . The amyloidogenic (pathogenic) pathway begins with BACE1, instead of α -secretase, releasing sAPP β , a shorter fragment.

The determinant of amyloidogenesis depends on the initial proteolytic cleavage at the membrane surface by either α - or β -secretase to create a soluble or insoluble fragment (Wolfe, 2007).

In the non-amyloidogenic pathway, α -secretase, a member of the ADAM (a disintegrin and metalloprotease domain) family, which is expressed on the surfaces of cells and anchored in the cell membrane, cleaves APP at the α -site releasing a soluble fragment – sAPP α – into the extracellular space (Jorissen *et al.*, 2010) and a C-terminal fragment with 83

amino acid residues (C-83). C-83 is subsequently cleaved by γ -secretase to form a non-toxic peptide with 3kD represented in Figure 1 by p3. This creates two subsequent fragments of the APP intracellular domain (AICD), released in the cytosol, and p3 which is released into the extracellular space and is not associated with plaque formation. It is believed that APP is preferentially cleaved through this pathway in a normal brain, with the balance shifting to the amyloidogenic pathway in AD (Stockley *et al.*, 2008).

Alternatively, the amyloidogenic (pathogenic) pathway begins with β -secretase or beta-site APP converting enzyme 1 (BACE1), instead of α -secretase. This enzyme also cleaves APP in the membrane surface, 18 amino acids towards the N-terminal, releasing a shorter soluble APP- β (sAPP β) fragment. The remaining C-terminal fragment of 99 amino acid residues (C-99) remains membrane bound until cleaved by γ -secretase. This releases two fragments: AICD and A β (Read *et al.*, 2013). Due to different cleavage sites of γ -secretase, A β species that are produced have different lengths, the longer being more hydrophobic and self-aggregation A β peptides. The two main species of A β produced are A β ₄₀ which ends at residue 40 of the preceding APP and A β ₄₂ which ends at residue 42 of the preceding APP. Although the A β ₄₂ specie seems to favor aggregation more than A β ₄₀ both species have been found in senile plaques.

It has been reported that endocytosis of lipid raft domains from the cell surface is required for BACE1 and APP to meet and generate A β (Ehehalt *et al.*, 2003).

From here we can see three different mechanisms involving the secretases that allow the non-amyloidogenic pathway or a decrease of A β in brain: the stimulation of α -secretase activity and the inhibition of both β - and γ - secretase activity.

As both pathways use the same target, APP, the non-amyloidogenic pathway can overcome the amyloidogenic pathway by simply having the α -secretase cleaving APP before BACE1 does it. This competition still raises scientific debate and there is evidence suggesting that the inhibition of α -secretase does not increase BACE1 activity *in vitro* (Kuhn *et al.*, 2010). Noteworthy, the species formed by the non-amyloidogenic pathway have shown many benefits and are very important in the maintenance of neuronal growth and factor. The sAPP α has shown to have neurotrophic and neuroprotective properties as well as to promote neurite expansion, synapse production and cell adhesion (Turner *et al.*, 2003), while AICD has a role in p53 expression and caspase 3 activation, both associated with cell death,

and in maintaining cellular actin dynamics (Muller *et al.*, 2007). Also, the sAPP α fragment modulates BACE1 activity decreasing A β peptide generation (Obregon *et al.*, 2012).

Thus, the activation of APP cleavage by α -secretase has two potential beneficial effects for AD: a decrease in the levels of A β peptide and an increase in neuroprotective sAPP α . Many studies verify a decrease in A β levels as a result of α -secretase over-expression (Donmez *et al.*, 2010). As a consequence of this decrease, amyloid plaque and inflammation in the brain are diminished along with an improvement in long-term potentiation and cognitive functions (Postina *et al.*, 2004). This indicates that a moderate activation of this secretase may be therapeutically beneficial in the treatment of AD but, given that only ADAM10 cleaves over than 30 different substrates, a carefully evaluation of the consequences of chronic ADAMs activation and consequently α -secretase activation is necessary (Dislich *et al.*, 2012).

Inhibition of γ -secretase could also be a therapeutic approach since it would decrease the processing of APP and, in consequence, the levels of A β . The main problem with this method is that γ -secretase cleavage regulates a variety of signaling events by releasing the cytoplasmic domain of many transmembrane proteins, allowing these domains to transduce signals to the nucleus (Golde *et al.*, 2013). The γ -secretase regulates intramembrane proteolysis, which mean that, through γ -secretase activity, cells can transmit and regulate signals across the lipid bilayer and in other cases can also play a role in transmembrane protein turnover (Golde *et al.*, 2003, Kopan *et al.*, 2004). These roles of γ -secretase make it a less safe target than the modulation of the activity of the other two secretases.

Lastly, the modulation of β -secretase's activity seems to be a very promising therapeutic strategy. No mutations in this secretase have been reported to cause AD, but enhanced activity of this enzyme has been detected in the brains of patients with SAD (Citron, 2010). This secretase is the initiating enzyme in A β generation and it is considered a prime drug target to low cerebral A β levels in AD patients. BACE1 null mice have proven to be sustainable, with few but not fatal phenotypical abnormalities, suggesting that inhibition of this enzyme could be clinically possible with few side effects (Luo *et al.*, 2001, Nishitomi *et al.*, 2006). The therapeutic potential of BACE1 was accentuated when the genetic inhibition of this enzyme was shown to rescue memory deficits in AD animals (Ohno *et al.*, 2004).

1.1.3 BACE 1 as a therapeutic target for Alzheimer's disease

β -secretase, also known as beta-site amyloid precursor protein cleaving enzyme (BACE 1), or membrane-associated aspartic protease 2 (memapsin 2) or aspartyl protease 2 (Asp2), is a 501 amino acid type I transmembrane aspartic acid protease related to the pepsin and retroviral aspartic protease family (Lin *et al.*, 2000). It has a large 434 amino acid ectodomain, a 21 amino acid N-terminal prodomain, a 21 amino acid transmembrane domain and a 24 amino acid cytoplasmatic tail (Sathya *et al.*, 2012).

The BACE1 gene is located on chromosome 11 and the protein is synthesized in the endoplasmic reticulum (Capell *et al.*, 2000). With its activity having a low optimum pH of 4.5 – 5.5 (Vassar *et al.*, 1999), this enzyme is mostly localized in acidic intracellular compartments, such as the endosomes and the trans-Golgi network, with its active site in the lumen of the vesicle, where it contacts with APP (Kinoshita *et al.*, 2003).

The normal biological role of β -secretase is still unclear. BACE1 knockout mice showed to be deficient in $A\beta$ production which indicates that there are no compensatory mechanisms for BACE1 cleavage in mice (Citron, 2010). Behavioral changes have also been reported in BACE1 knockout mice (Harrison *et al.*, 2003, Laird *et al.*, 2005) however it is unclear how BACE1 inhibition will affect human's phenotypes.

The first crystallographic structure of BACE1 (Figure 2) was discovered in 2000 when this secretase was complexed with a peptidomimetic inhibitor. It revealed a high degree of similarity with other mammalian and fungal proteases such as renin, cathepsin D and pensillopepsin (Hong *et al.*, 2000).

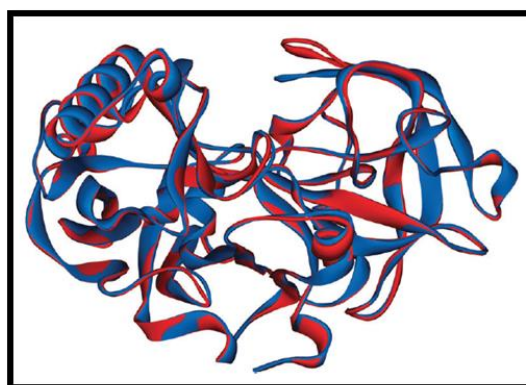


Figure 2 - Conformation of mature BACE1. Represented in red is the open flap and in blue the closed flap (Ghosh *et al.*, 2014).

The active site of BACE1 is covered by a flexible antiparallel β -hairpin, called a flap, which is believed to control substrate access to the active site and set the substrate into the correct geometry for the catalytic process. Therefore, mature BACE1 has two major conformations, flap - a β -sheet structure - open conformation and flap closed conformation as it is shown in Figure 2. Free BACE1 acquires the flap open conformation. This conformation is energetically stable and is held by optimal hydrogen bonds (Hong *et al.*, 2004). The catalytic domain is folded into conserved N-terminal and C-terminal lobes with oligosaccharides limiting the motion and orientation of this domain. When BACE1 interacts with a substrate its conformation changes and the secretase adopts a flap closed conformation.

For this change in conformation to occur there is a breakage of hydrogen bonds between some of the amino acids of this protein. This destabilization in the hydrogen bonds indicate that a conformational change must take place upon binding of the inhibitor/substrate to the active site and may participate kinetically in substrate binding in the closed conformation and product release in the open conformation. (Ghosh *et al.*, 2014).

The majority β -secretase activity is exhibit in neural tissue and neuronal cell lines (Seubert *et al.*, 1993). *In vitro*, β -secretase mediated APP cleavage and $A\beta$ production appears to be substantially less effective in astrocytes than in neurons. Indeed, neurons can have a strong β -secretase activity and are an important source of $A\beta$ in the brain (Zhao *et al.*, 1996).

After the discovery of BACE1, a close membrane-bound aspartyl protease homologue was identified (Yan *et al.*, 1999). BACE2, memapsin I or Asp1, is located in chromosome 21 and exhibit 64% amino acid similarity with BACE1 (Sathya *et al.*, 2012). BACE2 is expressed predominantly in astrocytes (Basi *et al.*, 2003) and in peripheral tissues like pancreas and kidney (Bennett *et al.*, 2000) however is not detected in neurons and microglia where only BACE1 seems to be present.

Studies have shown that BACE2 overexpression decrease the levels of $A\beta$ in primary neuronal cultures derived from APP transgenic mice (Sun *et al.*, 2005) and can function as an antagonist of BACE1 (Basi *et al.*, 2003), cleaving within $A\beta$ sequence and promoting the non-amyloidogenic pathway. However, *in vitro*, BACE2 is capable of cleaving APP at BACE1 cleavage site (Farzan *et al.*, 2000, Hussain *et al.*, 2000).

BACE2 plays very important roles in the pancreas, where regulates pancreatic β cell function (Esterhazy *et al.*, 2011) and in the skin it interacts with pigmentation, processing

(PMEL) (Rochin *et al.*, 2013). In the design of new BACE1 inhibitors it is important to be aware of BACE2 functions because, due to their high homology, BACE1 inhibitors are likely to interact also with BACE2 leading to unwanted side effects.

1.1.4 BACE I inhibitors development

Since the identification of BACE1, many efforts have been made to develop small-molecule BACE1 inhibitors as drugs for AD. Many inhibitors have been described however few had presented a balance between the *in vitro* potency and the necessary pharmacokinetic properties to achieve *in vivo* effectiveness. The first generation of BACE1 inhibitors were peptide-based mimetics and, like most inhibitors of aspartate proteases, originated from substrate and transition state analog-based design (Oehlrich *et al.*, 2014). This allowed for subsite specificity, hydrogen bonding and hydrophobic interactions to be conserved or enhanced through new side chain choices (Ghosh *et al.*, 2014).

Peptidomimetic inhibitors can be classified based on their transition state isostere. The most common used transition-states isosteres are statins, norstatines, tert-hydroxyl, hydroxyethylenes, hydroxyethylamines and reduced amides, whose structures are represented in Figure 3.

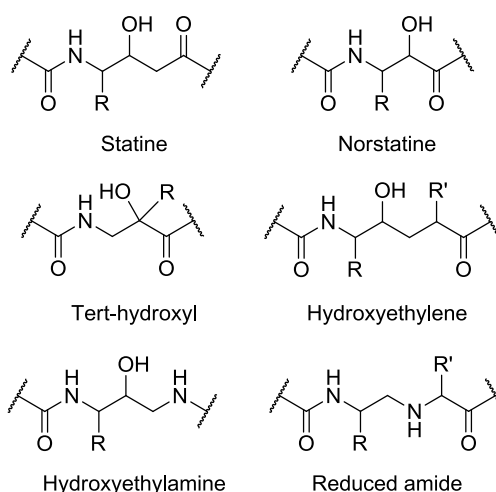


Figure 3 - Most common transition-states isosteres used to design new BACE1 inhibitors.

In addition of peptidic features and molecular size, these inhibitors must overcome many barriers in order to be efficient *in vivo*. One of the most important is the selectivity over

other aspartic proteases such as BACE2, pepsin, renin, cathepsin D, cathepsin B among others. These aspartic proteases are present in nearly all body tissues and its inhibition may cause unwanted side effects. Only in the case of cathepsin D (CatD), its unselective inhibition can lead to seizures, blindness and neuronal ceroid lipofuscinosis (Koike *et al.*, 2000). This implies that the subsite specificity in the active site of β -secretase must be taken into consideration during the design of new inhibitors.

Another big challenge of BACE1 inhibitors has been the large size of the catalytic site. This requires large molecules which will have poor cell membrane and blood-brain barrier permeability and consequently will not be effective *in vivo*. Decreasing the size of the peptidic inhibitor had shown a decrease in potency (Gruninger-Leitch *et al.*, 2002) because these inhibitors would not be able to fill the catalytic pocket of the enzyme properly. To overcome this difficulty, the affinity of the inhibitor with BACE1 active site must be increased by increasing interactions with the enzyme.

As a result of all the obstacles presented by peptidomimetic inhibitors new nonpeptide inhibitors began to be studied. These inhibitors are smaller and have evolved from high-throughput screening and fragment based screening followed by chemical optimization (Ghosh *et al.*, 2014). This new class of inhibitors can also be developed based on computational screening and modeling methods creating large compounds libraries.

The major objectives of this new approach were to develop inhibitors smaller in size, with less peptide character and better metabolic stability. These characteristics lead to molecules with better blood-brain barrier permeation and a lower efflux by the P-glycoprotein.

While no BACE1 inhibitor have been approved to date, in recent years, several β -secretase inhibitors are entering AD clinical trials (Vassar, 2014). A summary table of the inhibitors who are currently in clinical trials is shown below in Table 2.

Table 2 - BACE1 inhibitors currently in clinical trials, adapted from (Barao et al., 2016).

| Compound | Company | Phase | Population | Next Milestone |
|--------------|--------------------------|--------------|---|--|
| MK-8931 | Merck | Phase III | Mild-to-moderate AD; Prodromal AD | Completion of Phase III trial in 2017 (mild-to-moderate AD) and in 2019 (prodromal AD) |
| AZD3293 | AstraZeneca Eli Lilly | Phase II/III | Prodromal-to-mild AD | Completion of Phase II/III trials in 2019 |
| E2609 | Eisai Biogen Idec | Phase II | Prodromal-to-mild AD Early-stage AD | Completion of Phase II trial and started Phase III in 2016 |
| JNJ-54861911 | Shionogi Janssen | Phase II | pathophysiology (asymptomatic) and prodromal AD | Started Phase II/III adaptive AD prevention study in 2015 |
| CNP520 | Novartis Amgen | Phase I/II | ApoE4+/+ | Phase I/II results |
| PF-06648671 | Pfizer | Phase I | - | Phase I results |
| LY-3202626 | Eli Lilly | Phase I | - | Phase I results |

The most promisor of all these inhibitors is a small molecule inhibitor of BACE1 and BACE2, MK-8931 or Verubecestat. This inhibitor developed by Merck is currently in Phase 3 trials after proving its safety, tolerability and pharmacology in Phase I, when administered to patients with mild to moderate AD and with renal insufficiency. In Phase 2 showed a reduction in CSF A β by up to 90 percent.

I.1.5 Limits of BACE1 inhibitors

Initially BACE1 knockout mice were described as having no major phenotype and chronic inhibition of BACE1 had been proposed as a potentially attractive therapy for AD. However, subsequent studies showed that BACE1^{-/-} mice, that is, mice with total inhibition of BACE1, present some cognitive and neurochemical phenotypes which are related to a mechanism-based side effect. In fact, recent studies have identified innumerable substrates for BACE1 (Hemming *et al.*, 2009) and therefore a total inhibition of BACE1 activity might have adverse effects. The BACE1^{-/-} mouse phenotypes, many of which involve the CNS, are resumed in Table 3.

Table 3 - Most common phenotypes observed in mice BACE1^{-/-}, adapted from (Vassar *et al.*, 2014).

| <i>Phenotype</i> | <i>Reference</i> |
|--|--|
| Astrogenesis increase, neurogenesis decrease | (Hu <i>et al.</i> , 2013) |
| Axon guidance defects | (Rajapaksha <i>et al.</i> , 2011) (Cao <i>et al.</i> , 2012) (Hitt <i>et al.</i> , 2012) |
| Hyperactivity | (Dominguez <i>et al.</i> , 2005) (Savonenko <i>et al.</i> , 2008) |
| Hypomyelination | (Willem <i>et al.</i> , 2006) (Hu <i>et al.</i> , 2006) (Hu <i>et al.</i> , 2008) |
| Memory deficits | (Ohno <i>et al.</i> , 2004) (Ohno <i>et al.</i> , 2006) (Ohno <i>et al.</i> , 2007) (Laird <i>et al.</i> , 2005) |
| Neurochemical deficit | (Harrison <i>et al.</i> , 2003) |
| Neurodegeneration with age | (Hu <i>et al.</i> , 2010) |
| Post-natal lethality, growth retardation | (Dominguez <i>et al.</i> , 2005) |
| Retinal pathology | (Cai <i>et al.</i> , 2012) |
| Schizophrenia endophenotypes | (Savonenko <i>et al.</i> , 2008) |
| Seizures | (Kim <i>et al.</i> , 2007) (Kobayashi <i>et al.</i> , 2008) (Hu <i>et al.</i> , 2010) (Hitt <i>et al.</i> , 2010) |
| Spine density reduction | (Savonenko <i>et al.</i> , 2008) |
| Decreased synaptic plasticity | (Laird <i>et al.</i> , 2005) (Kobayashi <i>et al.</i> , 2008) (Wang <i>et al.</i> , 2008) (Filser <i>et al.</i> , 2015) |
| Reduced spine density | (Savonenko <i>et al.</i> , 2008) |
| Timid and less exploratory | (Harrison <i>et al.</i> , 2003) |

Another limiting factor of this therapy is the high homology between BACE1 and BACE2. This means that an inhibitor of BACE1 is likely going to interact also with BACE2 and cause potential mechanism-based side effects due to BACE2 inhibition especially in pancreas and in skin but also in the brain.

Although these limits are real and observable in *in vivo* tests, those phenotypes result from a total inhibition of BACE1. Importantly, the risk of mechanism-based toxic effects depends on the level of BACE inhibition. Thus, it is advisable that BACE1 inhibitors will cause only a partial inhibition of this enzyme to allow for a remaining BACE1 activity in order to spare its physiological functions (Barao *et al.*, 2016). Indeed, in heterozygous mice, with a 50% reduction of BACE1 expression, leading to a small decrease in A β levels, the amyloid plaques and the synaptic pathology were significantly reduced in aged mice brain, suggesting that a slight reduction of A β levels in AD patients might impact significantly the disease progression (Mcconlogue *et al.*, 2007). In support of this hypothesis, the carriers of the APP-A673T mutation, which decreases APP processing by BACE1, are protected against age-dependent cognitive decline and AD (Jonsson *et al.*, 2012)

Therefore, the goal in the design of new BACE1 inhibitors is to find a safe therapeutic window in which the doses of BACE1 inhibitors allow to achieve a successful AD therapy without inducing mechanism-based side effects.

1.2 Fluorine atom in medicinal chemistry

Since French chemist Henri Moissan prepared elemental fluorine in 1906 this compound had been widespread throughout many areas, with special impact on medicinal chemistry. The substitution of various functional groups by fluorine has been creating more active, efficient and selective compounds. Nowadays is estimated that approximately 15% of drugs developed for pharmaceutical use incorporate one fluorine (Hagmann, 2008). This percentage can increase to 25% if considering one or more fluorine atoms (Gomes *et al.*, 2015).

During the last decades, fluorinated compounds have contributed to the advancement of many drug capable of acting in the central nervous system and as anticancer and antiviral agents, among others (Bassetto *et al.*, 2015).

1.2.1 Incorporation of fluorine atoms in BACE1 inhibitors

The fluorine is introduced in a molecule through diverse chemical environments as shown in Figure 4.

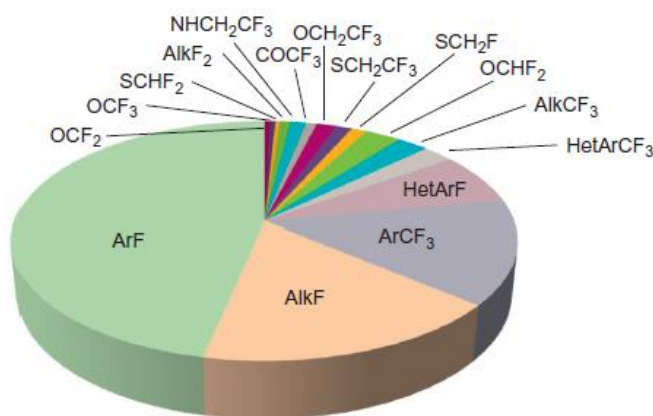


Figure 4 - Fluorine chemotypes in marketed drugs, adapted from (Lawton, 2015).

Although more than half of the drugs have a single fluorine atom, it has been increasing the number of drugs that include CF₃. In the case of BACE1 inhibitors it is possible to find progressively more compounds that include one or more fluorine atoms incorporated in the molecule, in many of the chemical environments shown in Figure 1 (Evin *et al.*, 2011, Ghosh *et al.*, 2012, Silvestri, 2009). Some compounds will be later analysed in detail and the

contribution of the incorporation of fluorine atoms will be explained as it was done by Steve Swallow.

1.2.1.1 General fluorine properties

Although there are several available elements in medicinal chemistry for modulating compounds properties, the unique properties of fluorine show a major interest.

The presence of fluorine atoms in a molecule causes several alterations in some atomic parameters. Its high ionization potential and low polarizability makes fluorinated compounds to have weak surface energies, dielectric constants and refracting indexes.

Table 4 - Atomic parameters of fluorine atom compared with other halogenes and atoms, adapted from (Swallow, 2015).

| Atom | Ionization Potential (kcal/mol) | Electron affinity (kcal/mol) | Atom polarizability (\AA^3) | Van Der Waals Radii (\AA) | Pauling's Electronegativity | Bond strength to Carbon |
|------|---------------------------------|------------------------------|--|--------------------------------------|-----------------------------|-------------------------|
| H | 313,6 | 17,7 | 0,667 | 1,20 | 2,20 | 98 |
| C | 240,5 | 29,0 | 1,76 | 1,70 | 2,55 | 83 |
| O | 314,0 | 33,8 | 0,82 | 1,52 | 3,44 | 84 |
| F | 401,8 | 79,5 | 0,557 | 1,47 | 3,98 | 105 |
| Cl | 299,0 | 83,3 | 2,18 | 1,75 | 3,16 | 77 |
| Br | 272,4 | 72,6 | 3,05 | 1,85 | 2,96 | 66 |

On the other hand, fluorine high electronegativity, small size, good overlap between its 2s or 2p orbitals with the correspondent orbitals of carbon and the presence of lone pairs of electrons make bonds between fluorine and carbon strongly polarized from the carbon (δ^+) to the fluorine (δ^-). These features associated with low polarizability of the fluorine atom implies that C-F bond has a reasonably important ionic character and a stronger energy than

between carbon and other halogens (Table 4). This property has been widely exploited by medicinal chemists as an attempt to block the metabolism of drug candidates, as it will be discussed ahead (Swallow, 2015).

This dipolar feature of C-F bond gives to fluorinated molecules a polar character and, consequently, their physicochemical properties are different from non-fluorinated compounds (Bégué, 2008), including the impact in lipophilicity, pK_a , conformation, molecular recognition and metabolic oxidation potential and allows the improvement of selectivity, potency, absorption and metabolism.

1.2.1.2 Impact of fluorine in lipophilicity of new potential BACE1 inhibitors

Lipophilicity, measured by $\log D$, is a prime characteristic when developing new compounds. Its influence in the potency, pharmacokinetics and toxicity of a molecule has been established for many years (Van De Waterbeemd *et al.*, 2001).

The absorption and distribution of a drug *in vivo* is controlled by its balance of lipophilicity and hydrophilicity as well as ionization (Ojima, 2009). So, enhanced lipophilicity allows the modulation of certain parameters such as absorption and biological barrier passage, which influences the transport into organs and cells, and the established interactions between the molecule and the macromolecular target (Bégué, 2008). However, if lipophilicity is too high there is an increased probability for that molecule to bind to multiple targets and the resultant pharmacologically induces toxicology, as well as poor solubility and metabolic clearance (Leeson *et al.*, 2007).

Several studies concluded that a fluorine substituent, in general, increases the lipophilicity. In aromatic systems, the substitution of a methyl group for a CF_3 group gives a slight increase in lipophilicity and at the same time converts the substituent into a powerful electron-withdrawing group (Swallow, 2015). However, this effect is not so linear in aliphatic systems. Changes in lipophilicity are, as said earlier, usually measured by the octanol-water partition coefficients under buffered conditions. Since these coefficients can be influenced by the presence of charged groups in the molecule, changes in pK_a can also influenced $\log D$. In general, the fluorination of saturated alkyl groups represents a decrease in lipophilicity due to strong electron withdrawing capabilities of fluorine. This decrease follows the sequence

$\text{CH}_3 < \text{CF}_3 < \text{CHF}_2 < \text{CH}_2\text{F}$ and in each case reflects the magnitude of the dipole (Huchet Q. A., 2013).

Since BACE1 inhibitors should have sufficient but not excessive lipophilicity to cross both plasma and endosomal membranes for gaining access to the vesicle lumen where the BACE1 active site is located (Vassar, 2014), incorporate fluorine atoms in molecules with potential inhibition of BACE1 represents a possible strategy that allows the molecule to reach the desired location in order to interact with the enzyme.

An example of this effect is seen in β -secretase inhibitors developed by Elan (Figure 5) where it was tried to improve the permeability and reduce the efflux potential of these molecules by adding fluorine atoms to the molecule structure (Oehlrich *et al.*, 2014).

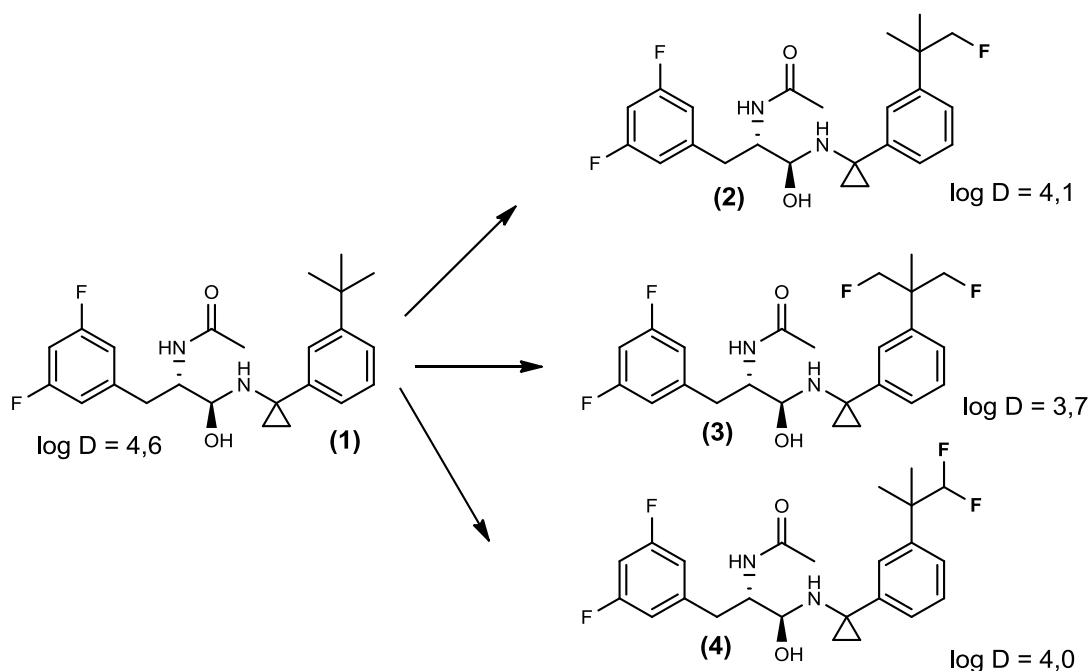


Figure 5 - Influence of fluorine atoms addition to the log D of BACE1 inhibitors.

In this case the purpose was to reduce the polarity of inhibitor I without introducing heteroatoms that could aggravate the efflux potential. So, and recognizing the polar hydrophobicity of fluorinated compounds, workers at Elan incorporated a fluorine atom in compound I. This led to a reduced log D and an improvement in permeability of compound 2 when compared with compound I. Beyond this structural modification, it was also studied the alteration in log D due to introduction of a second fluorine in the other methyl group - compound 3 - which led to a decrease in the log D of this compound when compared to compound 2. However, when the introduction of the second fluorine substituent was made

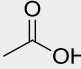
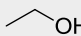
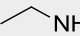
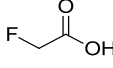
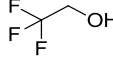
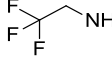
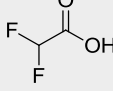
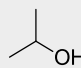
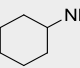
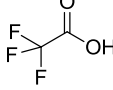
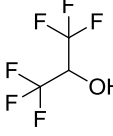
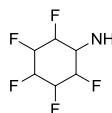
in the same carbon - compound 4 - the effect on log D proved to be additive (Swallow, 2015).

1.2.1.3 Impact of fluorine on pK_a of new potential BACE1 inhibitors

The influence of the acid-base dissociation constant, pK_a , on the molecular interactions and the physicochemical properties of a molecule has long been established in medicinal chemistry. Modulation of pK_a can impact on bioavailability by affecting the absorption process which in turn is related with charged and neutral species of an ionisable drug (Bégué, 2008). As the majority of drugs are weak acids or bases, knowing the dissociation constant in each case is necessary to understand the ionic form a molecule will take across a range of pH values (Manallack, 2008).

When a fluorine atom is added to a molecule, its pK_a is changed. There are many other forms to modulate pK_a but, due to the powerful inductive effect of fluorine coupled to its minor impact on size, shape and molecular weight, the substitution with fluorine around acidic and basic centres makes it a better form of pK_a modulation (Swallow, 2015). These changes are shown in Table 5 with examples of carboxylic acids, alcohols and amines.

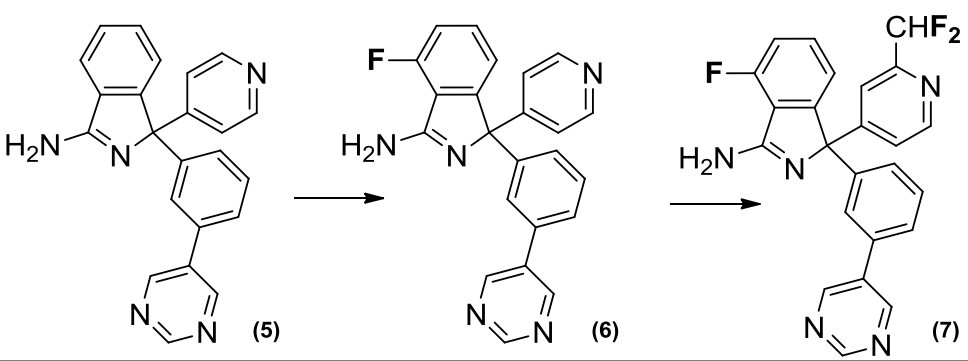
Table 5 - Effect of fluorine substitution on pK_a and pK_b values (Purser, 2007).

| Carboxylic acid | pK_a | Alcohol | pK_a | Amine | pK_b |
|---|--------|---|--------|--|--------|
|  | 4,76 |  | 15,9 |  | 10,6 |
|  | 2,59 |  | 12,4 |  | 5,7 |
|  | 1,34 |  | 19,2 |  | 4,6 |
|  | 0,52 |  | 5,1 |  | -0,36 |

As it can be seen in Table 5, the successive substitution of hydrogen atoms by fluorine atoms lead to a decrease of pK_a both in carboxylic acids and alcohols and a decrease in the basicity of amines.

An example of this effect can be seen in series of amino-isoindoles BACE1 inhibitors evaluated by AstraZeneca (Swahn *et al.*, 2012) shown in Table 6.

Table 6 - Effects of fluorine atom addition to the properties of a BACE1 inhibitor (Oehlrich, 2014).



| | (5) | (6) | AZD-3839 (7) |
|------------------------------|---------|---------|--------------|
| <i>BACE1 IC₅₀</i> | 500 nM | 124 nM | 35,1 nM |
| <i>Cell IC₅₀</i> | 90,3 nM | 8,25 nM | 16,7 nM |
| <i>pK_a</i> | 8,4 | 7,2 | 7,1 |
| <i>PgP efflux</i> | 12 | 1,9 | 0,9 |
| <i>hERG IC₅₀</i> | 16 μM | 3,1 μM | 4,8 μM |

The introduction of a fluorine atom ortho to the amidine (compound 6) was the key factor allowing to achieve an optimal pK_a , permeability and efflux. It was noticed that, in addition to a lower pK_a , the fluorine atom formed a weak internal hydrogen bond with the exocyclic nitrogen of the amidine, which was beneficial not only for permeability but also for P-glycoprotein (Pgp)-mediated efflux (Oehlrich *et al.*, 2014). Another characteristic observed was that this modification changed the affinity for the hERG (human Ether-à-go-go-Related Gene) ion channel. (both these parameters will be discussing in detail in the next section of this introduction.) Furthermore, they noticed that an addition of a lipophilic electron-withdrawing group in the 2-position of the pyridyl ring such as difluoromethyl group (or even trifluoromethyl group, not here represented) lowered the hERG liability and further

fine-tuned other properties. This molecule led to BACE1 inhibitor AZD-3839 which reached Phase I of clinical trials.

1.2.1.4 Increasing brain penetration through the incorporation of fluorine atoms in new potential BACE1 inhibitors

The pK_a has shown a very important role in the modulation of P-glycoprotein efflux (Gatlik-Landwojtowicz *et al.*, 2006). This influence is not just significant because Pgp mediates efflux, therefore limiting the absorption of drugs into the human system, but also because this protein is a very major limiting brain penetration factor for compounds that need to enter the CNS, as happens to be the case with BACE1 inhibitors.

The shift of cellular versus *in vitro* enzymatic activity also depends on the pK_a : basic compounds with a $pK_a \geq 7$ show a tendency for higher activity in the cell-based assay where compounds with a $pK_a < 7$ are more balanced or can even revert to have a higher potency in the enzymatic *in vitro* assay (Hilpert *et al.*, 2013).

Although several new scaffolds have been developed along the years as potential β -secretase inhibitors, the relationship between a good potency in both *in vitro* and cellular assays and the compound's physicochemical properties is very dependent of pK_a of the molecule. The modulation of this parameter will create leads with good brain penetrance and minimal hERG interactions (Oehlrich *et al.*, 2014). To achieve this purpose, fluorine substitution has been used. A good example is the optimization of several oxazines by Roche and its workers, where they studied the power of fluorine to lower the pK_a and thereby change the pharmacological profile of this class of BACE1 inhibitors (Hilpert *et al.*, 2013).

In their work, they described the compound 8 (presented in Table 7) as having good potency on the *in vitro* and cellular assays however showing very poor activity *in vivo*. This phenomenon was associated with the high basicity of this molecule that induced Pgp-mediated efflux, limiting its brain penetration. As an effort to reduce the pK_a , Roche workers performed an extensive study of the fluorine substitution in all available positions in the oxazine ring (Hilpert *et al.*, 2013).

This study shown the modification 9 as having an optimal balance of properties. Although the CF_3 group did not interact with the enzyme, it was exposed to the solvent and had a big impact on pK_a and in the efflux ratio, despite being distant from the basic center. The changes in properties of compound 8 to compound 9 are describe in table 7.

Table 7 - β -Secretase (BACE1) Inhibitors with high *in vivo* efficacy: effect of a trifluoromethyl group on the compound properties.

| | (8) | (9) |
|--|---------------|---------------|
| <i>BACE1</i> IC_{50} | 0.137 μ M | 0,012 μ M |
| Cell-based ($A\beta_{40}$) IC_{50} | 0,010 μ M | 0,002 μ M |
| pK_a | 9,7 | 7,0 |
| PgP efflux | 14,8 | 1,9 |

This change also had a huge impact on both *in vitro* and cellular assays potency with an associated improvement of *in vivo* activity. The compound 9 showed a 75% reduction of $A\beta_{40}$ production at 1mg/kg while compound 8 presented only a reduction of 13% at 10mg/kg

1.2.1.5 Impact of fluorine on hERG activity of new potential BACE1 inhibitors

Inhibition of hERG channels has become a huge preoccupation in medicinal chemistry. These ion channels are responsible for the electrical activity of the heart that coordinates the heart's beating (Vandenberg *et al.*, 2012) and when its capability to conduct electrical current across the cell membrane is inhibited or compromised it can lead to QT prolongation (Finlayson *et al.*, 2004), a fatal disorder.

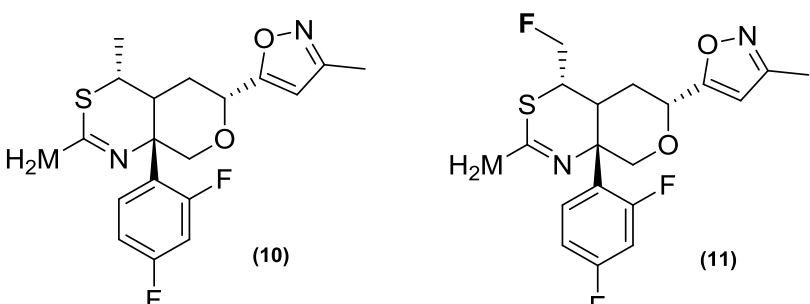
hERG channels activity is mostly associated with lipophilic bases (Aronov, 2008), so reducing lipophilicity and base pK_a will lead to a reduced activity of this channels. Thus,

introducing a fluorine close to the basic center of hERG active compounds have been a successful strategy to work around this problem.

An example of the strategic use of fluorine to reduce hERG inhibition, and simultaneously optimize other characteristics of potential inhibitors of BACE1, was published by Pfizer (Brodney *et al.*, 2015) and is presented in Table 8.

Briefly, they design compound 10 that incorporated two fluorine atoms. This compound had as major inconvenient the high IC₅₀ in hERG experiments. Pfizer workers then added a fluorine atom on the methyl substituent on the thioamidine heterocyclic in an attempt of reducing pK_a and thereby hERG activity, creating compound 11. Indeed, the objective was accomplished with a decrease of 0,7 points in pK_a and an increase of 8μM in the hERG IC₅₀ and this being achieved by a single fluorine atom addition.

Table 8 - Quantitative valuation of the Impact of fluorine substitution on P-gp mediated efflux, permeability, lipophilicity and metabolic stability of BACE1 inhibitors.



| | | |
|----------------------------|--------|---------|
| BACE1 CFA IC ₅₀ | 74 μM | 53 μM |
| Log D | 2,1 | 2,4 |
| pK _a | 7,7 | 7,0 |
| hERG IC ₅₀ | 2,1 μM | 10,1 μM |

1.2.1.6 Impact of fluorine in metabolism

One of the challenges in drug discovery relates to the metabolic processes that compounds face in live organisms, namely the drugs susceptibility to the oxidative metabolism catalysed by liver enzymes (Park *et al.*, 2001). Lipophilic compounds are more susceptible to this oxidation, so increasing the polarity of the compound by fluorine atoms

incorporation on a molecule can modify this metabolic process and even block the oxidative metabolism in both aromatic and aliphatic sites thereby changing the rate, route and extension of drug metabolism (Shah *et al.*, 2007).

At present the impact of fluorine incorporation in the metabolism of BACE1 inhibitors was not evaluated, but analysing this from a general perspective, the incorporation of fluorine atoms can not only help the metabolism but also can prevent the generation of reactive metabolites. An example is a study with the γ -secretase inhibitor that was made by Pettersson and its coworkers (Pettersson *et al.*, 2016).

Although fluorine is used to reduce metabolic clearance (Gillis *et al.*, 2015) and prevent the formation of reactive metabolites it can also lead to the formation of some specific metabolites that are known for its potential toxicity (Bégué, 2008) so its incorporation needs to be well analyzed.

1.2.1.7 Influence of fluorine in the conformation of new potential BACE1 inhibitors

The effects of the introduction of fluorine(s) in a molecule have been well reviewed through the years (Hunter, 2010, O'hagan, 2008). Namely, when a fluorine atom is introduced to a molecule it causes impact mostly due to the several features of the C-F bond.

The four principal effects caused by this molecular alteration are: changes in the geometry of the molecule, changes in charge-dipole interactions, hyperconjugation and changes in dipole-dipole interactions.

The change in geometry between carbon and fluorine occur due to high electronegativity of fluorine atom which leads to a reduction in the repulsion on the bonding electron pair between the carbon-fluorine and adjacent bonds.

The charge-dipole interactions are related with pK_a effect and lead to a conformational preference for gauche interactions between fluorine substitutions and protonate amines in open chain systems.

Another consequence of the high polarization of the bond between carbon and fluorine is the presence of a low-lying antibonding orbital that can embody electron density from bonds that are stereoelectronically aligned and are electron-rich bonds (e.g. oxygen and

nitrogen lone pairs) (O'hagan, 2008). Such interactions can lead to a stabilization of certain conformations.

An example is presented in fluorinated analogues of the HIV protease inhibitor Indinavir (Myers *et al.*, 2001). The HIV proteases also belong to the same type of proteolytic enzymes as BACE1, the aspartic proteases, as mentioned in section 1.1.2 of this Introduction. Thus, the fluorination on BACE I inhibitors can have similar effect.

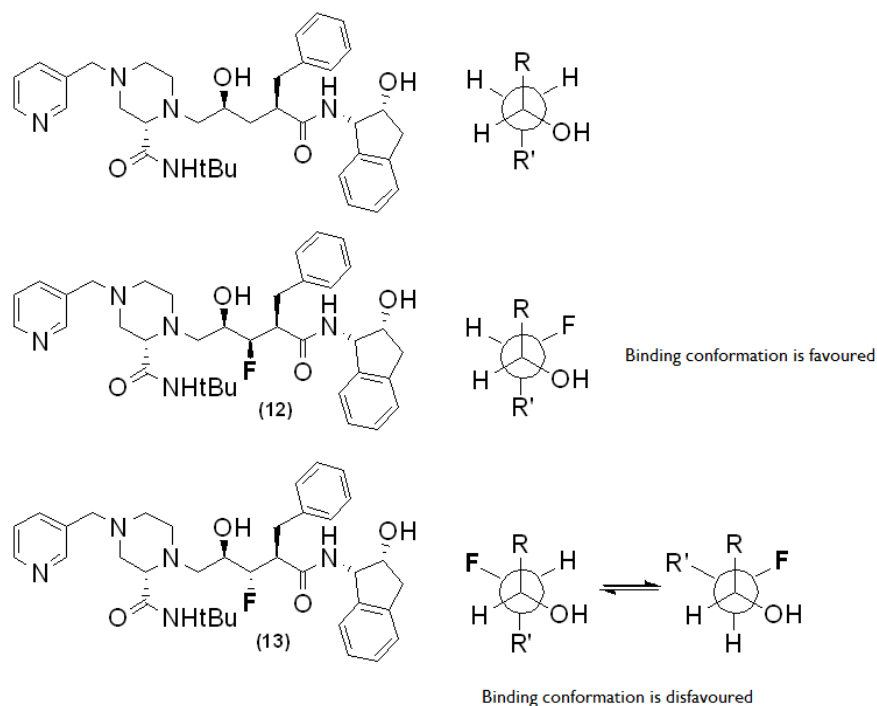


Figure 6 - Effects of fluorine atom in the preferential conformation of Indinavir.

In this example, represented in Figure 6, the diastereoisomer 12 of the compound Indinavir had a stabilized extended conformation that was observed in the crystal structure of Indinavir bound to HIV protease, leading to a potency comparable to that of Indinavir. By other hand, the diastereoisomer 13 had a disfavoured extended conformation leading to a much lower potency of this compound as an HIV protease inhibitor. This was explained by the gauche interactions that were preferred.

Another conformational change that occurs when the fluorine atom is incorporated in a molecule is the dipole-dipole interactions. The ionic character between carbon and fluorine bond leads to a large dipole moment which also plays an important role in determining the conformational behaviour of the fluorinated compounds.

Besides these alterations, other changes in molecule can include bonds attractions and repulsions with other functional groups in the molecule (Swallow, 2015).

1.2.2 Strategies of fluorination

Due to the many qualities of fluorine atoms when incorporated in molecules, several strategies of synthesis have been discovered and developed.

The chemistry of fluorinated compounds has been evolving during the last few decades with a special interest in new approaches which allow for the addition of more than one fluorine at a time. In particular, synthetic methods allowing the regio and chemoselective incorporation of fluorine atoms. Unfortunately, the task of introducing fluorine into organic molecules has presented a vast challenge to synthetic chemists (Liang *et al.*, 2013).

Initially the traditional techniques of fluorination involved unusual and corrosive reagents, like elemental fluorine, fluorhydric acid or sulphur tetrafluoride. As these chemicals were dangerous, difficult to handle and not very selective, the next strategy was to start from available compounds that already contained fluorine and prepare building blocks as starting chemicals. With this approach it was possible to handle more complex molecules and use methods to incorporate fluorine atoms in different chemical environments.

Two approaches are possible for synthesizing large and complex molecules containing one or several fluorine atoms. The first strategy is the use of fluorinated building blocks to synthesize the target compound. The second one is the synthesis of the non-fluorinated molecule and then introduce the fluorine atoms at a late stage of the synthesis by using fluorination, difluoromethylation or trifluoromethylation techniques (Bégué, 2008).

1.2.2.1 Monofluorination techniques

The incorporation of a single fluorine atom can only be achieved by electrophilic or nucleophilic attack or by a fluoro alkyl chain addition to the center structure of the drug (Stephenson *et al.*, 2007, Zhang *et al.*, 2005).

Concerning nucleophilic fluorination, the major challenges associated with this method derive from the high electronegativity of fluorine atom. This characteristic contributes to the high kinetic barriers in the formation of carbon-fluorine bonds despite the thermodynamic driving force of forming this bond being the strongest carbon-heteroatom single bond

known. (Liang *et al.*, 2013). Some nucleophilic fluorination reagents provided by Sigma Aldrich are shown in Figure 7.

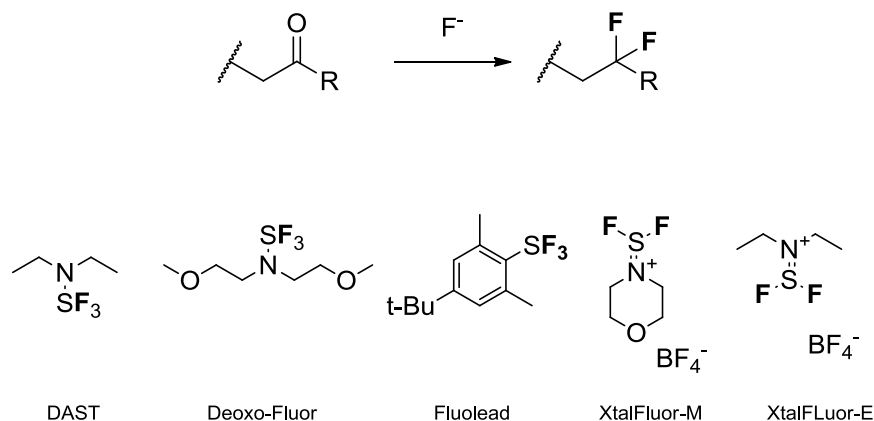


Figure 7 - Some reagents used for nucleophilic monofluorination.

Diethyl amino sulfur trifluoride (DAST) and Deoxo-fluor are the main reagents for nucleophilic fluorination. These reagents allow the direct transformation of a C–OH bond (alcohol) to a C–F bond (fluoride). The reaction is effective with primary, secondary and tertiary alcohols and are often stereoselective taking place with inversion of the configuration. Still, the cationic character of the substitution is often very pronounced.

Concerning electrophilic fluorination, the formation of an F⁺ specie does not exist under normal conditions and is energetically unfavorable. So there is the need to design F⁺ equivalents to implement nucleophilic fluorination in molecules. Some electrophilic fluorination reagents are shown in Figure 8.

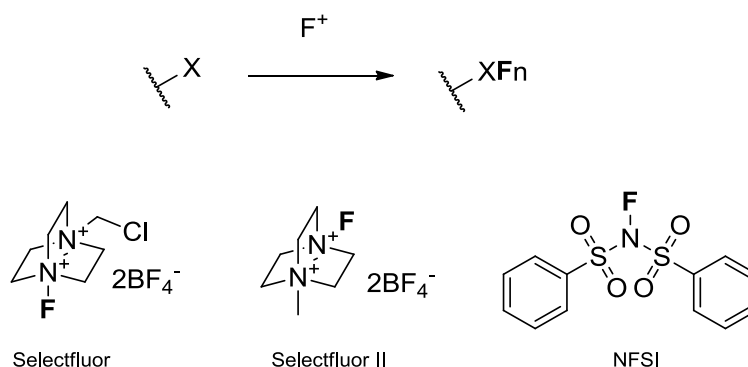


Figure 8 - Some reagents used for electrophilic monofluorination.

These reagents, in a general form, are safe and easy to use. In case of Selectfluor[®], this reagent is exceptionally stable and a very versatile electrophilic fluorinating agent that was developed by Banks and co-workers. This reagent become very popular and allows many applications, including fluorination of aril groups, nucleosides, steroids, carbon-metal bonds, and other substrates (Kirk, 2008).

1.2.2.2 Difluoromethylation techniques

The difluoromethyl group has been studied for its propensity to serve as a hydrogen bond donor and as potential replacement for hydroxyl groups (Jon A. Erickson, 1995). Some reagents are shown in Figure 9.

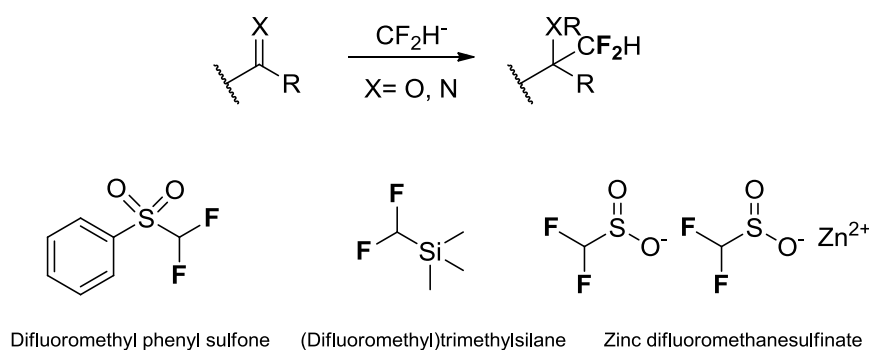


Figure 9 - Some reagents used for difluoromethylation reactions.

Of all these three reagents, it is necessary to highlight Zinc difluoromethanesulfinate that can directly add CF_2H to heterocycles under open flask conditions making it very operational to carry out difluoromethylation (Fujiwara *et al.*, 2012). Selectfluor[®] can also be used for difluorination in nucleosides (Bégué, 2008).

1.2.2.3 Trifluoromethylation techniques

Trifluoromethyl groups are electron-withdrawing substituents that increase the lipophilicity (Smart, 2001). This group can increase the metabolic stability of a molecule while retaining comparable cytotoxic potency. This is shown in an example with the anti-cancer epothilone, Fludelone (Rivkin *et al.*, 2002).

In comparison with mono and difluoromethylation, there are fewer synthesis strategies for the introduction of a trifluoromethyl group because three of the four substituents of the carbon atom are pre-determined and only the other substituent can be varied which limits the potential synthetic approaches (Liang *et al.*, 2013).

For nucleophilic trifluoromethylation, there are three major reagents represented in Figure 10. The Ruppert-Prakash reagent can add a CF_3 to carbonyls and imines (Nikolay E. Shevchenko, 2011) and also add this group to several other motifs in the presence of a transition metal catalysis (Furukawa *et al.*, 2011). The Colby Trifluoromethylation Reagent is an air-stable solid that adds CF_3 to ketones and thiols under mildly basic conditions (Sigma-Aldrich, 2013). Although these two examples of reagents are efficient in this type of reaction, nucleophilic trifluoromethylation with trifluoromethyl anion is a challenging process due to the competing fluoride elimination process pathway.

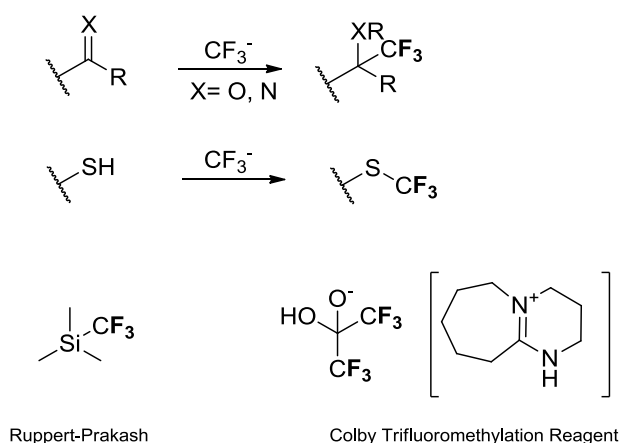


Figure 10 - Some reagents used in nucleophilic trifluoromethylation reactions.

Introduction of a trifluoromethyl group in a molecule is also possible through a radical process. Some reagents are represented in Figure 11.

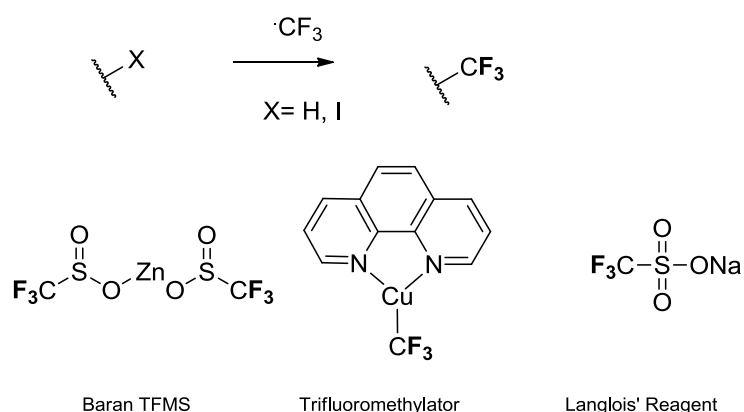


Figure 11 - Some reagents used in radical trifluoromethylation reactions.

The zinc trifluoromethanesulphinate, TFMS reagent, can be used to convert hydrogen of aryl and heteroaryl compounds into $-\text{CF}_3$ in mild conditions (Fujiwara *et al.*, 2012). Trifluoromethylator is another reagent capable of introducing a $-\text{CF}_3$ group into aryl systems (Morimoto *et al.*, 2011). Langlois reagent, or sodium trifluoromethanesulfinate, by other hand, is also capable of introducing a trifluoromethyl group into inactivated olefins (Deb *et al.*, 2013) being this the most relevant and important characteristic in relation to the other reagents.

Electrophilic trifluoromethylation is also possible and a preferable method in laboratory because these reagents tend to be crystalline and easily weighable and therefore easily to handle. Some reagents are shown in Figure 12.

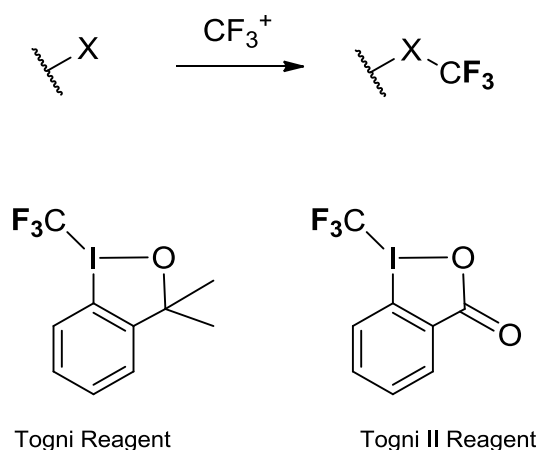


Figure 12 - Some reagents used in electrophilic trifluoromethylation reactions.

In particular, Togni reagents are easy to handle. These reagent can interact with β -ketoesters under phase-transfer catalysis conditions resulting in α -trifluoromethylated

derivatives (Eisenberger *et al.*, 2006). Besides that, Togni reagents can perform trifluoromethylations in α -nitroesters, which yield precursors to α -trifluoromethyl- α -amino acids (Kieltsch *et al.*, 2007). These reactions are very important because they occur in many functional groups and do not show significant solvent dependence, allowing them to be used in a later stage in the syntheses of complex molecules.

1.2.2.4 The use of fluorinated synthons

Alternatively to the use of the reagents referred in the sections above, the use of fluorinated synthons or fluorinated building-blocks can also be a strategy to introduce fluorine atoms in a molecule. In this strategy, the incorporation of low molecular weight polyfunctional fluorine-containing synthons becomes a key part of the synthetic scheme. Due to the synthetic versatility related with the synthon approach, this area of research has been very useful in compound development (Soloshonok, 2005).

Chapter II

Scientific objectives

2. Scientific objectives

2.1 General objectives

The introduction of a fluorine atom in key positions of a biological active molecule have been shown to improve absorption, lipophilicity, brain penetration and metabolism as well as to decrease toxicity in some BACE1 inhibitors.

Therefore, the aim of the present work is the design and synthesis of new potential BACE1 (β -secretase) inhibitors containing fluorine atoms.

2.2 Specific objectives

The main objective of this work consists in the structural modification of asiatic acid, a pentacyclic triterpenoid that can be isolated from *Centella Asiatica*, in order to obtain new semisynthetic derivatives that could act as new potential inhibitors of BACE1.

The preparation of the new asiatic acid derivatives should obey to the following structural considerations:

- The three hydroxyl groups present in the A-ring of asiatic acid should be acetylated;
- The C-28 carboxylic acid should be converted into amide;
- A fluorine atom should be inserted in the triterpenoid scaffold.

The structures of all new derivatives prepared should be elucidated using different mononuclear magnetic resonance techniques (NMR), such as ^1H NMR, ^{13}C NMR and distortionless enhancement by polarization transfer ($^{135}\text{DEPT}$).

Chapter III

Synthesis of new potential BACE1 inhibitors

3. Synthesis of new potential BACE1 inhibitors

3.1 Asiatic acid in Alzheimer's disease

The medical knowledge of medicinal plants have been accumulated over the years, with many active pharmacological compounds being identified for the treatment of various diseases (Chin *et al.*, 2006).

Nowadays, around 20% of the drugs in the market were derived from natural products (Newman, 2016). Triterpenoids represent an important class of natural compounds which are synthesized by the cyclization of squalene epoxide in different positions (Salvador, 2014). Asiatic acid is a natural pentacyclic triterpenoid extracted mainly from the medicinal herb *Centella Asiatica* (Zainol, 2008).

Centella Asiatica has been used since ancient times as a natural healing agent and a brain tonic (Jew *et al.*, 2000). In 1992, the extract was patented for the treatment of dementia and as a cognitive enhancer (European Patent Application, 1992). This extract had, besides asiatic acid, two other triterpenoids: asiaticoside and madecassid acid.

Asiatic acid is a well-studied compound with therapeutic potential in many different pathologies since its pharmacological activities include anti-hyperglycemic and anti-hyperlipidemic effects (Maulidiani *et al.*, 2016, Ramachandran *et al.*, 2013), anti-inflammatory (Lee *et al.*, 2016) and antioxidant activities (Tsao *et al.*, 2015), anticancer activity (Gonçalves, 2016, Li *et al.*, 2014), hepatoprotection (Yan *et al.*, 2014), and neuroprotection (Jiang *et al.*, 2016, Krishnamurthy *et al.*, 2009).

In 1990, De Souza *et al.* patented several derivatives of asiatic acid for the treatment of cognitive disorders, cerebral vascular diseases and diseases of the central nervous system. Since then, in order to further explore the potential neuroprotective effects of asiatic acid several new semisynthetic derivatives have been investigated.

New derivatives reported by Mook-Jung *et al.*, showed a strong prevention against A β toxicity, blocking A β -induced neuronal cell death (Mook-Jung *et al.*, 1999). Later, in structure-activity relationship studies the asiatic acid showed a protective activity of 97% against *in vitro* A β induced neurotoxicity (Jew *et al.*, 2000). In 2010, its activity was related with the modulation of multiple targets associated with APP processing. Namely, the protein levels of BACE1 were down regulated in a dose-dependent way in response to the

treatment of primary rat cortical neurons with Asiatic acid (Patil *et al.*, 2010). Taking in consideration the above mentioned studies, associated with the good results obtained in studies of docking of BACE1 with asiatic acid (Anthwal, 2015), this molecule is a potential good lead for the development of new BACE1 inhibitors.

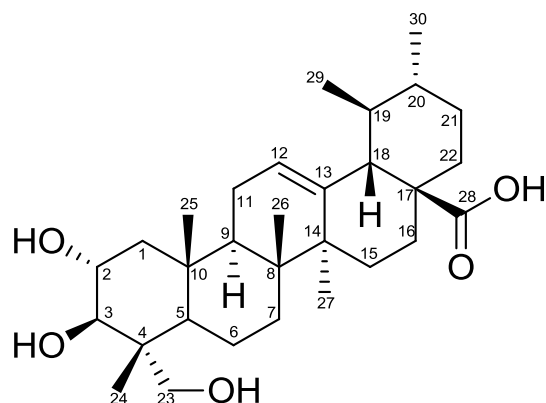


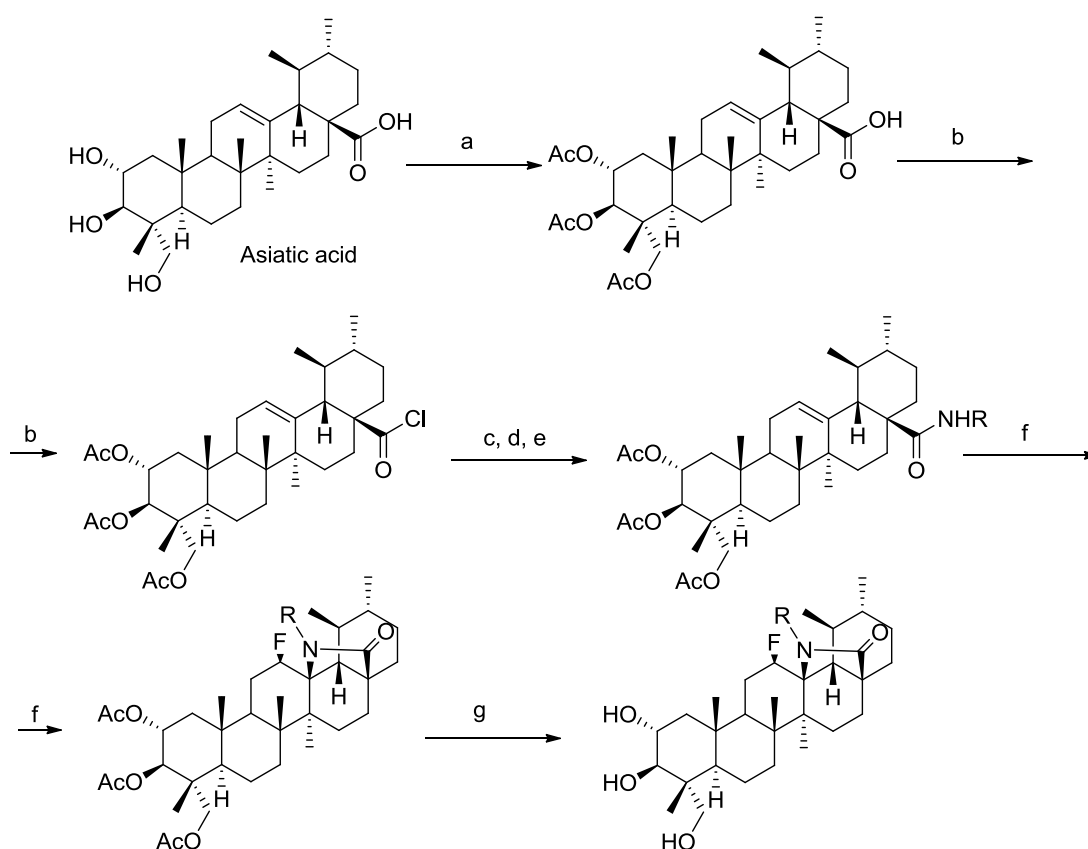
Figure 13 - Chemical structure of asiatic acid with the carbons numbered.

In addition, asiatic acid ($2\alpha,3\beta,23$ -trihydroxyurs-12-ene-28-oic acid), depicted in Figure 13, has three different types of functional groups: three hydroxyl groups at C2, C3 and C23, an olefin group at C12 and C13 and a carboxylic acid group at C28. The presence of this functional groups allows to perform various structural modifications which make this molecule an interesting candidate to designing new derivatives as BACE1 inhibitors.

3.2 Preparation and structural elucidation of Asiatic Acid derivatives

The structural modifications of asiatic acid present in this work were performed in order to obtain a series of fluorinated derivatives. The introduction of nitrogen – containing groups, in particular the amide bonds, was also explored due their versatile properties that can improve the pharmacokinetic profile of compounds (Mendes *et al.*, 2016).

The synthetic sequence designed to obtain the new derivatives started with an acylation, followed by the formation of the amide derivatives, the introduction of fluorine into the C ring to obtain 12 β -fluoro-13,28 β -lactones and a final step of hydrolysis. The general procedure is shown in the Scheme 2.

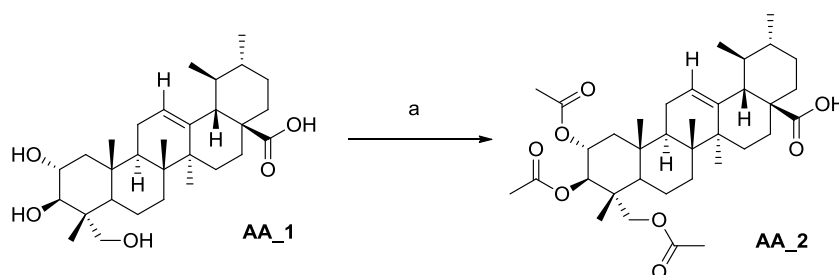


Scheme 2 - General synthetic scheme. Reagents and conditions: a) Acetic anhydride, DMAP, dry THF, room temperature; b) SOCl_2 , dry benzene, reflux temperature; c, d and e) amine, Et_3N , dry dichloromethane, room temperature; f) Selectfluor[®], dry dioxane, dry nitromethane, 80°C; g) 5% KOH in methanol, 30°C.

3.2.1 Preparation and structural elucidation of compound AA_2

The synthetic route was initiated with the protection of the three hydroxyl groups of asiatic acid (**AA_1**) affording the triacetate derivative **AA_2**. This step was performed to allow the selective preparation of amides from carboxylic acid.

The protection of hydroxyl groups was performed using acetic anhydride (Ac_2O), in the presence of a catalytic amount of 4-dimethylpyridine (DMAP), usually 10% of the substrate mass used in the reaction (Goncalves *et al.*, 2016) – Scheme 3.



Scheme 3 - Preparation of compound **AA_2**. Reagents and conditions: a) Acetic anhydride, DMAP, dry THF, room temperature.

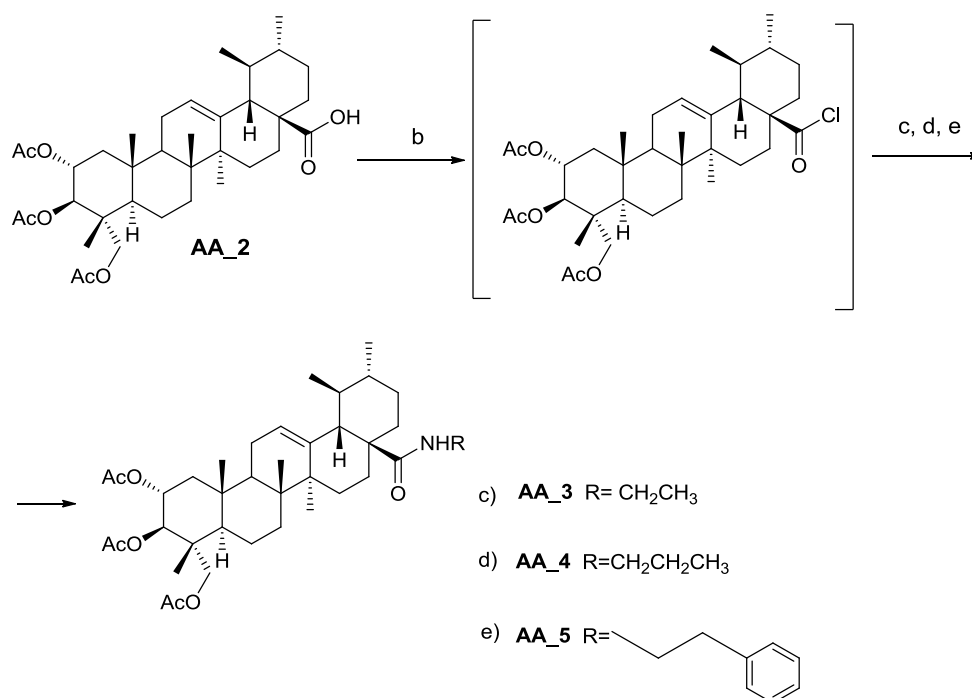
The structure of triacetylated asiatic acid **AA_2** was confirmed through the analysis of ¹H NMR, ¹³C NMR and ¹³⁵DEPT spectra and by comparison with data from literature (Gonçalves, 2016, Jew *et al.*, 2000).

3.2.2 Preparation and structural elucidation of the amide derivatives

The knowledge that carboxyl groups can be activated as acyl halides, acyl azides, ester, between others, is not new (Carpino, 1986).

There are some different ways of coupling carboxyl derivatives with an amine (Montalbetti, 2005) to afford amides. This work focused in the formation of an acyl chloride intermediate formed from carboxylic acid followed by the treatment with different amines.

Compound **AA_2** was treated with thionyl chloride in dry benzene, at 80°C, to afford the acyl chloride intermediate which, without previous purification, was then treated with different amines to generate the amide derivatives **AA_3**, **AA_4** and **AA_5** in good yields (Scheme 4).



Scheme 4 - Preparation of compounds **AA_3**, **AA_4** and **AA_5**. Reagents and conditions: b) SOCl₂, dry benzene, reflux temperature; c) ethylamine, Et₃N, dry dichloromethane, room temperature, d) propylamine, Et₃N, dry dichloromethane, room temperature; e) ethylbenzylamine, Et₃N, dry dichloromethane, room temperature.

3.2.2.1 Compound AA_3

Compound **AA_3**, seen in Figure 14, was prepared from acyl halide intermediate in dry dichloromethane in the presence of triethylamine by reaction with ethylamine.

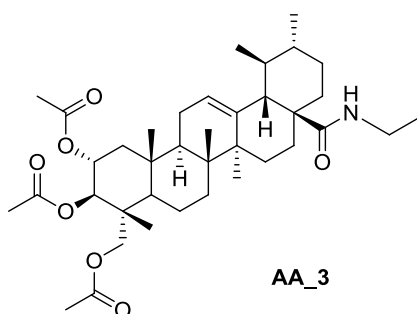


Figure 14 - Chemical structure of compound **AA_3**.

The structure of this compound was elucidated through NMR techniques.

In the ^1H NMR spectrum of compound **AA_3**, the formation of amide was confirmed by the presence of a triplet at 5.78 ppm ($J = 5.04$ Hz) corresponding to the proton attached to nitrogen atom. The signals for the methylene protons of amide were observed as two multiplets at 3.26 – 3.33 ppm and 3.06 – 3.15 ppm.

The signal for olefin proton at position 12 was observed as a triplet at 5.30 ppm with a coupling constant of 3.33 Hz

The signal of proton H-2 appeared as a multiplet between the chemical shifts of 5.12 and 5.19 ppm while the H-3 signal was observed as a doublet at 5.07 ppm with a coupling constant of 10.31 Hz. The signals of the hydrogens attached to C23 appeared as doublets at 3.84 ($J = 11.78$ Hz) and 3.57 ($J = 11.85$ Hz) ppm.

The hydrogens of the acetate groups were observed as three singlets at 2.08 ppm, 2.02 ppm and 1.98 ppm.

In the region between 0.79 and 1.10 ppm were observed seven signals corresponding to methyl protons.

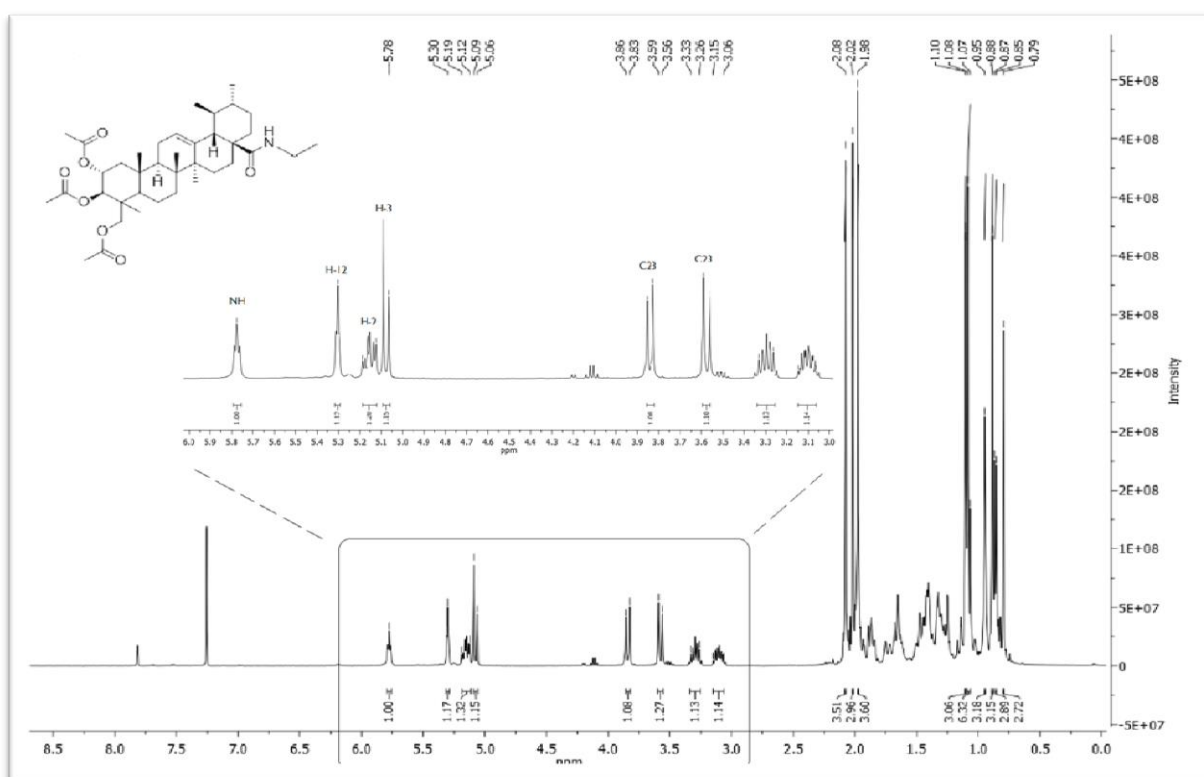


Figure 15 - ^1H NMR spectrum of compound **AA_3**.

The ^{13}C NMR spectrum confirmed the presence of 38 carbons.

The signal for carbonyl carbon of amide was observed at 177.71 ppm. At 170.35, ppm, 170.46 ppm and 170.79 ppm were observed the peaks corresponding to the carbonyl carbons of the acetate groups.

The peak corresponding to C13 appeared at 140.11 ppm and C12 at 124.93 ppm.

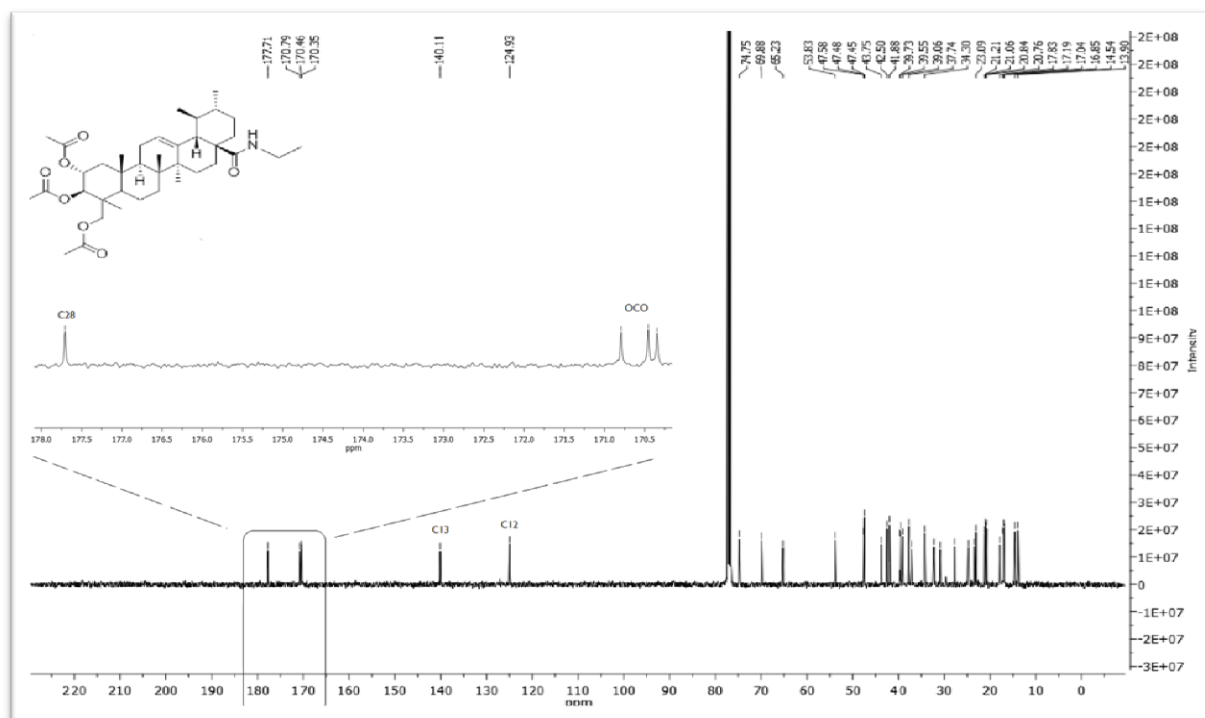


Figure 16 - ^{13}C NMR spectrum of compound AA_3.

$^{135}\text{DEPT}$ spectrum revealed that compound **AA_3** has ten CH_2 carbons and eighteen CH or CH_3 carbons remaining ten quaternary carbons that are not visible using technique.

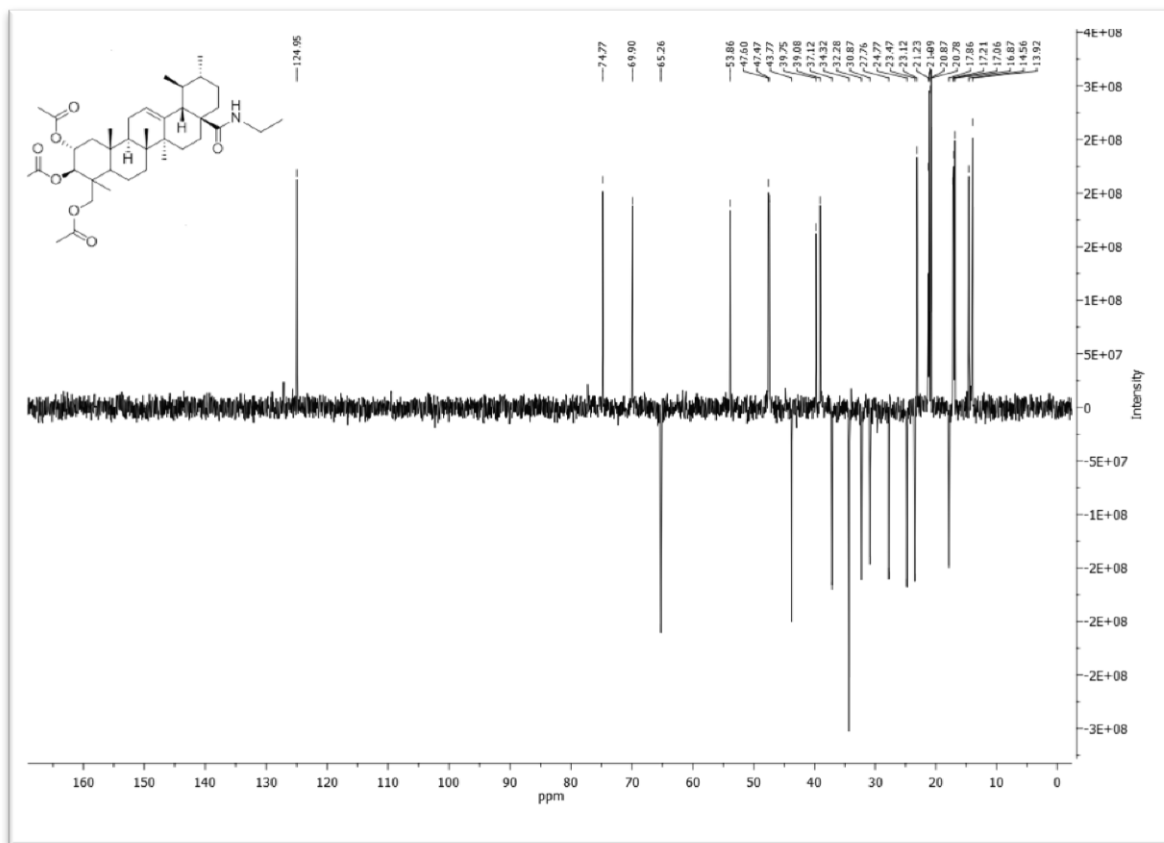


Figure 17 - $^{135}\text{DEPT}$ spectrum of compound AA_3.

3.2.2.2 Compound AA_4

Compound **AA_4**, seen in Figure 18, was prepared from acyl halide intermediate in dry dichloromethane in the presence of triethylamine by reaction with propylamine.

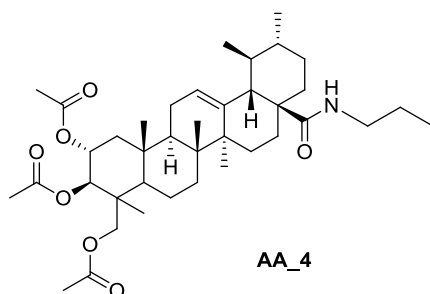


Figure 18 - Chemical structure of compound AA_4.

The introduction of the amide function in compound **AA_4** was confirmed in the ^1H NMR spectrum by a triplet at 5.85 ppm ($J = 5.26$ Hz) for the proton of the amide function. The protons of the methylene attached to nitrogen were observed as two multiplets which appeared between 2.92 – 3.00 ppm and 3.25 – 3.33 ppm.

The vinylic hydrogen signal appeared as a triplet at 5.30 ppm ($J = 3.41$ Hz).

The signal correspondent to H-2 was observed as a multiplet between 5.12 – 5.19 ppm, while the signal of H-3 appeared as a doublet at 5.08 ppm ($J = 10.20$ Hz). The signals for H-23 protons appeared as doublets at 3.84 ppm ($J = 12.42$ Hz) and 3.57 ppm ($J = 11.10$ Hz).

The presence of the acetate groups was confirmed through the singlets at 2.08, 2.02 and 1.98 ppm.

In the region between 0.79 and 1.10 ppm were observed the signals corresponding to methyl protons.

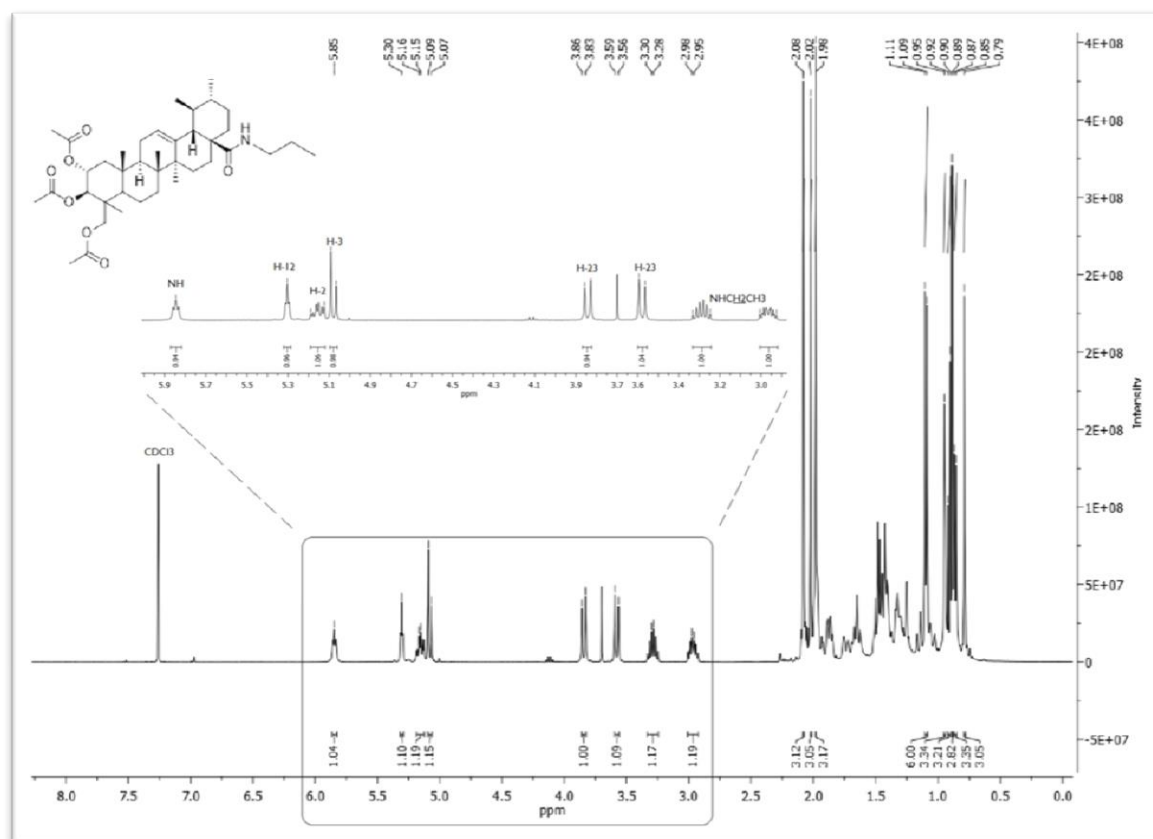


Figure 19 - ^1H NMR spectrum of compound **AA_4**.

The ^{13}C -NMR spectrum of compound **AA_4** confirmed the presence of 39 carbons.

At 177.78 ppm was observed the signal of C28 confirming the introduction of the amide function in this compound. At 170.36, ppm, 170.46 ppm and 170.81 ppm appeared the signals corresponding to the carbonyl carbons of the acetate groups.

The signal corresponding to C13 appeared at 140.15 ppm and the signal of C12 was observed at 124.92 ppm.

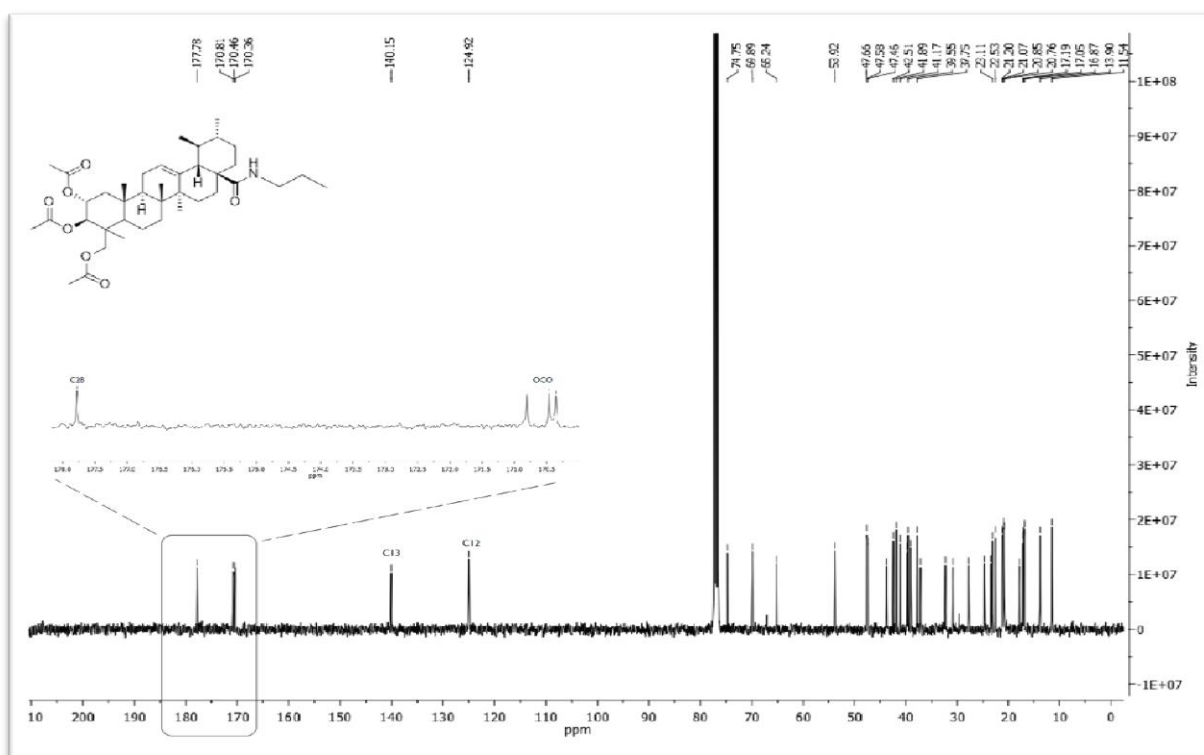


Figure 20 - ^{13}C NMR spectrum of compound **AA_4**.

$^{135}\text{DEPT}$ spectrum revealed that this compound has eleven CH_2 carbons and eighteen CH or CH_3 carbons remaining ten quaternary carbons that are not visible using technique.

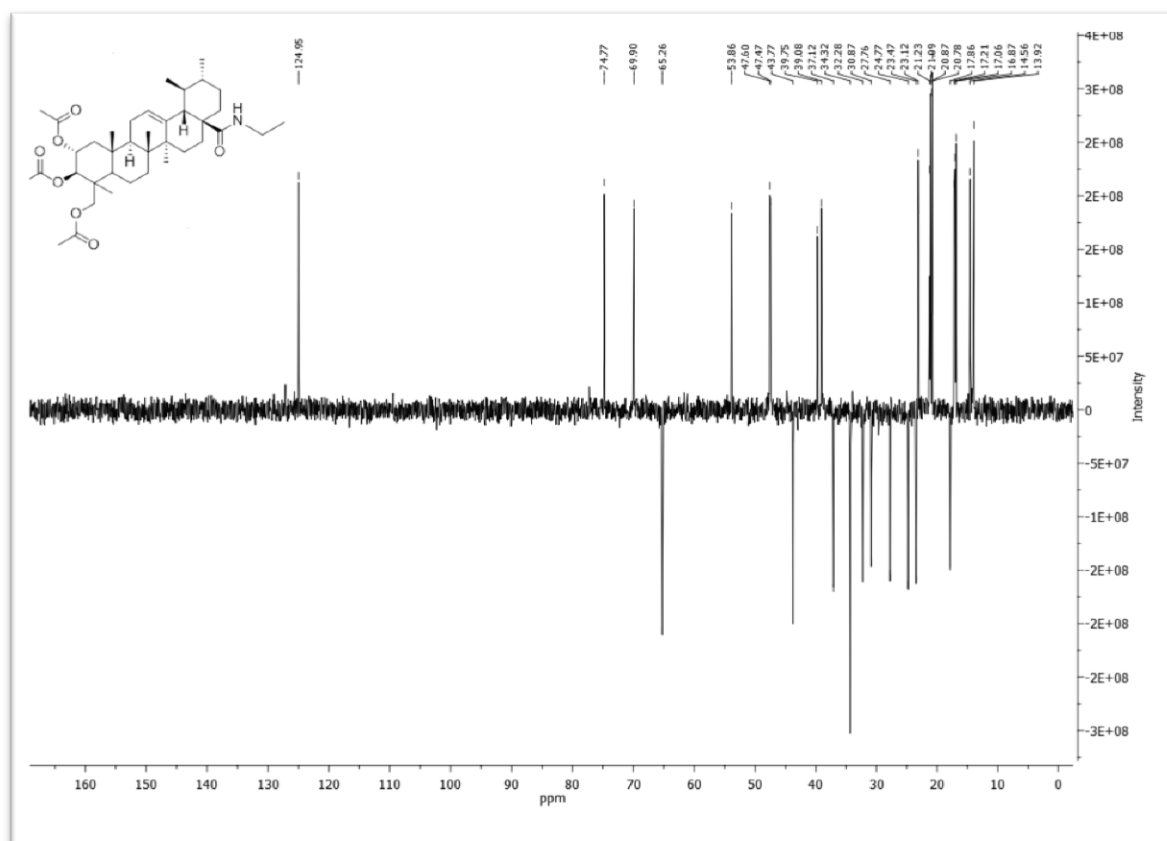


Figure 21 - 135 DEPT spectrum of compound AA_4.

3.2.2.3 Compound AA_5

Compound **AA_5**, seen in Figure 22, was prepared from acyl halide intermediate in dry dichloromethane in the presence of triethylamine by reaction with ethylbenzylamine.

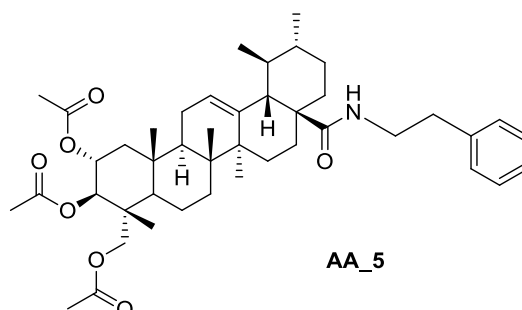


Figure 22 - Chemical structure of compound AA_5.

The presence in the $^1\text{H-NMR}$ spectrum of a multiplet between 5.78 – 5.81 ppm corresponding to the hydrogen attached to nitrogen atom and the characteristic peaks of the aromatic ring placed at 7 ppm confirmed the formation of ethylbenzylamide in this compound.

The signal of vicinal hydrogen appeared as a triplet at 4.86 ppm ($J = 3.33$ Hz).

The signals for H-2 and H-3 were observed as a multiplet between 5.12 and 5.19 ppm and a doublet at 5.06 ppm ($J = 10.03$ Hz) respectively. Hydrogens attached to C23 appeared as doublets at 3.82 ppm ($J = 11.94$ Hz) and 3.56 ppm ($J = 11.69$ Hz).

The presence of the acetate groups was confirmed through the singlets at 2.06, 2.02 and 1.98 ppm. In the region between 0.79 and 1.05 ppm were observed the signals corresponding to methyl protons.

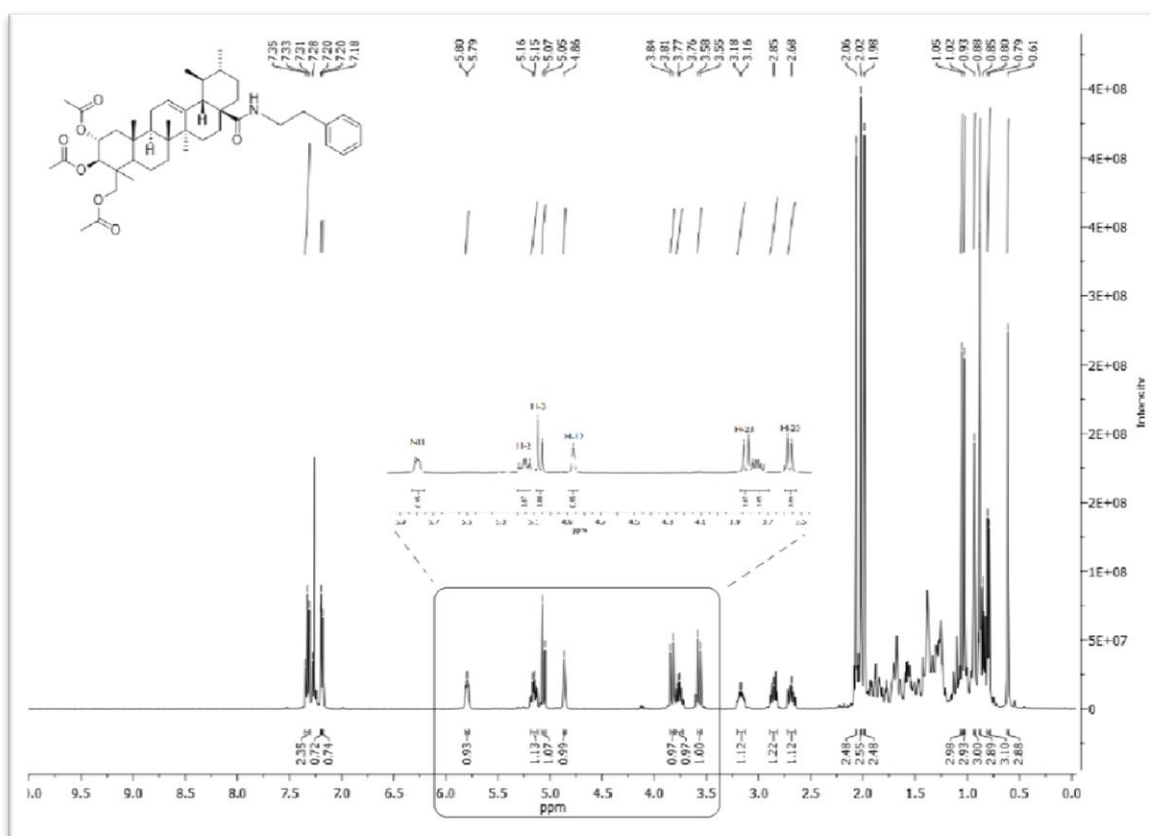


Figure 23 - ^1H NMR spectrum of compound AA_5.

In the ^{13}C -NMR spectrum of compound **AA_5** were observed 44 carbons.

At 177.92 ppm was possible to observe the signal of the carbonyl carbon C28. The signals for the benzylic carbons were observed at 126.64 ppm, 128.67 ppm and 128.75 ppm. This information is in good agreement with the introduction of an amide group in the molecule.

The signals corresponding to the carbons of the acetate groups were seen at 170.34, ppm, 170.49 ppm and 170.78 ppm.

The peak corresponding to C12 was found at 125.10 ppm.

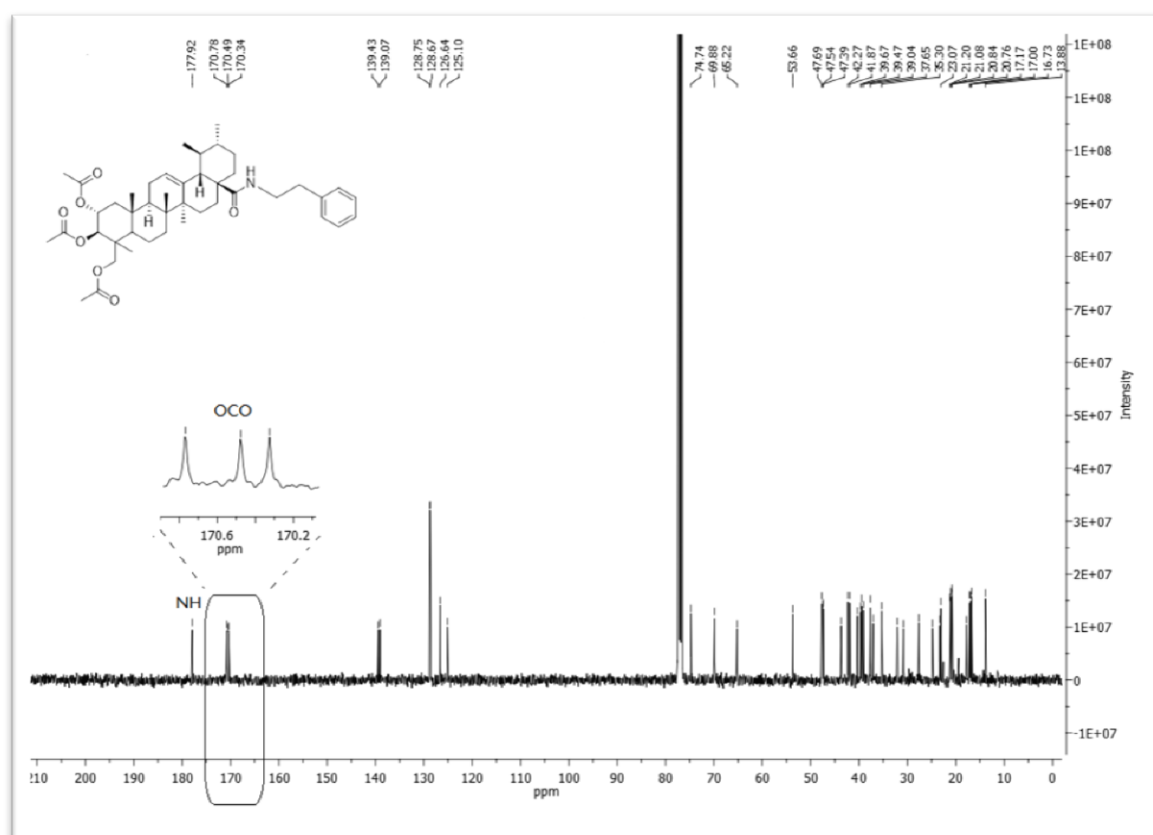


Figure 24 - ^{13}C NMR spectrum of compound **AA_5**.

$^{135}\text{DEPT}$ spectrum revealed that compound **AA_5** has eleven CH_2 carbons and twenty-two CH or CH_3 carbons, remaining eleven quaternary carbons that are not visible using this technique. This information corroborate the data obtained in the carbon spectrum.

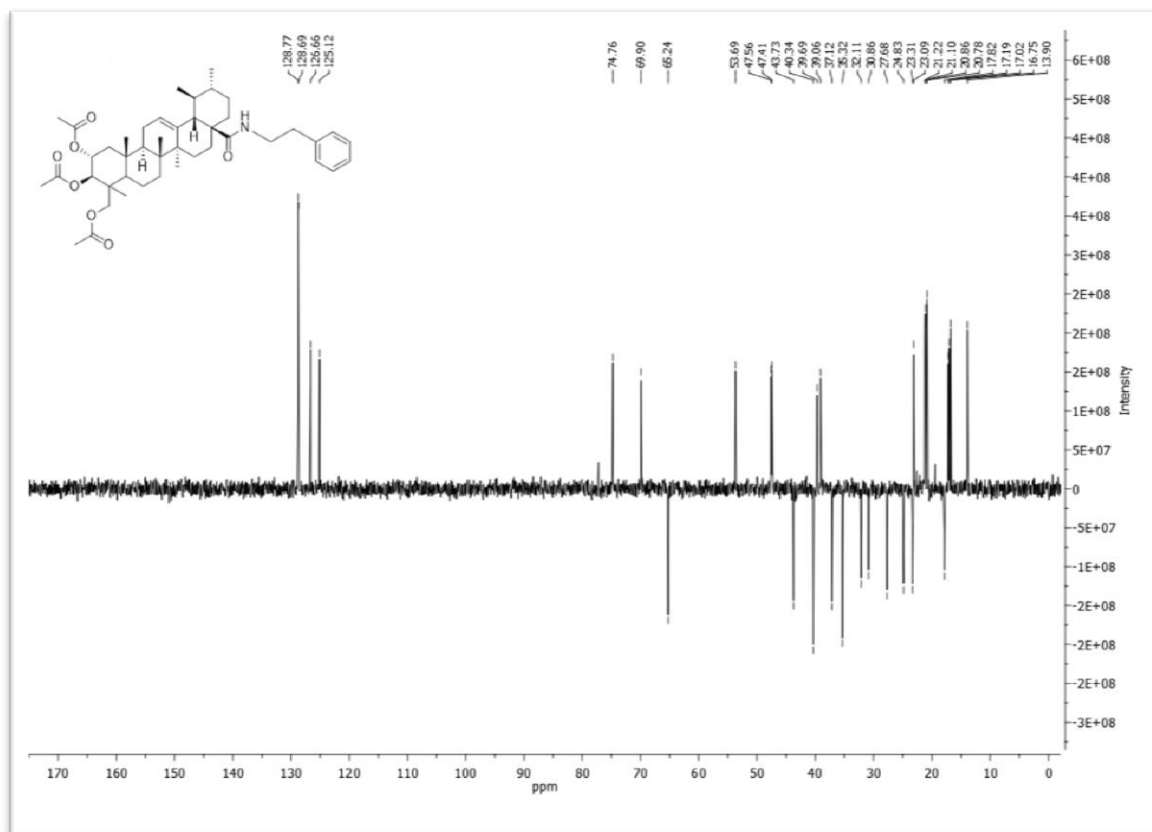


Figure 25 - $^{135}\text{DEPT}$ spectrum of compound AA_5.

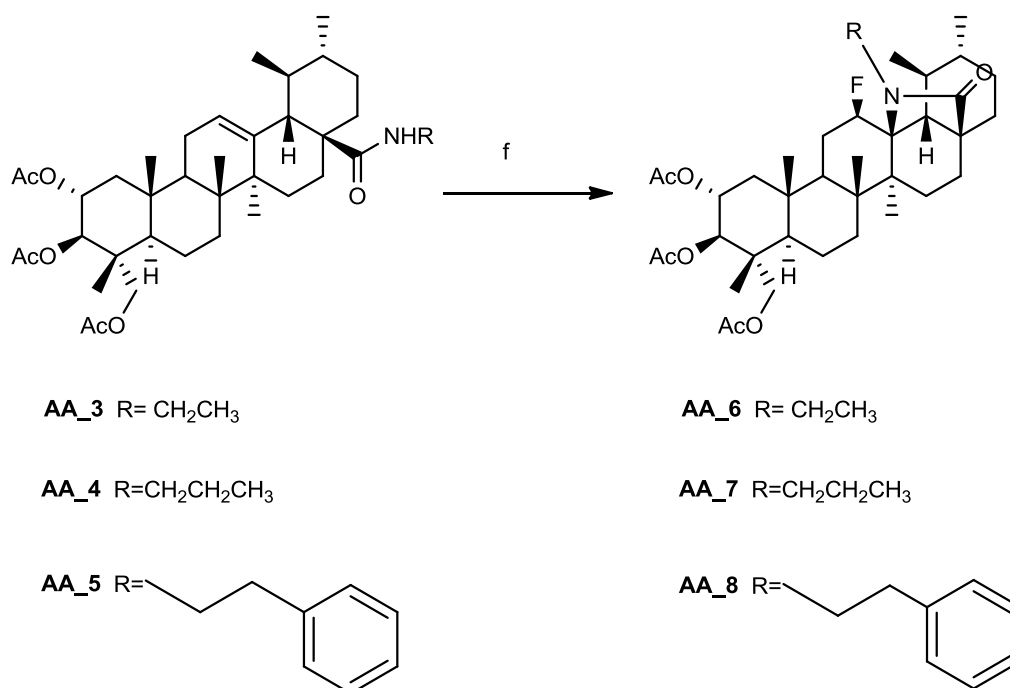
3.2.3 Preparation and structural elucidation of the fluorolactam derivatives

The fluorinated derivatives **AA_6**, **AA_7** and **AA_8** were prepared using the electrophilic fluorination reagent Selectfluor[®], in a mixture of dry dioxane and dry nitromethane, at 80°C.

Selectfluor[®] [(1-chloromethyl-4-fluoro-1,4-diazoniabicyclo [2.2.2] octane bis(tetrafluoroborate), or F-TEDA)] is an electrophilic fluorination reagent, user friendly, stable at high temperatures and easy to work with (Banks, 1997). Its versatility allows the fluorination of different functionalized compounds with high selectivity and high yields (Nyffeler *et al.*, 2004).

Some papers describe the reaction of Selectfluor[®] with alkenes, in the presence of a nucleophilic donor (Goncalves *et al.*, 2016). In this case, with the introduction of fluorine at C12, the nitrogen atom of amide carries out a nucleophilic attack on C13 promoting the

cyclization allowing the formation of the β isomer of 12-fluorolactams (Leal et al., 2012)
AA_6, **AA_7** and **AA_8** – Scheme 5.



Scheme 5 - Preparation of compounds **AA_6**, **AA_7** and **AA_8**. Reagents and conditions: f) Selectfluor[®], dry dioxane, dry nitromethane, 80°C.

3.2.3.1 Compound AA_6

The structure of compound **AA_6** - Figure 26 - was elucidated through NMR techniques.

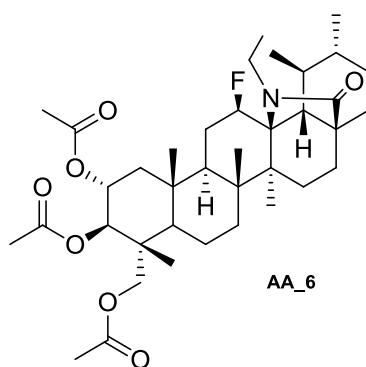


Figure 26 - Chemical structure of compound **AA_6**.

The formation of the 12 β -fluorolactam **AA_6** was confirmed by the presence in the ¹H NMR spectra of a double quartet at 4.86 ppm, with a coupling constant of 45.73 Hz, characteristic of the geminal proton for the fluorine (Leal *et al.*, 2012). The inductive effect triggered by fluorine causes a spin-spin splitting in the peak of geminal proton as we can see in this spectra (Pavia, 2013).

The signal for the hydrogen attached to C3 appeared as a doublet at 5.07 ppm ($J = 10.30$ Hz) while the signal for hydrogen attached to C2 was observed as a multiplet at 5.16 - 5.23 ppm.

The multiplet observed with the chemical shift between 3.28 ppm and 3.40 ppm was attributed to the hydrogens of the methylene group bonded to the nitrogen atom.

The signals corresponding to H-23 protons were observed as two doublets at 3.60 ppm ($J = 11.90$ Hz) and 3.80 ppm ($J = 11.90$ Hz).

The presence of the acetate groups was confirmed by the observation of three methyl peaks at 1.99 ppm, 2.02 ppm and 2.08 ppm.

In the region between 0.88 and 1.22 ppm were observed the signals corresponding to methyl protons.

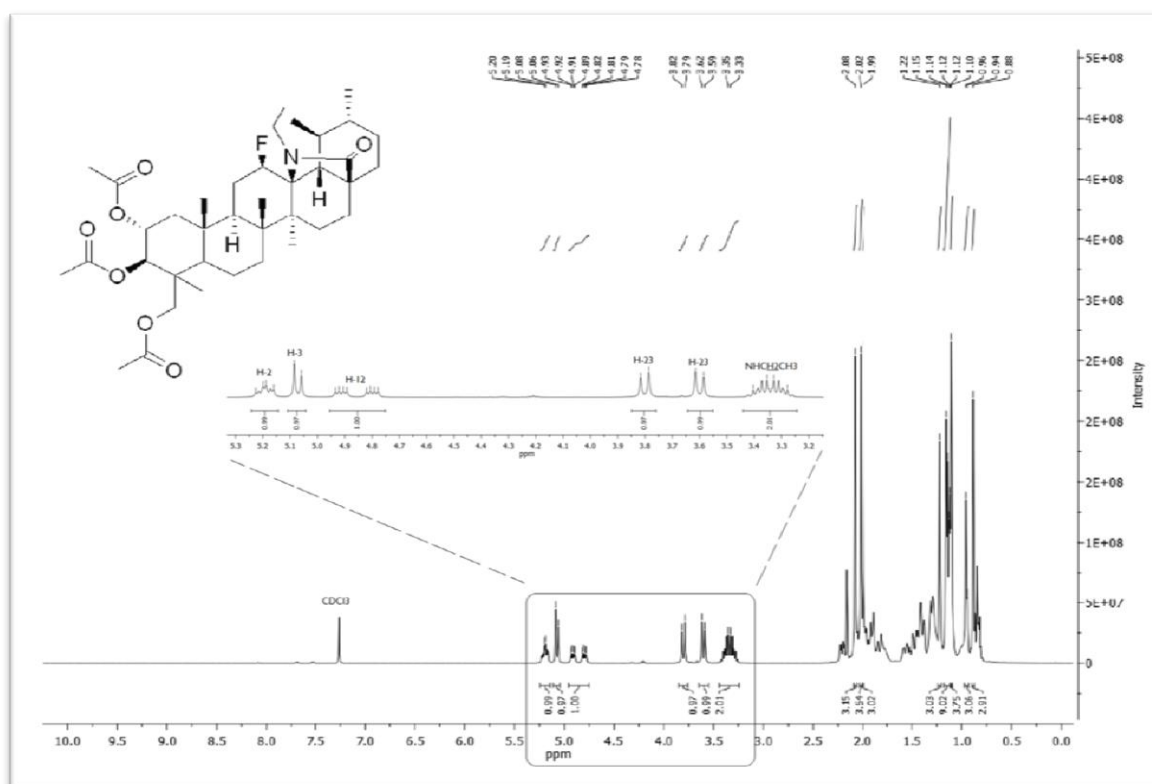


Figure 27 - ¹H NMR spectrum of compound **AA_6**.

In the ^{13}C -NMR spectrum of compound **AA_6** were observed 38 carbons.

The signal of C12 was observed as a doublet at 89.80 ppm with a coupling constant of 185.15 Hz, and the signal of C13 was found as a doublet at 90.49 ppm with a coupling constant of 14.22 Hz. This profile is characteristic of the β -isomer of the fluorolactam derivative.

At 164.77 ppm was possible to observe the signal of carbonyl carbon C28. The peaks corresponding to the carbonyl carbons of the acetate groups were observed at 170.27 and 170.79 ppm.

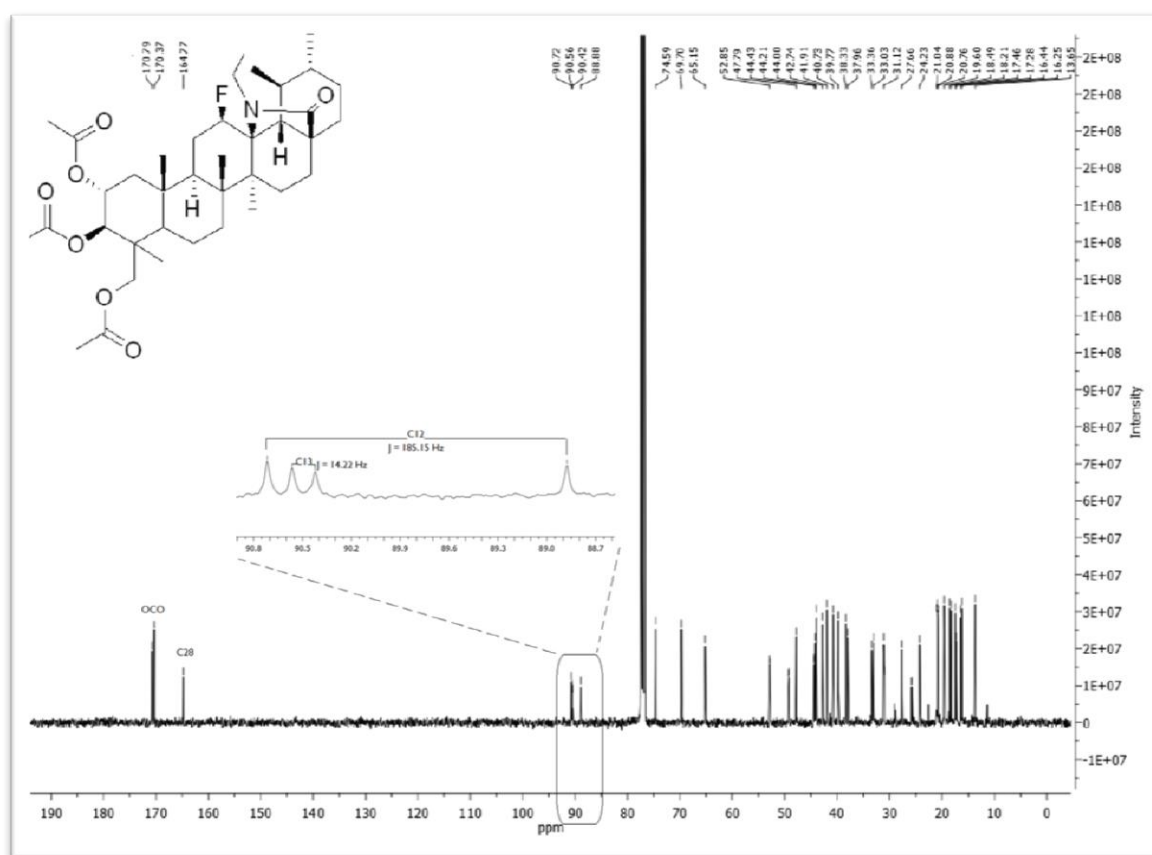


Figure 28 - ^{13}C NMR spectrum of compound **AA_6**.

$^{135}\text{DEPT}$ spectrum of compound **AA_6** - Figure 29 - revealed ten CH_2 carbons and eighteen CH or CH_3 carbons, remaining ten quaternary carbons. The tertiary carbon C12 appeared as a doublet at 89.80 ppm, while the quaternary C13 was not observed in this technique.

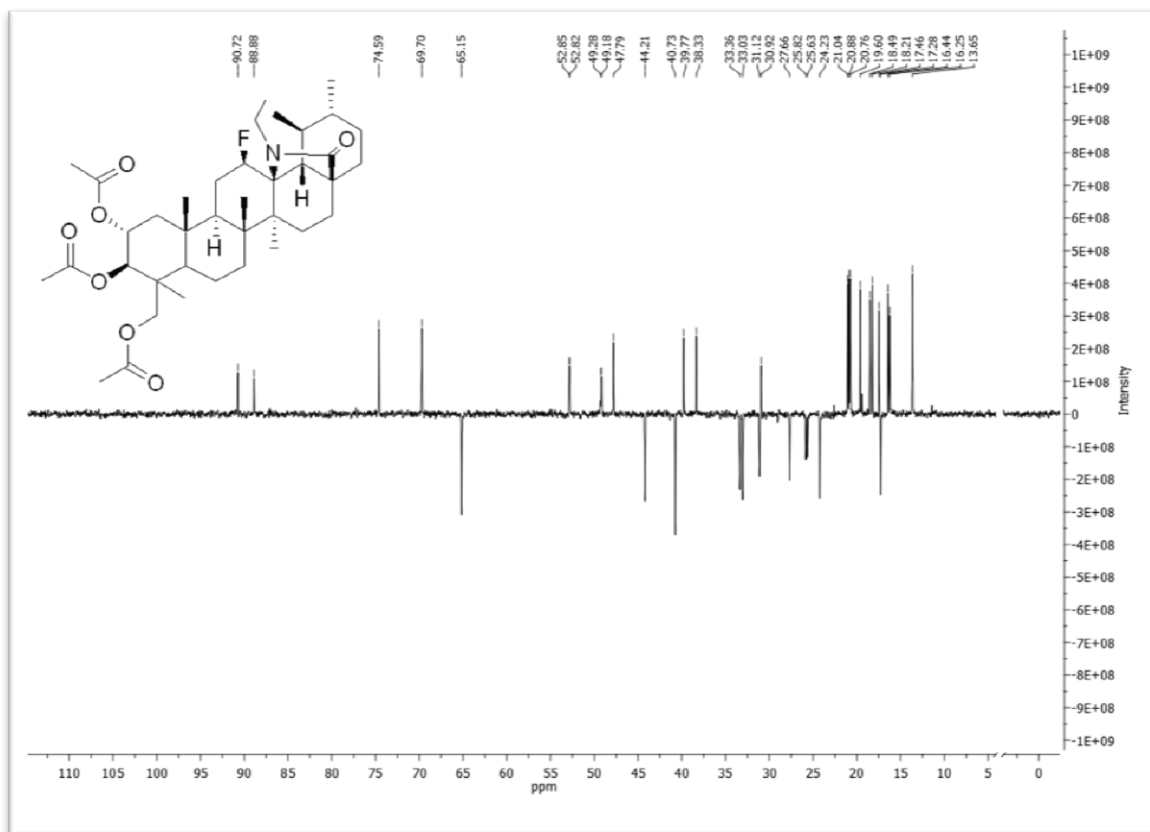


Figure 29 - $^{135}\text{DEPT}$ spectrum of compound AA_6.

3.2.3.2 Compound AA_7

The structure of compound **AA_7** - Figure 30 - was elucidated through NMR.

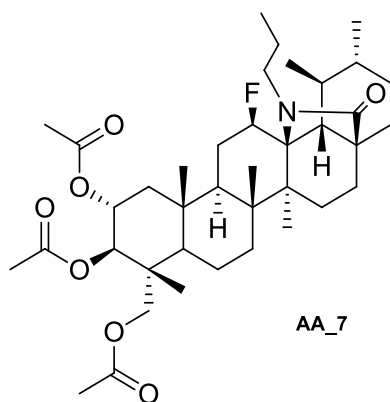


Figure 30 - Chemical structure of compound AA_7.

The ^1H NMR spectrum of compound **AA_7** is very similar to the spectrum of compound **AA_6** with the signal for the H-12, germinal to fluorine atom, appearing as a double quartet at 4.86 ppm, with a coupling constant of 45.52 Hz.

At 5.07 ppm was observed a doublet signal corresponding to the proton bounded to C3 ($J = 10.38$ Hz). The signal for the proton bounded to C2 was found as a multiplet at 5.16–5.23 ppm.

The multiplet signals corresponding to the hydrogens of the methylene group bonded to amide were observed at 3.18 – 3.25 ppm and 3.28 – 3.35 ppm.

The two protons bounded to C23 appeared as doublets at 3,61 ppm ($J = 11,70$ Hz) and 3,81 ppm ($J = 11,98$ Hz).

The hydrogens for the methyl peaks of the three acetate groups were observed as distinctive singlets at 1,99 ppm, 2,02 ppm and 2,08 ppm.

In the region between 0.89 and 1.22 ppm were observed the signals corresponding to methyl protons.

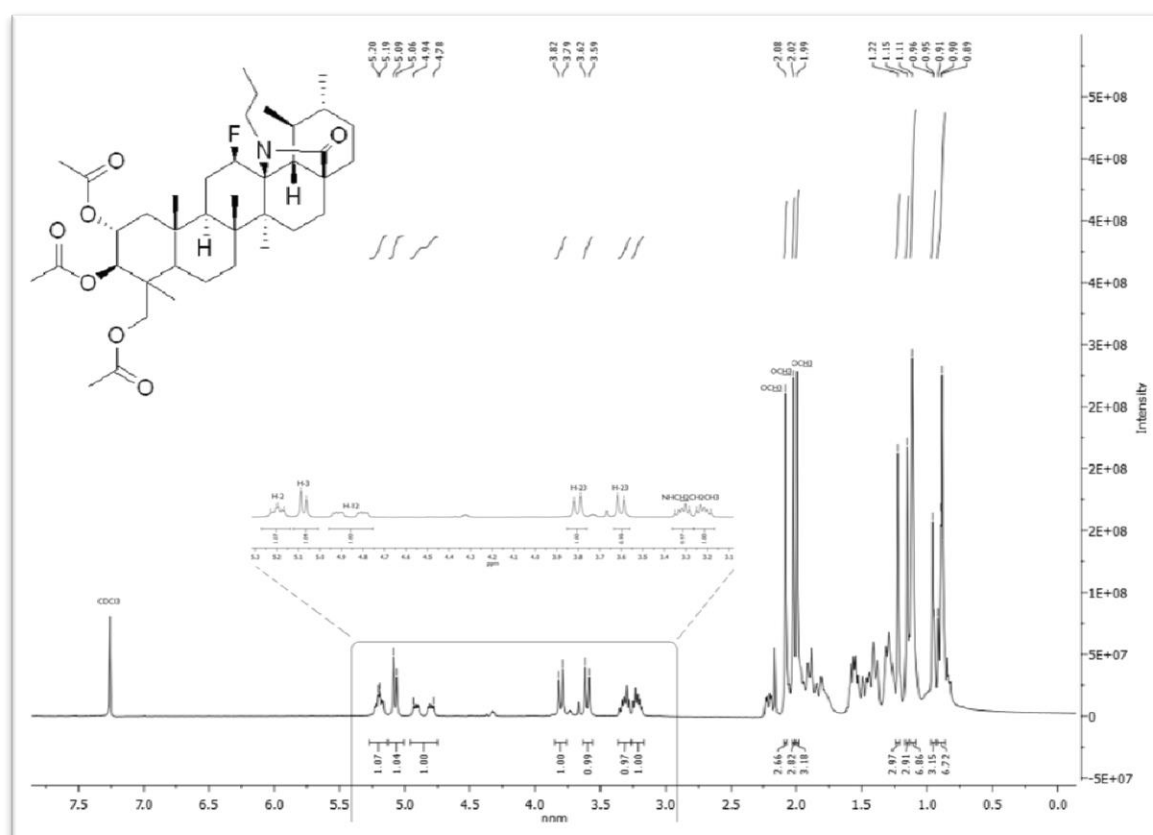


Figure 31 - ^1H NMR spectrum of compound **AA_7**.

In the ^{13}C -NMR spectrum of compound **AA_7** were observed 39 carbons.

The signal of C12 was observed as a doublet at 89.78 ppm with a coupling constant of 185.41 Hz, while the signal of C13 was found as a doublet at 90.38 ppm with a coupling constant of 13.90 Hz.

The ^{13}C NMR signal for the carbonyl carbon of lactam appeared 164.75 ppm. At 170.35 ppm were observed two peaks corresponding to the carbonyl carbons of the acetate groups being the third found at 170.77 ppm.

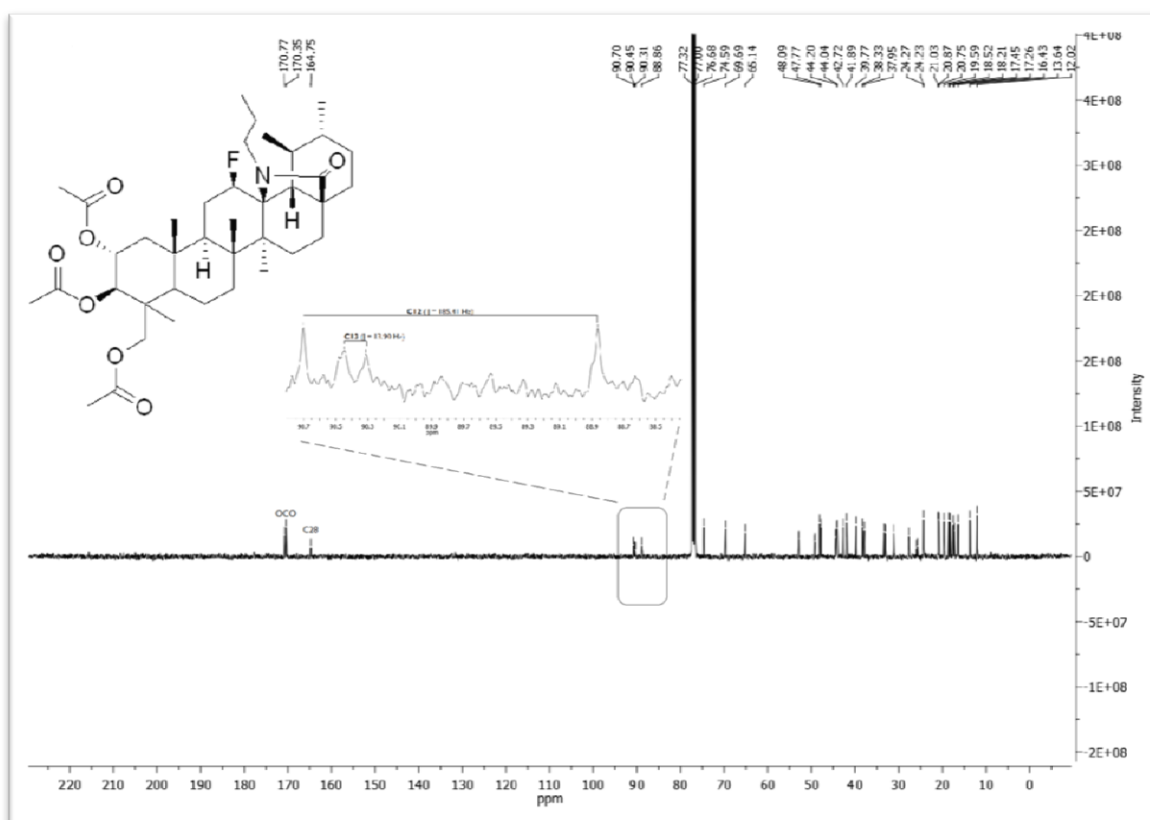


Figure 32 - ^{13}C spectrum of compound **AA_7**.

$^{135}\text{DEPT}$ spectrum for this compound, revealed eleven CH_2 carbons and eighteen CH or CH_3 carbons remaining ten quaternary carbons.

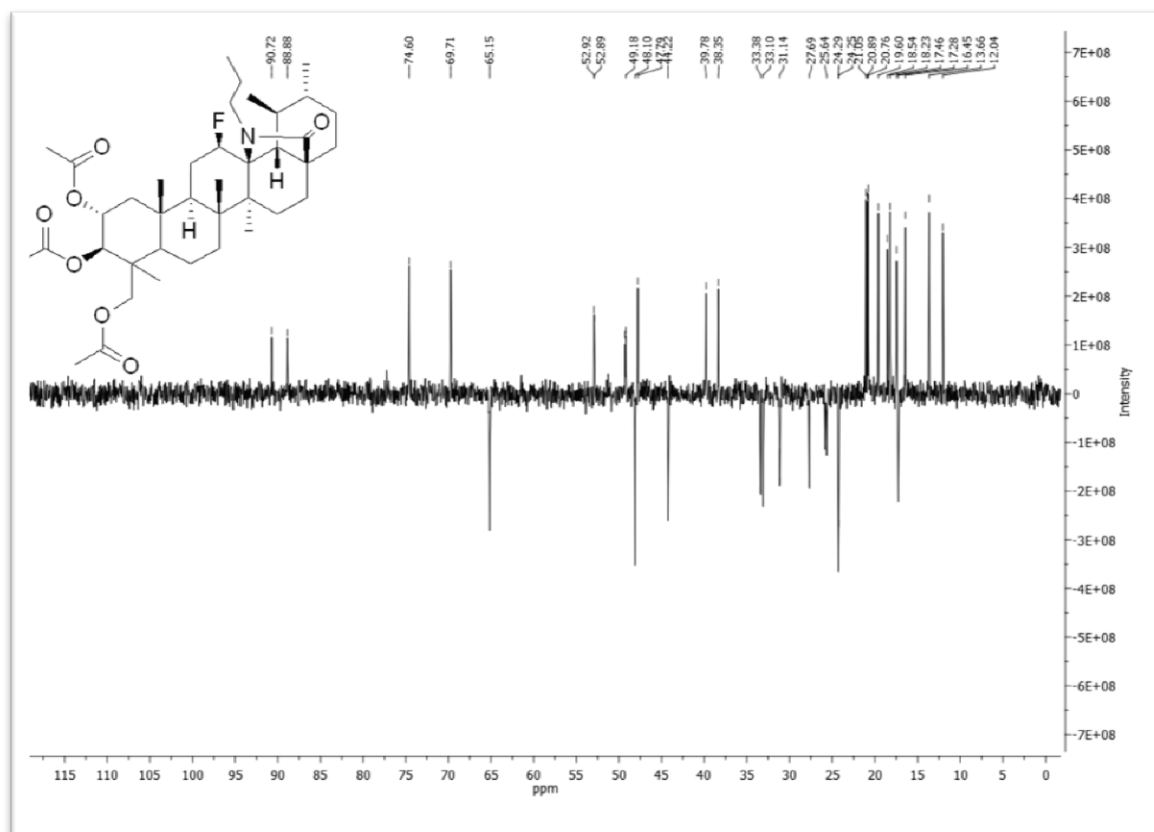


Figure 33 - $^{135}\text{DEPT}$ spectrum of compound AA_7.

3.2.3.3 Compound AA_8

The structure of compound **AA_8** - Figure 34 - was elucidated using NMR techniques.

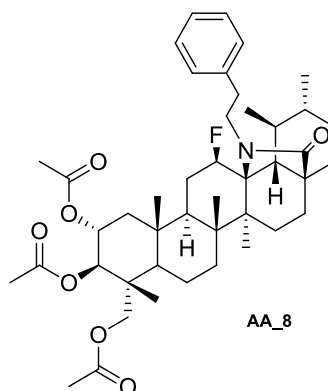


Figure 34 - Chemical structure of compound AA_8.

In the $^1\text{H-NMR}$ spectrum of compound **AA_8** the presence of the benzene side chain was confirmed by the signals corresponding to benzyl protons observed in 7.16 ppm – 7.29 ppm, characteristic of aromatic protons. The methylene protons of amide were observed as multiplets at 3.56 – 3.63 and 2.80 – 2.92 ppm.

The introduction of β -fluorine atom was confirmed through the double quartet present at 4.85 ppm ($J = 45.53$ Hz), belonging to H-12, the hydrogen geminal to fluorine.

The signal for the proton H-2 was observed as a multiplet between 5.16 ppm and 5.22 ppm and the signal for proton H-3 was found at 5.07 ppm as a doublet with a coupling constant of 10.41 Hz.

The doublet at 3.80 ppm ($J = 11.77$ Hz) and the multiplet at 3.46 – 3.53 ppm were attributed to the hydrogens attached to C23.

The presence of the acetate groups was confirmed through the distinctive singlets at 2.08, 2.02 and 1.99 ppm.

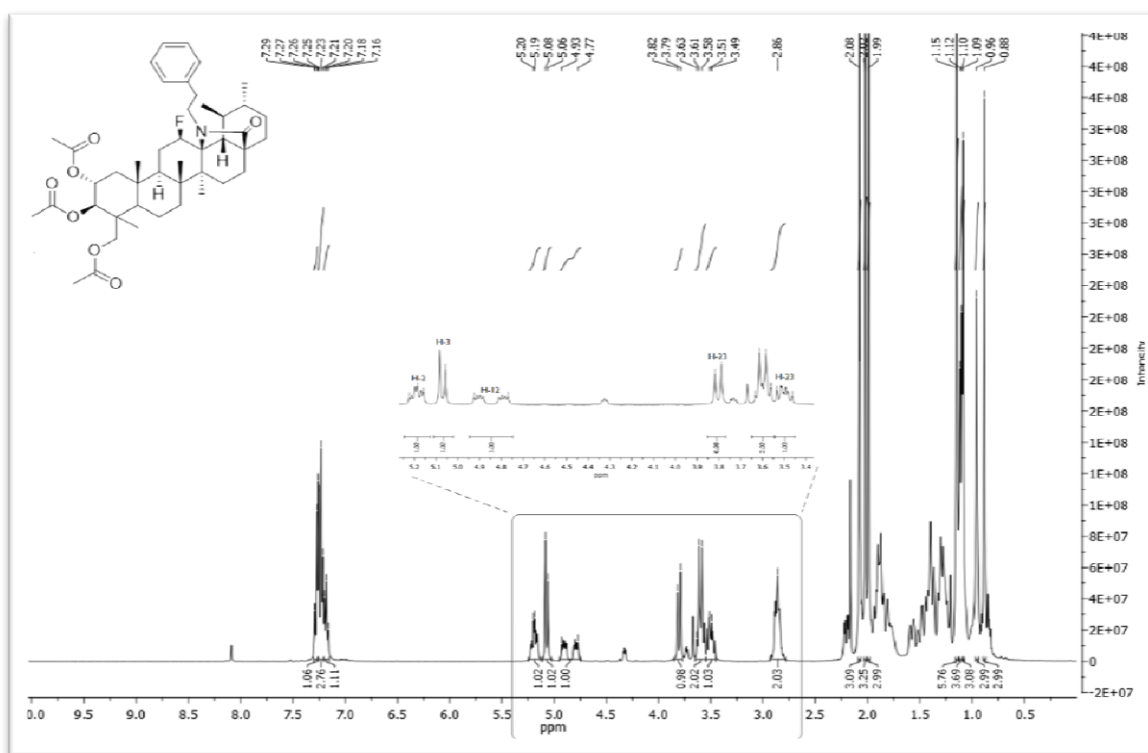


Figure 35 - ^1H NMR spectrum of **AA_8**.

In the ^{13}C -NMR spectrum of compound **AA_8** were observed the presence of 44 carbons.

The presence of lactam was verified through the signal at 165.34 ppm representing the carbonyl carbon of lactam. The signal of C12 was observed as a doublet at 89.68 ppm, with a coupling constant of 185.48 Hz. At 90.77 ppm appeared the signal for C13 as a doublet with a coupling constant of 14.00 Hz.

At 125.81 ppm, 128.19 ppm, 128.92 and 140.83 ppm were observed the signals corresponding to the benzylic carbons.

At 170.33, and 170.75 ppm were observed the peaks corresponding to the carbonyl carbons of the acetate groups.

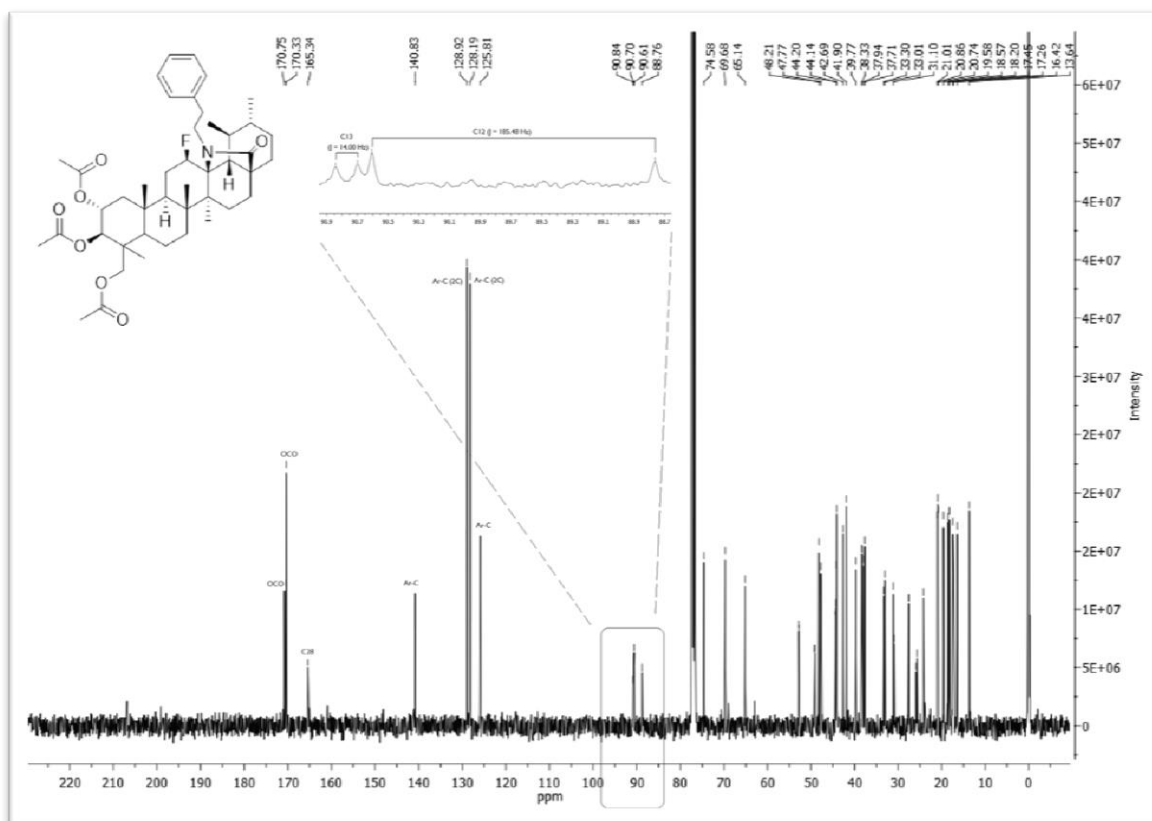


Figure 36 - ^{13}C NMR spectrum of compound **AA_8**.

$^{135}\text{DEPT}$ spectrum of compound **AA_8** revealed eleven CH_2 carbons and twenty-two CH or CH_3 carbons. This information was according to the expected for this compound.

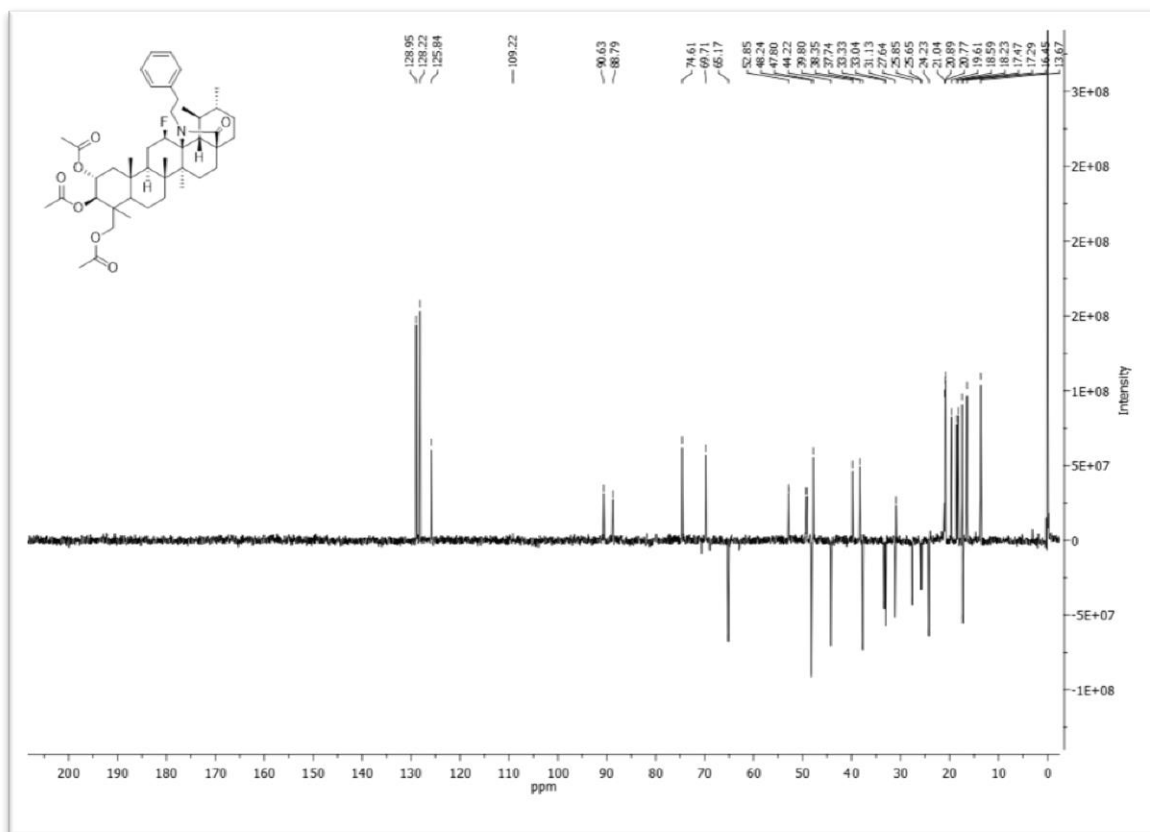
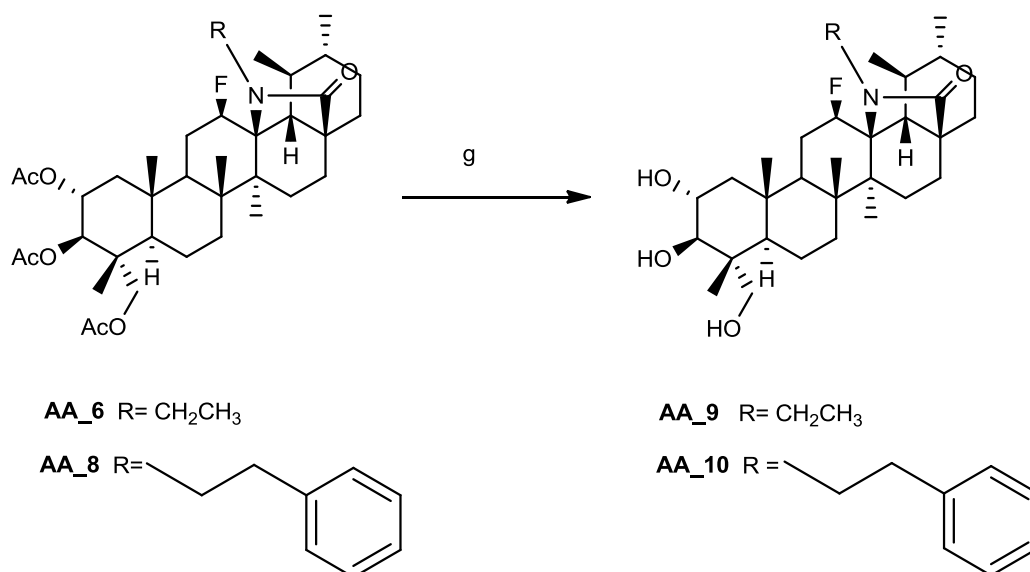


Figure 37 - 135 DEPT spectrum of compound AA_8.

3.2.4 Preparation and structural elucidation of the hydrolysed derivatives

The final step consisted in the deprotection of the hydroxyl groups, previously protected as acetate groups.

In this step, the deacetylation of compounds **AA_6** and **AA_8** was performed in a stirred solution of 5% potassium hydroxide (KOH) in methanol to give compounds **AA_9** and **AA_10** Scheme 6.



Scheme 6 - Preparation of compounds **AA_9** and **AA_10**. Reagents and conditions: g) 5% KOH in methanol, 30°C.

3.2.4.1 Compound AA_9

The structure of compound **AA_9** - Figure 38 - was elucidated using NMR techniques.

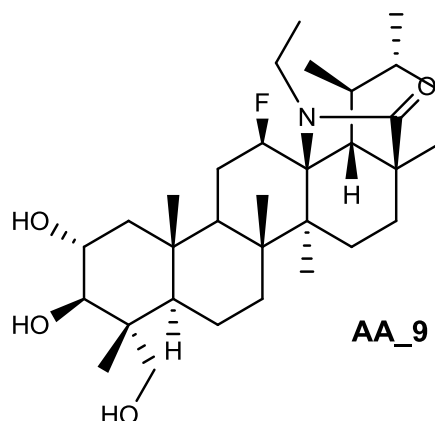


Figure 38 - Chemical structure of compound **AA_9**.

Through NMR analysis it was possible to conclude that the ¹H spectrum of this compound was similar to ¹H spectrum of **AA_6** with the disappearance of the signals corresponding to the methyl protons of acetate groups, the characteristic signals around 2 ppm and the appearance of the broad singlet corresponding to the protons of free hydroxyl groups. This peak presents exchange broadening due to intermolecular proton exchange (Charisiadis *et al.*, 2014).

The signal for the proton H-12 was seen as a double triplet at 4.87 ppm, with a coupling constant of 45.21 ppm. It was also possible to observe a multiplet between 3.27 and 3.44 ppm corresponding to the methylene protons attached to nitrogen atom and to the two hydrogens attached to C23.

The doublet signal of H-3 proton was found at 3.62 ppm ($J = 10.44$ Hz) and the multiplet signal corresponding to H-2 was observed at 3.76–3.83 ppm.

In the region between 0.82 and 1.21 ppm were observed the signals corresponding to methyl protons.

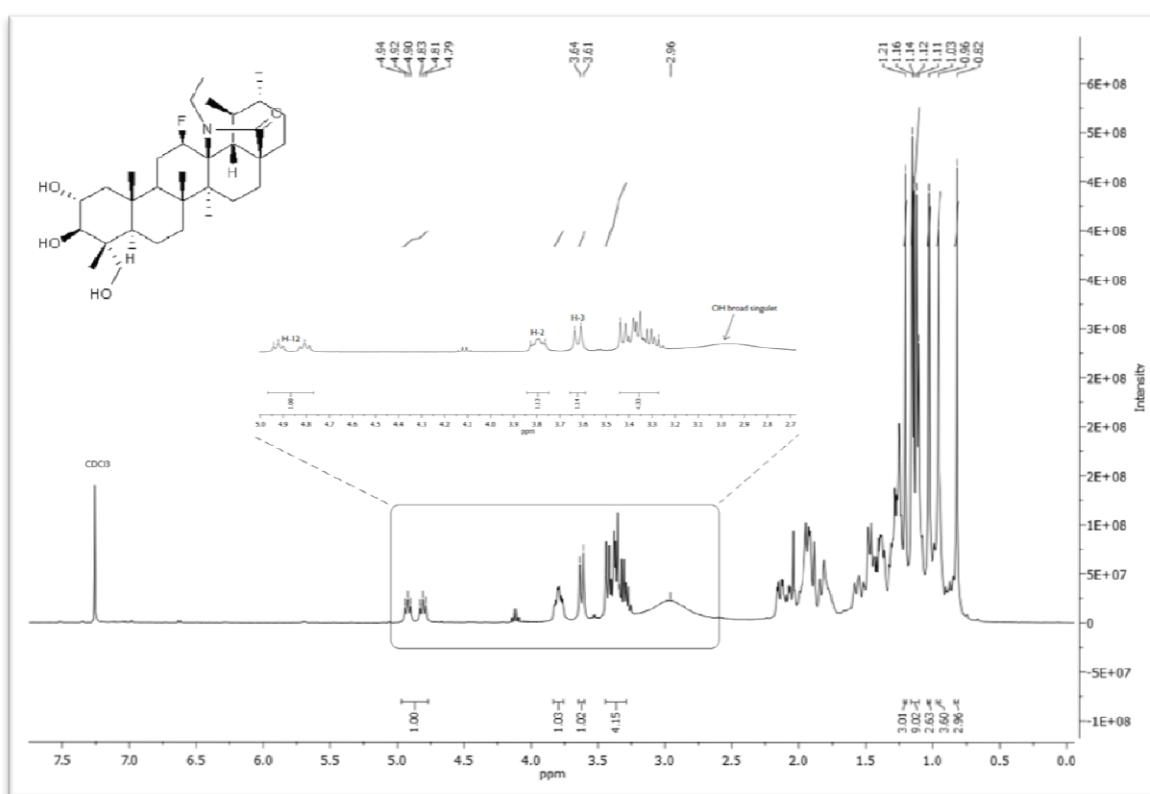


Figure 39 - ^1H NMR spectrum of compound **AA_9**.

The analysis of ^{13}C - NMR spectrum of compound **AA_9** revealed the presence of 32 carbons.

The ^{13}C NMR signal for C12 was observed as a doublet at 89,92 ppm with a coupling constant of 185,00 Hz. In the same zone of this spectrum, at 90,86 ppm, was observed the doublet corresponding to C13 with a coupling constant of 13,46 Hz.

The signal for the carbonyl carbon of the amide was found at 165.50 ppm. The absence of the peaks corresponding to the carbonyl carbons of the acetate groups confirmed the efficacy of the hydrolysis step.

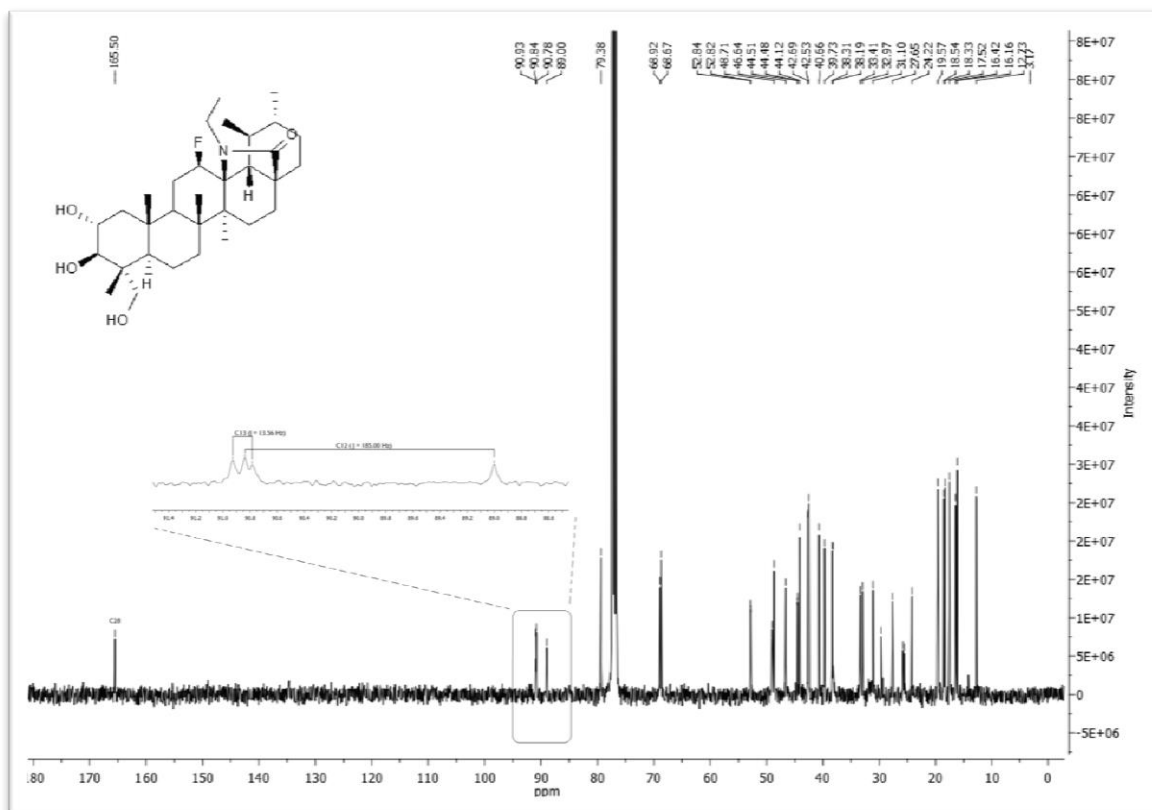


Figure 40 - ^{13}C NMR spectrum of compound AA_9.

$^{135}\text{DEPT}$ spectrum of compound **AA_9** revealed ten CH_2 carbons and fifteen CH or CH_3 carbons. This information was according to the expected for this compound.

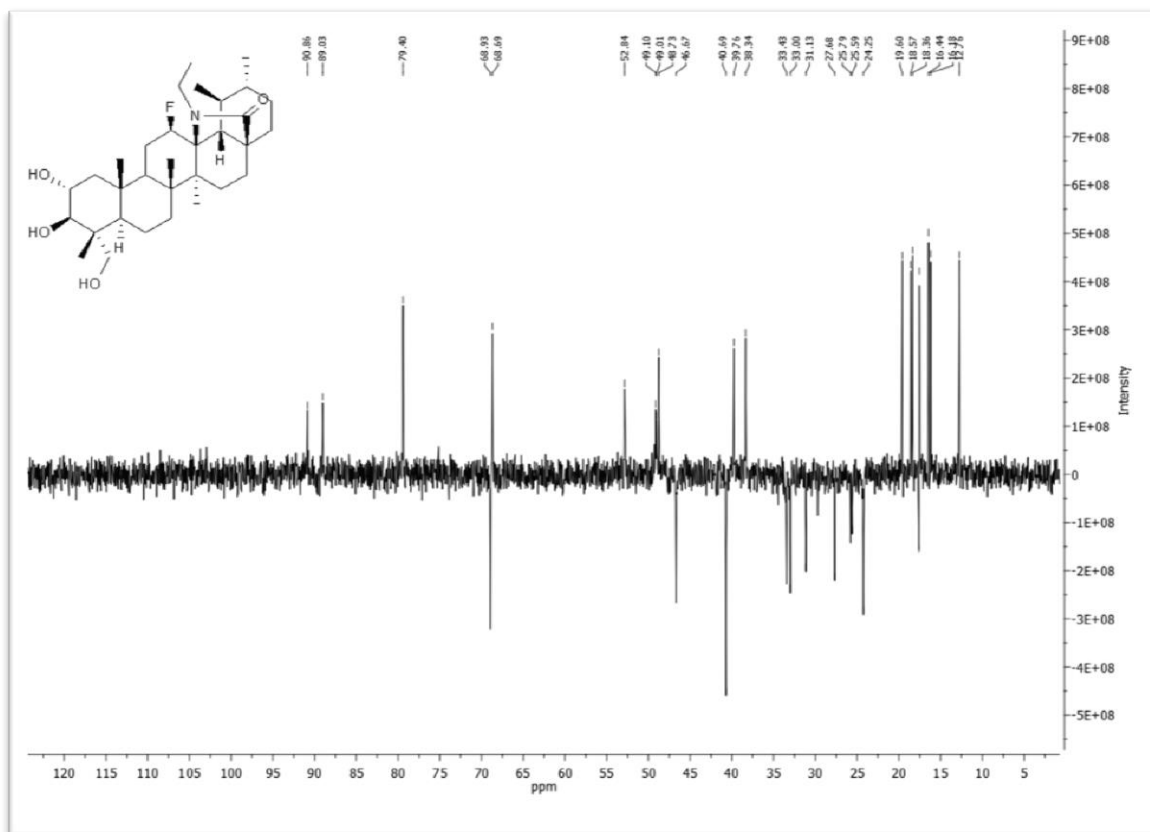


Figure 41 - 135 DEPT spectrum of compound AA_9.

3.2.4.2 Compound AA_10

The structure of compound **AA_10** - Figure 42 - was elucidated through NMR.

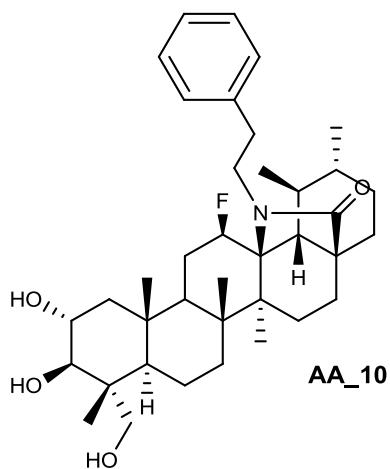


Figure 42 - Structure of compound AA_10.

The ^1H NMR spectrum of this compound was similar to ^1H NMR spectrum of **AA_8** with the disappearance of the signals corresponding to the acetates groups and the appearance of a broad signal, corresponding to the protons of free hydroxyl groups.

The characteristic signals observed downfield around 7 ppm indicate the presence of the aromatic ring in the structure of this compound.

The signal for H-12 was observed as a double triplet as 4.88 ppm, with a coupling constant of 45.74 Hz.

It was also possible to observe a multiplet between 3.79 ppm and 3.85 ppm corresponding H-2 and a doublet signal at 3.65 ppm ($J = 9.18$ Hz) corresponding to H-3. The signals for H-23 protons appeared as two doublets at 3.45 ppm ($J = 9.51$ Hz) and 3.39 ppm ($J = 10.25$ Hz)

The signals for the four methylene protons of amide were observed as multiplets with chemical shifts between 3.59 – 3.63 ppm, 3.49 – 3.56 ppm and 2.87 – 2.92 ppm.

In the region between 0.86 and 1.18 ppm were observed the signals corresponding to methyl protons.

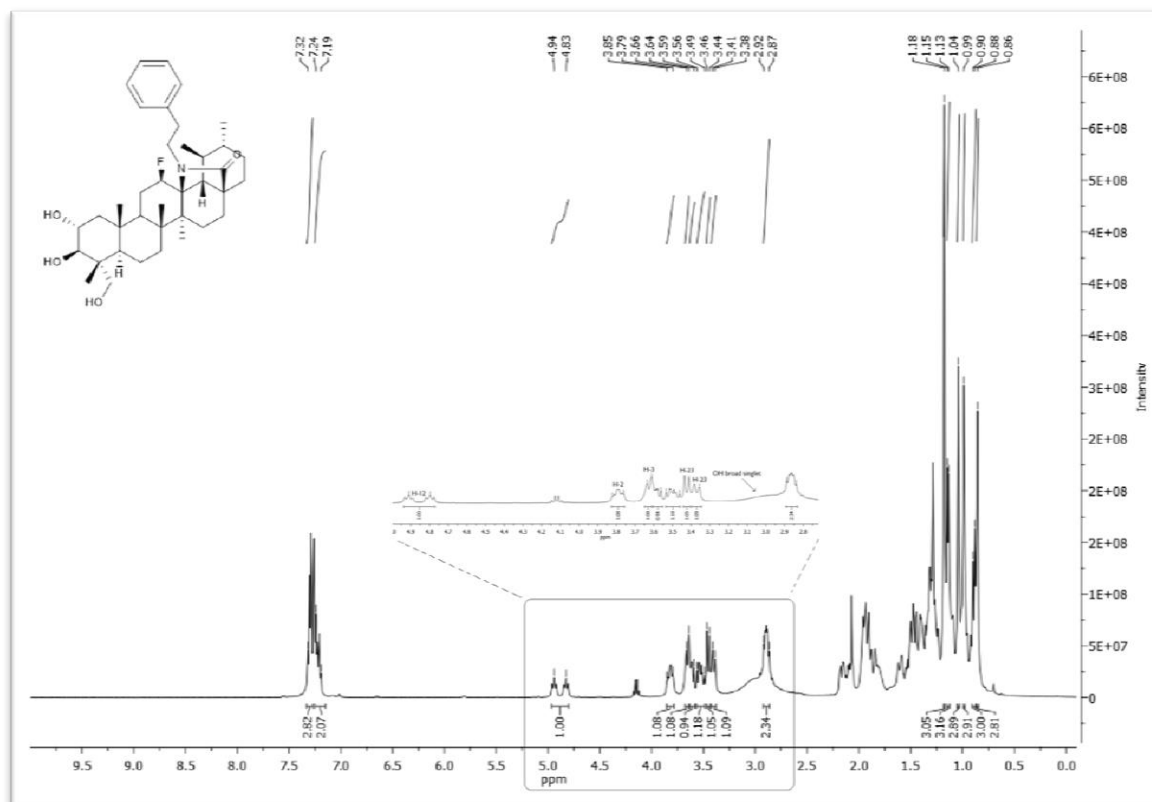


Figure 43 - ^1H NMR spectrum of compound AA_10.

The analysis of ^{13}C NMR spectrum of compound **AA_10** revealed the presence of 38 carbons. The signal for C12 was observed as a doublet at 89,83 ppm with a coupling constant of 184,95 Hz. At 91,09 ppm, was observed the doublet signal corresponding to C13 with a coupling constant of 14,86 Hz.

The signal for the carbonyl carbon of the lactam was found at 165.94 ppm. The absence of the peaks corresponding to the carbonyl carbons of the acetate groups confirmed the successful hydrolysis of compound **AA_8**.

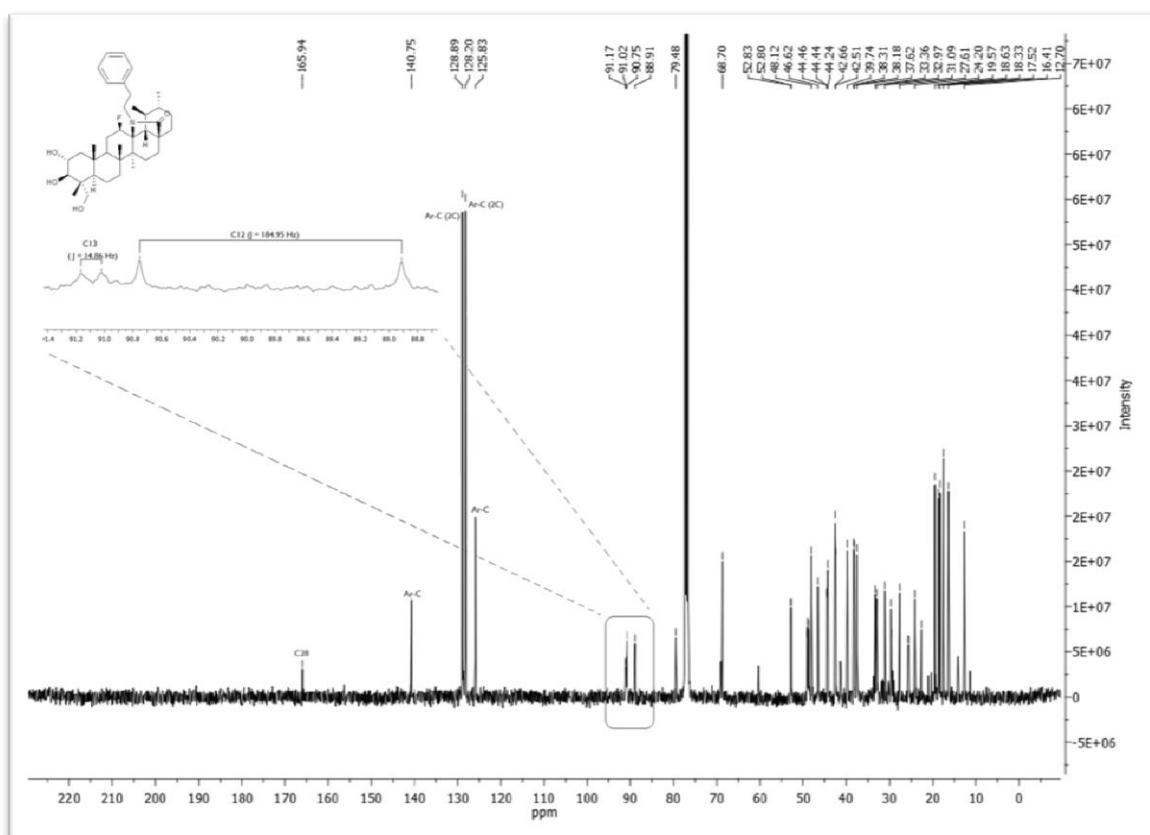


Figure 44 - ^{13}C NMR spectrum of compound **AA_10**.

$^{135}\text{DEPT}$ spectrum revealed that compound **AA_10** has eleven CH_2 carbons and nineteen CH or CH_3 carbons, remaining eight quaternary carbons that are not visible using this technique. This information corroborate the data obtained in the carbon spectrum.

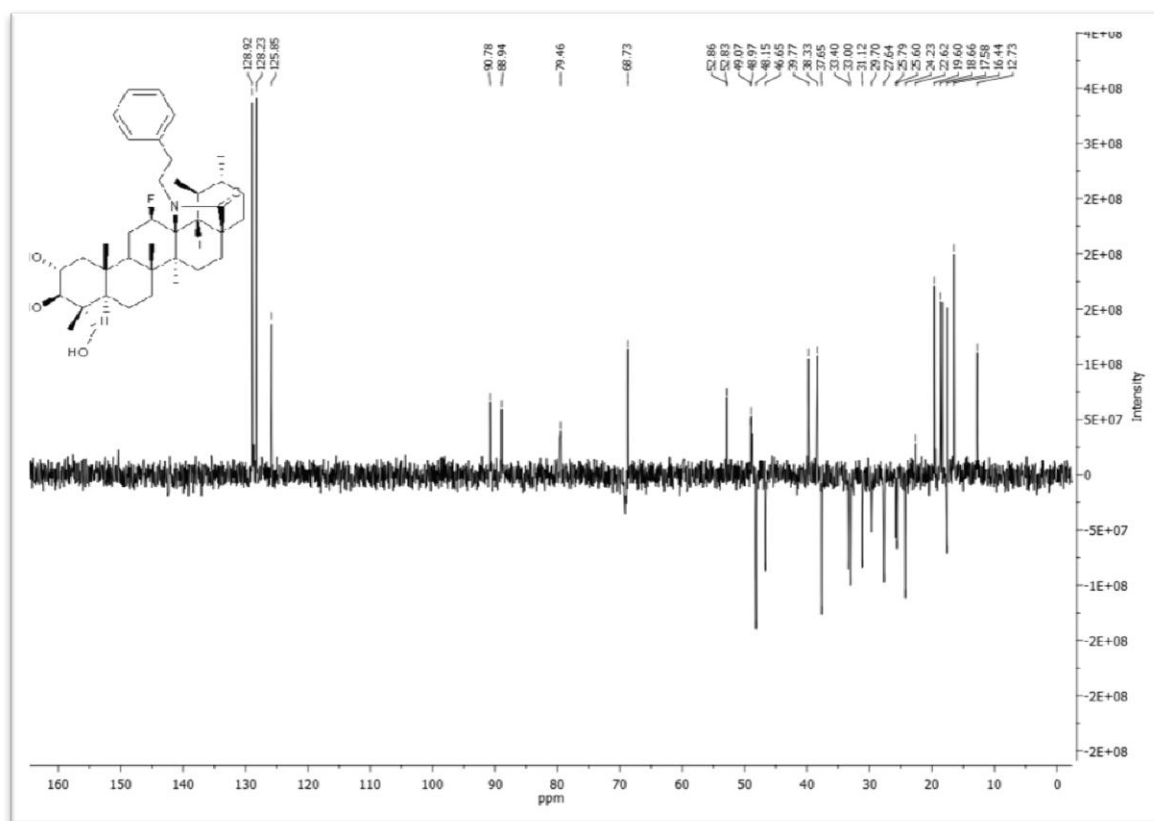


Figure 45 - 135 DEPT spectrum of compound AA_10.

3.3 Experimental section

3.3.1 Chemical

The solvents used in the reactions were previously purified and dried according to the literature procedures. The solvents used in the workups were of analytical grade and purchased from VWR Portugal. Reagents were all purchased from Sigma Aldrich and Merck.

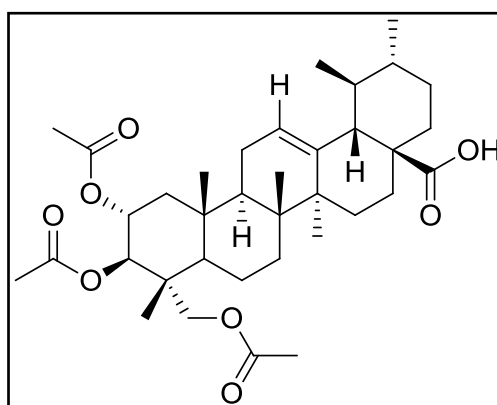
For thin layer chromatography (TLC) it was used Kieselgel 60 F₂₅₄ and revealed in a mixture of ethanol-sulfuric acid (95:5) with heat.

¹H, ¹³C and DEPT-135 NMR spectra were recorded in a Bruker Avance III 400 MHz spectrometer. The chemical shifts were recorded in δ (ppm) using CDCl₃. Chemical shifts measures were given in part per million (ppm) and coupling constants (J) in hertz (Hz). As internal standard was used $\delta = 7.26$ ppm of CHCl₃ in ¹H and $\delta = 77.00$ ppm in ¹³C.

3.3.2 Experimental procedure

Compound AA_2

According to literature (Goncalves *et al.*, 2016), to a solution of **AA_1** (400 mg, 0,82 mmol) in dry THF (12.3 mL), acetic anhydride (0.46 mL, 4.91 mmol) and a catalytic amount of DMAP (40mg) were added. The mixture was stirred at room temperature in anhydrous conditions. After 4h, the reaction mixture was evaporated under reduced pressure to remove the organic phase. The obtained

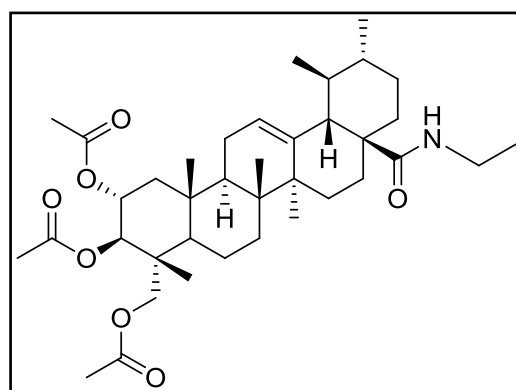


crude was dispersed by water (50 mL) and aqueous phase was extracted with EtOAc (3 x 50 mL). The resulting organic phase was washed with 5% HCl (2 x 30 mL), 10% NaHCO₃ (2 x 30 mL) and water (30 mL), dried over Na₂SO₄, filtered and concentrated under vacuum to afford compound **AA_2** as a white powder (568,8 mg, quantitative). ¹H-NMR (400 MHz, CDCl₃): $\delta = 5.23$ (t, J = 3.2 Hz, 1H, H12), 5.19 - 5.13 (m, 1H, H2), 5.08 (d, J = 10.3 Hz, 1H,

H3), 3.85 (d, $J = 11.9$ Hz, 1H, H23), 3.58 (d, $J = 11.9$ Hz, 1H, H23), 2.08 (s, 3H, CH₃CO), 2.02 (s, 3H, CH₃CO), 1.97 (s, 3H, CH₃CO), 1.10 (s, 3H), 1.07 (s, 3H), 0.94 (d, $J = 5.3$ Hz, 3H), 0.87 (s, 3H), 0.85 (d, $J = 5.4$ Hz, 3H), 0.76 (s, 3H) ppm; ¹³C NMR (100 MHz, CDCl₃): $\delta = 183.1$ (C28), 170.9 (OCO), 170.5 (OCO), 170.4 (OCO), 138.0, 125.3, 74.8, 69.9, 65.3, 52.5, 47.9, 47.6, 47.8, 43.7, 42.0, 41.9, 39.5, 39.0, 38.8, 37.8, 36.6, 32.4, 30.5, 27.9, 24.0, 23.4, 23.3, 21.1, 21.1, 20.9, 20.8, 17.9, 17.0, 16.9, 16.9, 13.9 ppm.

Compound AA_3

To a stirred solution of **AA_2** (400 mg, 0.65 mmol), in dry benzene (8 mL), thionyl chloride (0.1 mL, 1.37 mmol) was slowly added. The resultant solution was heat-refluxed at 80°C. After 4h30, the solvent was removed by evaporation under reduced pressure and petroleum ether (approximately 3 mL) was added to the residue

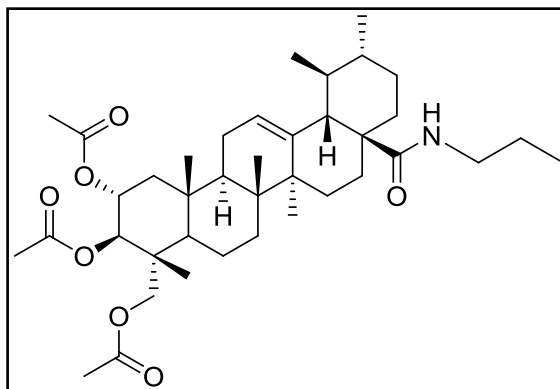


and concentrated to dryness to give the acyl chloride derivative. Without purification, the obtained acyl chloride was dissolved in dry dichloromethane (10 mL), added triethylamine (0.22 mL, 1.58 mmol) and a solution of ethylamine (sol. 2M in THF) (1.26 mL, 2.53 mmol). The resultant mixture was stirred at room temperature. After 6h, the solvent was removed by evaporation under reduced pressure. The obtained crude was dispersed with water (50 mL) and extracted with ethyl acetate (3 x 50 mL). The combined organic phase was washed with 5% aqueous HCl (2 x 50 mL), 10% aqueous NaHCO₃ (2 x 50 mL) and water (2 x 50 mL), dried over Na₂SO₄, filtered and concentrated under vacuum to afford a light yellow solid (369.3 mg, 88.51%). ¹H-NMR (400 MHz, CDCl₃): $\delta = 5.78$ (t, $J = 5.04$ Hz, 1H, NHCH₂CH₃), 5.30 (t, $J = 3.33$ Hz, 1H, H12), 5.19 - 5.12 (m, 1H, H2), 5.07 (d, $J = 10.31$ Hz, 1H, H3), 3.84 (d, $J = 11.78$ Hz, 1H, H23), 3.57 (d, $J = 11.85$ Hz, 1H, H23), 3.33 - 3.26 (m, 1H, NHCH₂CH₃), 3.15 - 3.06 (m, 1H, NHCH₂CH₃), 2.08 (s, 3H, CH₃CO), 2.02 (s, 1H, CH₃CO), 1.98 (s, 1H, CH₃CO), 1.10 (s, 3H), 1.07 (d, $J = 7.36$ Hz, 6H), 0.95 (s, 3H), 0.88 (s, 3H), 0.86 (d, $J = 6.38$ Hz, 3H), 0.79 (s, 3H) ppm; ¹³C NMR (100 MHz, CDCl₃): $\delta = 177.71$ (C28), 170.79 (OCO), 170.46 (OCO), 170.35 (OCO), 140.11 (C13), 124.93 (C12), 74.75, 69.88, 65.23, 53.83, 47.58, 47.48, 47.45, 43.75, 42.50, 41.88, 39.73, 39.55, 39.06, 37.74, 37.10,

34.30, 32.26, 30.85, 27.73, 24.75, 23.45, 23.09, 21.21, 21.06, 20.84, 20.76, 17.83, 17.19, 17.04, 16.85, 14.54, 13.90 ppm.

Compound AA_4

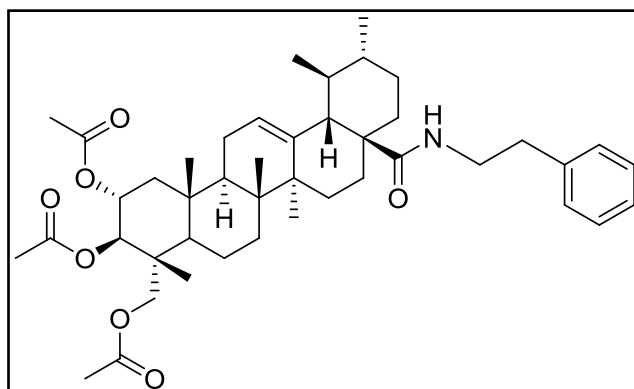
To a stirred solution of **AA_2** (550 mg, 0.89 mmol), in dry benzene (8 mL), thionyl chloride (0.2 mL, 2.77 mmol) was slowly added. The resultant solution was heat-refluxed at 80°C. After 3h, the solvent was removed by evaporation under reduced pressure and petroleum ether (approximately 3 mL) was added to the residue and concentrated to



dryness to give the acyl chloride derivative. Without purification, the obtained acyl chloride was dissolved in dry dichloromethane (12.5 mL), added triethylamine (0.27 mL, 1.97 mmol) and a solution of propylamine (0.26 mL, 3.16 mmol). The resultant mixture was stirred at room temperature. After 18h propylamine was added (0.1 mL, 0.78 mmol). After 22h, the solvent was removed by evaporation under reduced pressure. The obtained crude was dispersed with water (50 mL) and extracted with ethyl acetate (3 x 50 mL). The combined organic phase was washed with 5% aqueous HCl (2 x 50 mL), 10% aqueous NaHCO₃ (2 x 50 mL) and water (2 x 50 mL), dried over Na₂SO₄, filtered and concentrated under vacuum to afford a light yellow solid (508.7 mg, 87.14%). ¹H-NMR (400 MHz, CDCl₃): δ = 5.85 (t, J = 5.26 Hz, 1H, NH), 5.30 (t, J = 3.41 Hz, 1H, H12), 5.19 – 5.12 (m, 1H, H2), 5.08 (d, J = 10.20 Hz, 1H, H3), 3.84 (d, J = 12.42 Hz, 1H, H23), 3.57 (d, J = 11.10 Hz, 1H, H23), 3.33 – 3.25 (m, 1H, NHCH₂CH₂CH₃), 3.00 – 2.92 (m, 1H, NHCH₂CH₂CH₃), 2.08 (s, 3H, CH₃CO), 2.02 (s, 3H, CH₃CO), 1.98 (s, 3H, CH₃CO), 1.10 (s, 3H), 1.09 (s, 3H), 0.95 (s, 3H), 0.90 – 0.85 (m, 9H), 0.79 (s, 3H) ppm; ¹³C NMR (100 MHz, CDCl₃): δ = 177.78 (C28), 170.81 (OCO), 170.46 (OCO), 170.36 (OCO), 140.15 (C13), 124.92 (C12), 74.75, 69.89, 65.24, 53.92, 47.66, 47.58, 47.46, 43.75, 42.51, 41.89, 41.17, 39.73, 39.55, 39.07, 37.75, 37.20, 32.28, 30.86, 27.74, 24.76, 23.45, 23.11, 22.53, 21.20, 21.07, 20.85, 20.76, 17.84, 17.19, 17.05, 16.87, 13.90, 11.54 ppm.

Compound AA_5

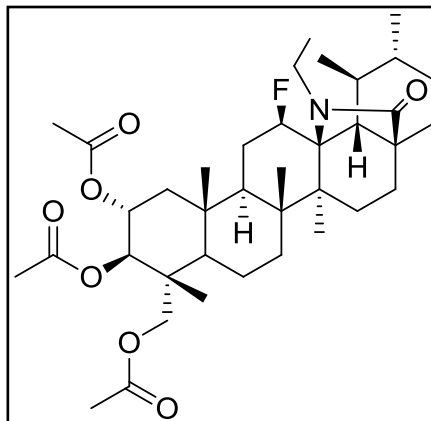
To a stirred solution of **AA_2** (200 mg, 0.32 mmol), in dry benzene (5 mL), thionyl chloride (0.07 mL, 1.0 mmol) was slowly added. The resultant solution was heat-refluxed at 80°C. After 3h15, the solvent was removed by evaporation under reduced pressure and petroleum ether (approximately 3 mL) was added to



the residue and concentrated to dryness to give the acyl chloride derivative. Without purification, the obtained acyl chloride was dissolved in dry dichloromethane (5 mL), triethylamine (0.11 mL, 0.79 mmol) and phenylethylamine (0.16 mL, 1.26 mmol) were added. The resultant mixture was stirred at room temperature. After 2h, the solvent was removed by evaporation under reduced pressure. The obtained crude was dispersed with water (30 mL) and extracted with ethyl acetate (3 x 30 mL). The combined organic phase was washed with 5% aqueous HCl (2 x 30 mL), 10% aqueous NaHCO₃ (2 x 30 mL) and water (2 x 30 mL), dried over Na₂SO₄, filtered and concentrated under vacuum to afford a light yellow solid (223.0 mg, 97.06%). ¹H-NMR (400 MHz, CDCl₃): δ = 7.35 – 7.18 (m, 5H, Ar-H), 5.81 – 5.78 (m, 1H, NH), 5.19 – 5.12 (m, 1H, H2), 5.06 (d, J = 10.03 Hz, 1H, H3), 4.86 (t, J = 3.33 Hz, 1H, H12), 3.82 (d, J = 11.94 Hz, 1H, H23), 3.79 – 3.72 (m, 1H), 3.56 (d, J = 11.69 Hz, 1H, H23), 3.21 – 3.13 (m, 1H), 2.89 – 2.82 (m, 1H), 2.72 – 2.65 (m, 1H), 2.06 (s, 3H, CH₃CO), 2.02 (s, 3H, CH₃CO), 1.98 (s, 3H, CH₃CO), 1.05 (s, 3H), 1.02 (s, 3H), 0.93 (s, 3H), 0.88 (s, 3H), 0.87 – 0.82 (m, 3H), 0.79 (d, J = 6.55 Hz, 3H); ¹³C NMR (100 MHz, CDCl₃): δ = 177.92 (C28), 170.78 (OCO), 170.49 (OCO), 170.34 (OCO), 139.43, 139.07, 128.75 (2C, Ar-C), 128.67 (2C, Ar-C), 126.64 (Ar-C), 125.10 (C12), 74.74, 69.88, 65.22, 53.66, 47.69, 47.54, 47.39, 43.71, 42.27, 41.87, 40.32, 39.67, 39.47, 39.04, 37.65, 37.10, 35.30, 32.09, 30.83, 27.66, 24.81, 23.29, 23.07, 21.20, 21.08, 20.84, 20.76, 17.80, 17.17, 17.00, 16.73, 13.88 ppm.

Compound AA_6

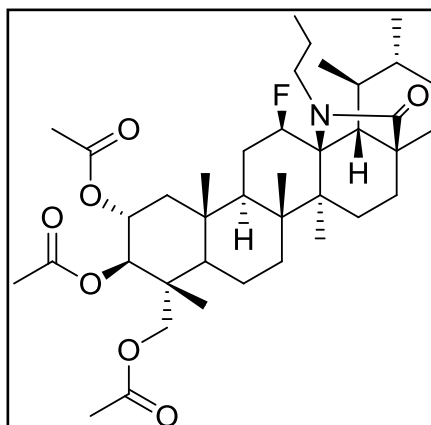
To a stirred solution of **AA_3** (350 mg, 0.54 mmol) in dry nitromethane (14 mL) and dry dioxane (9.1 mL) at 80°C, Selectfluor® (579.51 mg, 1.64 mmol) was added. The mixture was stirred at 80°C, in anhydrous conditions. After 24h30, Selectfluor® (193.17 mg, 0.54 mmol) was added. After 68h, the solvent was removed by evaporation under reduced pressure. The obtained crude was dispersed with water (50 mL). Aqueous phase



was extracted with EtOAc (3 x 50 mL), the combined organic phase was washed with water (4 x 50 mL), dried over Na₂SO₄, filtered, and concentrated under vacuum to afford **AA_6** (389.9 mg, quantitative). ¹H-NMR (400 MHz, CDCl₃): δ = 5.23 – 5.16 (m, 1H, H2), 5.07 (d, J = 10.30 Hz, 1H, H3), 4.86 (dq, J = 45.73 Hz, 5.61 Hz, 1H, H12), 3.80 (d, J = 11.90 Hz, 1H, H23), 3.60 (d, J = 11.90 Hz, 1H, H23), 3.40 – 3.28 (m, 2H, NCH₂CH₃), 2.08 (s, 3H, CH₃CO), 2.02 (s, 3H, CH₃CO), 1.99 (s, 3H, CH₃CO), 1.22 (s, 3H), 1.14 (m, 9H), 1.11 (m, 3H), 0.95 (d, J = 4.59 Hz, 3H), 0.88 (s, 3H) ppm; ¹³C NMR (100 MHz, CDCl₃): δ = 170.79 (OCO), 170.27 (2C, OCO), 164.77 (C28), 90.49 (d, J = 14.22 Hz, C13), 89.80 (d, J = 185.15 Hz, C12), 74.59, 60.70, 65.15, 52.84 (d, J = 2.63 Hz), 49.23 (d, J = 9.47 Hz), 47.79, 44.44 (d, J = 3.16 Hz), 44.21, 44.00, 42.74, 41.91, 40.73, 39.77, 38.33, 37.96, 33.36, 33.03, 31.12, 27.66, 25.73 (d, J = 19.90 Hz), 24.23, 21.04, 20.88, 20.76, 19.60, 18.49, 18.21, 17.46, 17.28, 16.44, 16.25, 13.65 ppm.

Compound AA_7

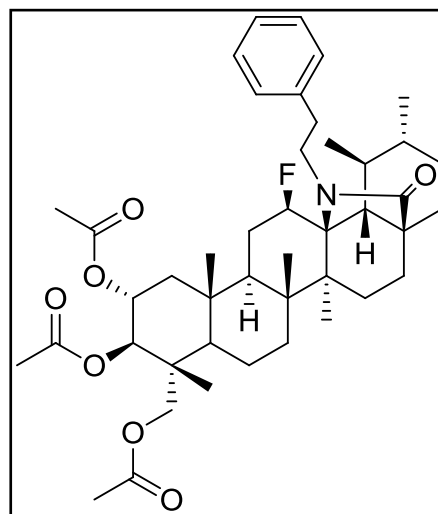
To a stirred solution of **AA_4** (461.2 mg, 0.70 mmol) in dry nitromethane (18.45 mL) and dry dioxane (12 mL) at 80°C, Selectfluor® (742.79 mg, 2.10 mmol) was added. The mixture was stirred at 80°C, in anhydrous conditions. After 24h, the solvent was removed by evaporation under reduced pressure. The obtained crude was dispersed with water (60 mL). Aqueous phase was extracted with EtOAc (3 x 60 mL).



the combined organic phase was washed with water (4 x 60 mL), dried over Na₂SO₄, filtered, and concentrated under vacuum to afford **AA_7** (500.8 mg, quantitative). ¹H-NMR (400 MHz, CDCl₃): δ = 5.23 – 5.16 (m, 1H, H2), 5.07 (d, J = 10.38 Hz, H3), 4.86 (dq, J = 45.52 Hz, 5.51 Hz, 1H, H12), 3.81 (d, J = 11.98 Hz, 1H, H23), 3.61 (d, J = 11.70 Hz, 1H, H23), 3.35 – 3.28 (m, 1H, NCH₂CH₂CH₃), 3.25 – 3.18 (m, 1H, NCH₂CH₂CH₃), 2.08 (s, 3H, CH₃CO), 2.02 (s, 3H, CH₃CO), 1.99 (s, 3H, CH₃CO), 1.22 (s, 3H), 1.15 (s, 3H), 1.11 (s, 6H), 0.95 (d, J = 5.05 Hz, 3H), 0.89 (d, J = 3.40 Hz, 6H) ppm; ¹³C NMR (100 MHz, CDCl₃): δ = 170.77 (OCO), 170.35 (2C, OCO), 164.75 (C28), 90.38 (d, J = 13.90 Hz, C13), 89.78 (d, J = 185.41 Hz, C12), 74.59, 69.69, 65.15, 52.89 (d, J = 2.82 Hz), 49.22 (d, J = 9.64 Hz), 48.09, 47.77, 44.44 (d, J = 2.93 Hz), 44.20, 44.04, 42.72, 41.89, 39.77, 38.33, 37.95, 33.36, 33.08, 31.12, 27.66, 25.73 (d, J = 19.61 Hz), 24.27, 24.23, 21.03, 20.87, 20.75, 19.59, 18.52, 18.21, 17.45, 17.26, 16.43, 13.64, 12.02 ppm.

Compound **AA_8**

To a stirred solution of **AA_5** (200 mg, 0.28 mmol) in dry nitromethane (8 mL) and dry dioxane (5.2 mL) at 80°C, Selectfluor[®] (296.05 mg, 0.84 mmol) was added. The mixture was stirred at 80°C, in anhydrous conditions. After 25h, the solvent was removed by evaporation under reduced pressure. The obtained crude was dispersed with water (30 mL). Aqueous phase was extracted with EtOAc (3 x 30 mL). the combined organic phase was washed with water (4 x 30 mL), dried over Na₂SO₄, filtered, and concentrated under vacuum to

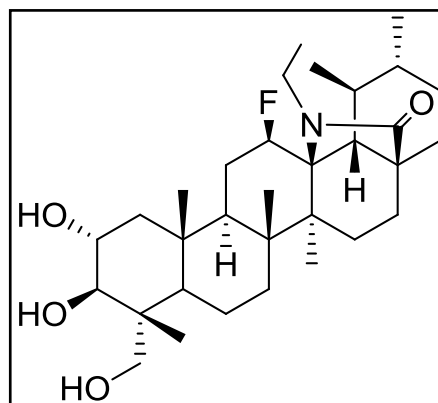


afford **AA_8** (210.0 mg, quantitative). ¹H-NMR (400 MHz, CDCl₃): δ = 7.29 – 7.16 (m, 5H, Ar-H), 5.22- 5.16 (m, 1H, H2), 5.07 (d, J = 10.41 Hz, 1H, H3), 4.85 (dq, J = 45.53 Hz, 5.66 Hz, 1H, H12), 3.80 (d, J = 11.77 Hz, 1H, H23), 3.63 – 3.56 (m, 2H), 3.53 – 3.46 (m, 1H, H23), 2.92 – 2.80 (m, 2H), 2.08 (s, 3H, CH₃CO), 2.02 (s, 3H, CH₃CO), 1.99 (s, 3H, CH₃CO), 1.15 (s, 6H), 1.11 (d, J = 6.13 Hz, 3H), 1.09 (s, 3H), 0.96 (s, 3H), 0.88 (s, 3H) ppm; ¹³C NMR (100 MHz, CDCl₃): δ = 170.75 (OCO), 170.33 (2C, OCO), 165.34 (C28), 140.83 (Ar-C), 128.92 (2C, Ar-C), 128.19 (2C, Ar-C), 125.81 (Ar-C), 90.77 (d, J = 14.00 Hz, C13), 89.68 (d, J = 185.48 Hz, C12), 74.58, 69.68, 65.14, 52.82 (d, J = 2.98 Hz), 49.19 (d, J = 9.01 Hz), 48.21,

47.77, 44.39 (d, $J = 2.66$ Hz), 44.20, 44.14, 42.69, 41.90, 39.77, 38.33, 37.94, 37.71, 33.30, 33.01, 31.10, 27.61, 25.72 (d, $J = 20.17$ Hz), 24.20, 21.01, 20.86, 20.74, 19.58, 18.57, 18.20, 17.45, 17.26, 16.42, 13.64 ppm.

Compound AA_9

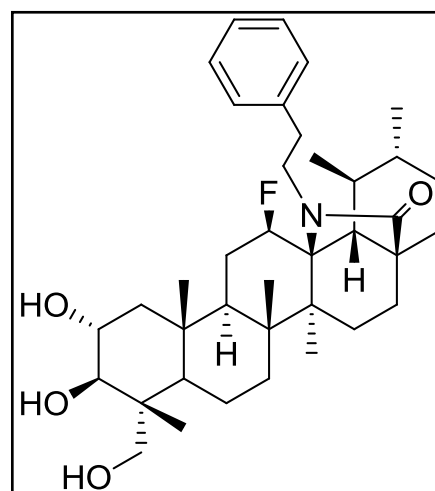
To a stirred solution of **AA_6** (350 mg, 0.53 mmol) in methanol (20 mL), KOH (1.0022 g) was added. The reaction mixture was heated under reflux. After 20h the reaction mixture was evaporated under reduced pressure to remove the methanol. The obtained crude was dispersed with water (40 mL) and extracted with ethyl acetate (3 x 40 mL). The resulting organic phase was washed with water (3 x 40 mL) and



brine (40 mL), dried over Na_2SO_4 , filtered and concentrated under vacuum to afford **AA_9** as a light yellow powder (194.0 mg, 68.58%). $^1\text{H-NMR}$ (400 MHz, CDCl_3): $\delta = 4.87$ (dt, $J = 45.21$ Hz, 8.39 Hz, 1H, H12), 3.83 – 3.76 (m, 1H, H2), 3.62 (d, $J = 10.44$ Hz, 1H, H3), 3.44 – 3.27 (m, 4H, H23 and NHCH_2CH_3), 1.21 (s, 3H), 1.16 (s, 3H), 1.14 – 1.11 (m, 6H), 1.03 (s, 3H), 0.95 (d, $J = 5.71$ Hz, 3H), 0.82 (s, 3H) ppm; $^{13}\text{C NMR}$ (100 MHz, CDCl_3): 165.50 (C28), 90.86 (d, $J = 13.46$ Hz, C13), 89.92 (d, $J = 185.00$ Hz, C12), 79.38, 68.92, 68.67, 52.83 (d, $J = 2.75$ Hz), 49.03 (d, $J = 9.42$ Hz), 48.71, 46.64, 44.49 (d, $J = 2.86$ Hz), 44.12, 42.69, 42.53, 40.66, 39.73, 38.31, 38.19, 33.41, 32.97, 31.10, 29.67, 27.65, 25.66 (d, $J = 19.44$ Hz), 24.22, 19.57, 18.54, 18.33, 17.52, 16.42, 16.16, 12.73 ppm.

Compound AA_10

To a stirred solution of **AA_8** (194.9 mg, 0.26 mmol) in methanol (20 mL), KOH (1.0020 g) was added. The reaction mixture was heated under reflux. After 22h the reaction mixture was evaporated under reduced pressure to remove the methanol. The obtained crude was dispersed with water (30 mL) and extracted with ethyl acetate (3 x 30 mL). The resulting organic phase



was washed with water (3 x 30 mL) and brine (30 mL), dried over Na₂SO₄, filtered and concentrated under vacuum to afford **AA_10** as a light yellow powder (147.5 mg, 93.02%).
¹H-NMR (400 MHz, CDCl₃): δ = 7.32 – 7.19 (m, 5H, Ar-H), 4.88 (dt, J = 45.74 Hz, 8.77 Hz, 1H, H12), 3.85 – 3.79 (m, 1H, H2), 3.65 (d, J = 9.18 Hz, 1H, H3), 3.63 – 3.59 (m, 1H), 3.56 – 3.49 (m, 1H), 3.45 (d, J = 9.51 Hz, 1H, H23), 3.39 (d, J = 10.25 Hz, 1H, H23), 2.92 – 2.87 (m, 2H), 1.18 (s, 3H), 1.14 (d, J = 6.48 Hz, 3H), 1.04 (s, 3H), 0.99 (s, 3H), 0.90 – 0.88 (m, 3H), 0.86 (s, 3H) ppm; ¹³C NMR (100 MHz, CDCl₃): 165.94 (C28), 140.75 (Ar-C), 128.89 (2C, Ar-C), 128.20 (2C, Ar-C), 125.83 (Ar-C), 91.09 (d, J = 14.86 Hz, C13), 89.83 (d, J = 184.95 Hz, C12), 79.48, 68.70, 52.81 (d, J = 3.05 Hz), 48.99 (d, J = 9.95 Hz), 48.12, 46.62, 44.45 (d, J = 3.05 Hz), 44.24, 42.66, 42.51, 39.74, 38.31, 38.18, 37.62, 33.36, 23.97, 31.09, 29.67, 29.63, 27.61, 25.66 (d, J = 19.11 Hz), 24.20, 22.59, 19.57, 18.63, 18.33, 17.52, 16.41, 12.70 ppm.

Chapter IV

Concluding remarks and future prospects

Concluding remarks and future prospects

In this work a panel of five new derivatives of asiatic acid was designed and successfully synthesized.

The introduction of an amide group in compounds AA_3, AA_4 and AA_5 was accomplished through the formation of an acyl halide intermediate. The successful preparation of the amide derivatives was confirmed by appearance in the ¹H NMR spectrum of a signal around 5.8 ppm for the NH proton of amide. In the ¹³C NMR spectrum, the presence of the amide function was confirmed by the observation of a signal around 175 ppm corresponding to the carbonyl carbon of amide group, which was different from the signal observed for the carboxylic acid carbonyl carbon at 183.1 ppm.

The introduction of 12β-fluorolactam function in compounds AA_6, AA_7 and AA_8 was confirmed by the observation of ¹H NMR signals for H -12 and H -13 in ¹H NMR spectrum and for C12 and C13 in ¹³C NMR spectrum, which were characteristics of the β-isomer.

The final step of hydrolysis was confirmed by the disappearance of the protons of acetate groups and the appearance of a broad singlet in ¹H NMR. In ¹³C NMR spectrum, the signals for carbonyl carbons of acetate groups also disappeared.

The versatility of these reactions associated with high yields and the use of simple cost effective and easy to handle techniques make these compounds a good starting point for the development of new potential inhibitors of BACE1.

These compounds warrant additional studies to investigate their ability to inhibit the BACE1 and to establish a structure - activity relationship.

Chapter V

Bibliographic references

Bibliographic references

- ANTHWAL, P., SEMWAL, P., KAPOOR, T. THAPLIYAL, M., THAPLIYAL, A. (2015) - Azadirachtin, cardiofolioside, and kutkin can be vital phytochemicals for the modulation of secretase enzymes for the treatment of alzheimer's: an in-silico analysis. "Asian Journal of Pharmaceutical and Clinical Research." 8. 4 (2015). 108-112.
- ARONOV, A. M. (2008) - Ligand structural aspects of hERG channel blockade. "Curr Top Med Chem." 8. 13 (2008). 1113-27.
- BANKS, R. B. (1997) - Selectfluor reagent F-TEDA-BF, in action: tamed fluorine at your service "Journal of Fluorine Chemistry." 87. (1997). 1-17.
- BARAO, S.[et. al.] (2016) - BACE1 Physiological Functions May Limit Its Use as Therapeutic Target for Alzheimer's Disease. "Trends Neurosci." 39. 3 (2016). 158-69.
- BARD, F.[et. al.] (2000) - Peripherally administered antibodies against amyloid beta-peptide enter the central nervous system and reduce pathology in a mouse model of Alzheimer disease. "Nat Med." 6. 8 (2000). 916-9.
- BARUCH-SUCHODOLSKY, R.[et. al.] (2009) - Abeta40, either soluble or aggregated, is a remarkably potent antioxidant in cell-free oxidative systems. "Biochemistry." 48. 20 (2009). 4354-70.
- BASI, G.[et. al.] (2003) - Antagonistic effects of beta-site amyloid precursor protein-cleaving enzymes 1 and 2 on beta-amyloid peptide production in cells. "J Biol Chem." 278. 34 (2003). 31512-20.
- BASSETTO, M.[et. al.] (2015) - Polyfluorinated groups in medicinal chemistry. "Future Med Chem." 7. 4 (2015). 527-46.
- BÉGUÉ, J. P., BONNET-DELPON, D. (2008)- Bioorganic and medicinal chemistry of fluorine. John Wiley & Sons, Inc, (2008). Chapter Available from: WWW: <<http://onlinelibrary.wiley.com/book/10.1002/9780470281895>>.
- BENNETT, B. D.[et. al.] (2000) - Expression analysis of BACE2 in brain and peripheral tissues. "J Biol Chem." 275. 27 (2000). 20647-51.
- BRODNEY, M. A.[et. al.] (2015) - Utilizing structures of CYP2D6 and BACE1 complexes to reduce risk of drug-drug interactions with a novel series of centrally efficacious BACE1 inhibitors. "J Med Chem." 58. 7 (2015). 3223-52.
- BUSH, A. I.[et. al.] (1994) - Rapid induction of Alzheimer A beta amyloid formation by zinc. "Science." 265. 5177 (1994). 1464-7.

- CAI, J.[et. al.] (2012) - beta-Secretase (BACE1) inhibition causes retinal pathology by vascular dysregulation and accumulation of age pigment. "EMBO Mol Med." 4. 9 (2012). 980-91.
- CAO, L.[et. al.] (2012) - The precision of axon targeting of mouse olfactory sensory neurons requires the BACE1 protease. "Sci Rep." 2. (2012). 231.
- CAPELL, A.[et. al.] (2000) - Maturation and pro-peptide cleavage of beta-secretase. "J Biol Chem." 275. 40 (2000). 30849-54.
- CARPINO, L. A., AMHERST, B. J. C. (1986) - ((9-Fluorenylmethyl)oxy)carbonyl (Fmoc) Amino Acid Chlorides. Synthesis, Characterization, and Application to the Rapid Synthesis of Short Peptide Segments "J. Org. Chem. ." 51. (1986). 3732-3734
- CHARISIADIS, P.[et. al.] (2014) - ¹H-NMR as a structural and analytical tool of intra- and intermolecular hydrogen bonds of phenol-containing natural products and model compounds. "Molecules." 19. 9 (2014). 13643-82.
- CHENG, H.[et. al.] (2007) - Mechanisms of disease: new therapeutic strategies for Alzheimer's disease--targeting APP processing in lipid rafts. "Nat Clin Pract Neurol." 3. 7 (2007). 374-82.
- CHIN, Y. W.[et. al.] (2006) - Drug discovery from natural sources. "AAPS J." 8. 2 (2006). E239-53.
- CITRON, M. (2010) - Alzheimer's disease: strategies for disease modification. "Nat Rev Drug Discov." 9. 5 (2010). 387-98.
- CORDER, E. H.[et. al.] (1993) - Gene dose of apolipoprotein E type 4 allele and the risk of Alzheimer's disease in late onset families. "Science." 261. 5123 (1993). 921-3.
- CUMMINGS, J. L. (1995) - Dementia: the failing brain. "Lancet." 345. 8963 (1995). 1481-4.
- CZIRR, E.[et. al.] (2012) - The immunology of neurodegeneration. "J Clin Invest." 122. 4 (2012). 1156-63.
- DEB, A.[et. al.] (2013) - Oxidative trifluoromethylation of unactivated olefins: an efficient and practical synthesis of alpha-trifluoromethyl-substituted ketones. "Angew Chem Int Ed Engl." 52. 37 (2013). 9747-50.
- DISLICH, B.[et. al.] (2012) - The Membrane-Bound Aspartyl Protease BACE1: Molecular and Functional Properties in Alzheimer's Disease and Beyond. "Front Physiol." 3. (2012). 8.
- DOMINGUEZ, D.[et. al.] (2005) - Phenotypic and biochemical analyses of BACE1- and BACE2-deficient mice. "J Biol Chem." 280. 35 (2005). 30797-806.

- DONMEZ, G.[et. al.] (2010) - SIRT1 suppresses beta-amyloid production by activating the alpha-secretase gene ADAM10. "Cell." 142. 2 (2010). 320-32.
- EHEHALT, R.[et. al.] (2003) - Amyloidogenic processing of the Alzheimer beta-amyloid precursor protein depends on lipid rafts. "J Cell Biol." 160. 1 (2003). 113-23.
- EISENBERGER, P.[et. al.] (2006) - Novel 10-I-3 hypervalent iodine-based compounds for electrophilic trifluoromethylation. "Chemistry." 12. 9 (2006). 2579-86.
- ESLER, W. P.[et. al.] (2001) - A portrait of Alzheimer secretases--new features and familiar faces. "Science." 293. 5534 (2001). 1449-54.
- ESTERHAZY, D.[et. al.] (2011) - Bace2 is a beta cell-enriched protease that regulates pancreatic beta cell function and mass. "Cell Metab." 14. 3 (2011). 365-77.
- EUROPEAN PATENT APPLICATION, HOECHST AKTIENGESELLSCHAFT, EP 0 383171 A2 (1992) - (1992).
- EVIN, G.[et. al.] (2011) - BACE inhibitors as potential drugs for the treatment of Alzheimer's disease: focus on bioactivity. "Recent Pat CNS Drug Discov." 6. 2 (2011). 91-106.
- FARZAN, M.[et. al.] (2000) - BACE2, a beta -secretase homolog, cleaves at the beta site and within the amyloid-beta region of the amyloid-beta precursor protein. "Proc Natl Acad Sci U S A." 97. 17 (2000). 9712-7.
- FILSER, S.[et. al.] (2015) - Pharmacological inhibition of BACE1 impairs synaptic plasticity and cognitive functions. "Biol Psychiatry." 77. 8 (2015). 729-39.
- FINLAYSON, K.[et. al.] (2004) - Acquired QT interval prolongation and HERG: implications for drug discovery and development. "Eur J Pharmacol." 500. 1-3 (2004). 129-42.
- FORSTL, H.[et. al.] (1999) - Clinical features of Alzheimer's disease. "Eur Arch Psychiatry Clin Neurosci." 249. 6 (1999). 288-90.
- FUJIWARA, Y.[et. al.] (2012) - Practical and innate carbon-hydrogen functionalization of heterocycles. "Nature." 492. 7427 (2012). 95-9.
- FURUKAWA, T.[et. al.] (2011) - Organocatalyzed regio- and enantioselective allylic trifluoromethylation of Morita-Baylis-Hillman adducts using Ruppert-Prakash reagent. "Org Lett." 13. 15 (2011). 3972-5.
- GATLIK-LANDWOJTOWICZ, E.[et. al.] (2006) - Quantification and characterization of P-glycoprotein-substrate interactions. "Biochemistry." 45. 9 (2006). 3020-32.
- GHOSH, A. K.[et. al.] (2012) - Developing beta-secretase inhibitors for treatment of Alzheimer's disease. "J Neurochem." 120 Suppl 1. (2012). 71-83.
- GHOSH, A. K.[et. al.] (2014) - BACE1 (beta-secretase) inhibitors for the treatment of Alzheimer's disease. "Chem Soc Rev." 43. 19 (2014). 6765-813.

- GILLIS, E. P.[et. al.] (2015) - Applications of Fluorine in Medicinal Chemistry. "J Med Chem." 58. 21 (2015). 8315-59.
- GOLDE, T. E.[et. al.] (2003) - Physiologic and pathologic events mediated by intramembranous and juxtamembranous proteolysis. "Sci STKE." 2003. 172 (2003). RE4.
- GOLDE, T. E.[et. al.] (2013) - gamma-Secretase inhibitors and modulators. "Biochim Biophys Acta." 1828. 12 (2013). 2898-907.
- GOMES, B.[et. al.] (2015) - The Potential Effect of Fluorinated Compounds in the Treatment of Alzheimer's Disease. "Curr Pharm Des." 21. 39 (2015). 5725-35.
- GONÇALVES, B. M. F., SALVADOR, J. A. R., MARÍNCD, S., CASCANTE, M. (2016) - Synthesis and biological evaluation of novel asiatic acid derivatives with anticancer activity. "RSC Adv." 6. (2016). 3967-3985.
- GONCALVES, B. M.[et. al.] (2016) - Synthesis and anticancer activity of novel fluorinated asiatic acid derivatives. "Eur J Med Chem." 114. (2016). 101-17.
- GOTZ, J.[et. al.] (2001) - Formation of neurofibrillary tangles in P301I tau transgenic mice induced by Abeta 42 fibrils. "Science." 293. 5534 (2001). 1491-5.
- GRUNINGER-LEITCH, F.[et. al.] (2002) - Substrate and inhibitor profile of BACE (beta-secretase) and comparison with other mammalian aspartic proteases. "J Biol Chem." 277. 7 (2002). 4687-93.
- HAAG, M. D.[et. al.] (2009) - Statins are associated with a reduced risk of Alzheimer disease regardless of lipophilicity. The Rotterdam Study. "J Neurol Neurosurg Psychiatry." 80. 1 (2009). 13-7.
- HAGMANN, W. K. (2008) - The many roles for fluorine in medicinal chemistry. "J Med Chem." 51. 15 (2008). 4359-69.
- HARDY, J.[et. al.] (2002) - The amyloid hypothesis of Alzheimer's disease: progress and problems on the road to therapeutics. "Science." 297. 5580 (2002). 353-6.
- HARRISON, S. M.[et. al.] (2003) - BACE1 (beta-secretase) transgenic and knockout mice: identification of neurochemical deficits and behavioral changes. "Mol Cell Neurosci." 24. 3 (2003). 646-55.
- HEMMING, M. L.[et. al.] (2009) - Identification of beta-secretase (BACE1) substrates using quantitative proteomics. "PLoS One." 4. 12 (2009). e8477.
- HENEKA, M. T.[et. al.] (2015) - Innate immunity in Alzheimer's disease. "Nat Immunol." 16. 3 (2015). 229-36.

- HERRUP, K. (2015) - The case for rejecting the amyloid cascade hypothesis. "Nat Neurosci." 18. 6 (2015). 794-9.
- HILPERT, H.[et. al.] (2013) - beta-Secretase (BACE1) inhibitors with high in vivo efficacy suitable for clinical evaluation in Alzheimer's disease. "J Med Chem." 56. 10 (2013). 3980-95.
- HITT, B. D.[et. al.] (2010) - BACE1^{-/-} mice exhibit seizure activity that does not correlate with sodium channel level or axonal localization. "Mol Neurodegener." 5. (2010). 31.
- HITT, B.[et. al.] (2012) - beta-Site amyloid precursor protein (APP)-cleaving enzyme 1 (BACE1)-deficient mice exhibit a close homolog of LI (CHLI) loss-of-function phenotype involving axon guidance defects. "J Biol Chem." 287. 46 (2012). 38408-25.
- HONG, L.[et. al.] (2000) - Structure of the protease domain of memapsin 2 (beta-secretase) complexed with inhibitor. "Science." 290. 5489 (2000). 150-3.
- HONG, L.[et. al.] (2004) - Flap position of free memapsin 2 (beta-secretase), a model for flap opening in aspartic protease catalysis. "Biochemistry." 43. 16 (2004). 4689-95.
- HU, X.[et. al.] (2008) - Genetic deletion of BACE1 in mice affects remyelination of sciatic nerves. "FASEB J." 22. 8 (2008). 2970-80.
- HU, X.[et. al.] (2013) - BACE1 regulates hippocampal astrogenesis via the Jagged1-Notch pathway. "Cell Rep." 4. 1 (2013). 40-9.
- HU, X.[et. al.] (2006) - Bace1 modulates myelination in the central and peripheral nervous system. "Nat Neurosci." 9. 12 (2006). 1520-5.
- HU, X.[et. al.] (2010) - BACE1 deficiency causes altered neuronal activity and neurodegeneration. "J Neurosci." 30. 26 (2010). 8819-29.
- HUCHET Q. A., KUHN B., WAGNER B., FISCHER H., KANSY M., ZIMMERLIN D. (2013) - On the polarity of partially fluorinated methyl groups. "J Fluor Chem." (2013).
- HUNTER, L. (2010) - The C-F bond as a conformational tool in organic and biological chemistry. "Beilstein J Org Chem." 6. (2010). 38.
- HUSSAIN, I.[et. al.] (2000) - ASPI (BACE2) cleaves the amyloid precursor protein at the beta-secretase site. "Mol Cell Neurosci." 16. 5 (2000). 609-19.
- HUTTON, M.[et. al.] (1998) - Association of missense and 5'-splice-site mutations in tau with the inherited dementia FTDP-17. "Nature." 393. 6686 (1998). 702-5.
- IGBAVBOA, U.[et. al.] (2009) - Amyloid beta-protein stimulates trafficking of cholesterol and caveolin-1 from the plasma membrane to the Golgi complex in mouse primary astrocytes. "Neuroscience." 162. 2 (2009). 328-38.

- JEW, S. S.[et. al.] (2000) - Structure-activity relationship study of asiatic acid derivatives against beta amyloid (A beta)-induced neurotoxicity. "Bioorg Med Chem Lett." 10. 2 (2000). 119-21.
- JIANG, W.[et. al.] (2016) - Neuroprotective effect of asiatic acid against spinal cord injury in rats. "Life Sci." 157. (2016). 45-51.
- JON A. ERICKSON, JIM I. MCLOUGHLIN (1995) - Hydrogen Bond Donor Properties of the Difluoromethyl Group. "J. Org. Chem. ." 60. (1995). 1626-1631.
- JONSSON, T.[et. al.] (2012) - A mutation in APP protects against Alzheimer's disease and age-related cognitive decline. "Nature." 488. 7409 (2012). 96-9.
- JORISSEN, E.[et. al.] (2010) - The disintegrin/metalloproteinase ADAM10 is essential for the establishment of the brain cortex. "J Neurosci." 30. 14 (2010). 4833-44.
- KIELTSCH, I.[et. al.] (2007) - Mild electrophilic trifluoromethylation of carbon- and sulfur-centered nucleophiles by a hypervalent iodine(III)-CF₃ reagent. "Angew Chem Int Ed Engl." 46. 5 (2007). 754-7.
- KIM, D. Y.[et. al.] (2007) - BACE1 regulates voltage-gated sodium channels and neuronal activity. "Nat Cell Biol." 9. 7 (2007). 755-64.
- KINOSHITA, A.[et. al.] (2003) - Demonstration by FRET of BACE interaction with the amyloid precursor protein at the cell surface and in early endosomes. "J Cell Sci." 116. Pt 16 (2003). 3339-46.
- KIRK, KENNETH L. (2008) - Fluorination in Medicinal Chemistry: Methods, Strategies, and Recent Developments. "Organic Process Research & Development." 12. (2008). 305–321.
- KOBAYASHI, D.[et. al.] (2008) - BACE1 gene deletion: impact on behavioral function in a model of Alzheimer's disease. "Neurobiol Aging." 29. 6 (2008). 861-73.
- KOIKE, M.[et. al.] (2000) - Cathepsin D deficiency induces lysosomal storage with ceroid lipofuscin in mouse CNS neurons. "J Neurosci." 20. 18 (2000). 6898-906.
- KOPAN, R.[et. al.] (2004) - Gamma-secretase: proteasome of the membrane? "Nat Rev Mol Cell Biol." 5. 6 (2004). 499-504.
- KRISHNAMURTHY, R. G.[et. al.] (2009) - Asiatic acid, a pentacyclic triterpene from *Centella asiatica*, is neuroprotective in a mouse model of focal cerebral ischemia. "J Neurosci Res." 87. 11 (2009). 2541-50.
- KUHN, P. H.[et. al.] (2010) - ADAM10 is the physiologically relevant, constitutive alpha-secretase of the amyloid precursor protein in primary neurons. "EMBO J." 29. 17 (2010). 3020-32.

- KUMAR, D. K.[et. al.] (2016) - Amyloid-beta peptide protects against microbial infection in mouse and worm models of Alzheimer's disease. "Sci Transl Med." 8. 340 (2016). 340ra72.
- LAIRD, F. M.[et. al.] (2005) - BACE1, a major determinant of selective vulnerability of the brain to amyloid-beta amyloidogenesis, is essential for cognitive, emotional, and synaptic functions. "J Neurosci." 25. 50 (2005). 11693-709.
- LAWTON, G., WITTY, D. R. (2015)- Progress in medicinal chemistry. Elsevier, (2015). Chapter Available
- LEAL, A. S.[et. al.] (2012) - Semisynthetic ursolic acid fluorolactone derivatives inhibit growth with induction of p21(waf1) and induce apoptosis with upregulation of NOXA and downregulation of c-FLIP in cancer cells. "ChemMedChem." 7. 9 (2012). 1635-46.
- LEE, J. W.[et. al.] (2016) - Asiatic acid inhibits pulmonary inflammation induced by cigarette smoke. "Int Immunopharmacol." 39. (2016). 208-17.
- LEESON, P. D.[et. al.] (2007) - The influence of drug-like concepts on decision-making in medicinal chemistry. "Nat Rev Drug Discov." 6. 11 (2007). 881-90.
- LI, J. F.[et. al.] (2014) - Synthesis and biological evaluation of novel aniline-derived asiatic acid derivatives as potential anticancer agents. "Eur J Med Chem." 86. (2014). 175-88.
- LIANG, T.[et. al.] (2013) - Introduction of fluorine and fluorine-containing functional groups. "Angew Chem Int Ed Engl." 52. 32 (2013). 8214-64.
- LIN, X.[et. al.] (2000) - Human aspartic protease memapsin 2 cleaves the beta-secretase site of beta-amyloid precursor protein. "Proc Natl Acad Sci U S A." 97. 4 (2000). 1456-60.
- LUO, Y.[et. al.] (2001) - Mice deficient in BACE1, the Alzheimer's beta-secretase, have normal phenotype and abolished beta-amyloid generation. "Nat Neurosci." 4. 3 (2001). 231-2.
- MA, H.[et. al.] (2007) - Involvement of beta-site APP cleaving enzyme 1 (BACE1) in amyloid precursor protein-mediated enhancement of memory and activity-dependent synaptic plasticity. "Proc Natl Acad Sci U S A." 104. 19 (2007). 8167-72.
- MANALLACK, D. T. (2008) - The pK(a) Distribution of Drugs: Application to Drug Discovery. "Perspect Medicin Chem." 1. (2008). 25-38.
- MASTERS, C. L.[et. al.] (2015) - Alzheimer's disease. "Nat Rev Dis Primers." 1. (2015). 15056.
- MAULIDIANI[et. al.] (2016) - Metabolic alteration in obese diabetes rats upon treatment with Centella asiatica extract. "J Ethnopharmacol." 180. (2016). 60-9.

- MCCONLOGUE, L.[et. al.] (2007) - Partial reduction of BACE1 has dramatic effects on Alzheimer plaque and synaptic pathology in APP Transgenic Mice. "J Biol Chem." 282. 36 (2007). 26326-34.
- MENDES, V. I.[et. al.] (2016) - Synthesis and cytotoxic activity of novel A-ring cleaved ursolic acid derivatives in human non-small cell lung cancer cells. "Eur J Med Chem." 123. (2016). 317-31.
- MONTALBETTI, C. A. G. N., FALQUE, V. (2005) - Amide bond formation and peptide coupling. "Tetrahedron " 61. (2005). 10827–10852
- MOOK-JUNG, I.[et. al.] (1999) - Protective effects of asiaticoside derivatives against beta-amyloid neurotoxicity. "J Neurosci Res." 58. 3 (1999). 417-25.
- MORIMOTO, H.[et. al.] (2011) - A broadly applicable copper reagent for trifluoromethylations and perfluoroalkylations of aryl iodides and bromides. "Angew Chem Int Ed Engl." 50. 16 (2011). 3793-8.
- MULLER, T.[et. al.] (2007) - Modulation of gene expression and cytoskeletal dynamics by the amyloid precursor protein intracellular domain (AICD). "Mol Biol Cell." 18. 1 (2007). 201-10.
- MYERS, A. G.[et. al.] (2001) - Asymmetric synthesis of chiral organofluorine compounds: use of nonracemic fluoroiodoacetic acid as a practical electrophile and its application to the synthesis of monofluoro hydroxyethylene dipeptide isosteres within a novel series of HIV protease inhibitors. "J Am Chem Soc." 123. 30 (2001). 7207-19.
- NEWMAN, D. J., CRAGG, G. M. (2016) - Natural Products as Sources of New Drugs from 1981 to 2014. "J. Nat. Prod." 79. (2016). 629–661.
- NIKOLAY E. SHEVCHENKO, KATJA VLASOV, VALENTINE G. NENAJDENKO , GERD-VOLKER ROSCHENTHALER (2011) - The reaction of cyclic imines with the RuppertePrakash reagent. Facile approach to a-trifluoromethylated nornicotine, anabazine, and homoanabazine. "Tetrahedron." 67 (2011). 69-74.
- NISHITOMI, K.[et. al.] (2006) - BACE1 inhibition reduces endogenous Abeta and alters APP processing in wild-type mice. "J Neurochem." 99. 6 (2006). 1555-63.
- NYFFELER, P. T.[et. al.] (2004) - Selectfluor: mechanistic insight and applications. "Angew Chem Int Ed Engl." 44. 2 (2004). 192-212.
- O'HAGAN, D. (2008) - Understanding organofluorine chemistry. An introduction to the C-F bond. "Chem Soc Rev." 37. 2 (2008). 308-19.
- OBREGON, D.[et. al.] (2012) - Soluble amyloid precursor protein-alpha modulates beta-secretase activity and amyloid-beta generation. "Nat Commun." 3. (2012). 777.

- OEHLRICH, D.[et. al.] (2014) - The evolution of amidine-based brain penetrant BACE1 inhibitors. "Bioorg Med Chem Lett." 24. 9 (2014). 2033-45.
- OHNO, M.[et. al.] (2006) - Temporal memory deficits in Alzheimer's mouse models: rescue by genetic deletion of BACE1. "Eur J Neurosci." 23. 1 (2006). 251-60.
- OHNO, M.[et. al.] (2007) - BACE1 gene deletion prevents neuron loss and memory deficits in 5XFAD APP/PS1 transgenic mice. "Neurobiol Dis." 26. 1 (2007). 134-45.
- OHNO, M.[et. al.] (2004) - BACE1 deficiency rescues memory deficits and cholinergic dysfunction in a mouse model of Alzheimer's disease. "Neuron." 41. 1 (2004). 27-33.
- OJIMA, IWAO (2009)- Fluorine in Medicinal Chemistry and Chemical Biology. Blackwell Publishing, (2009). Chapter Available
- PARK, B. K.[et. al.] (2001) - Metabolism of fluorine-containing drugs. "Annu Rev Pharmacol Toxicol." 41. (2001). 443-70.
- PATIL, S. P.[et. al.] (2010) - Withanolide A and asiatic acid modulate multiple targets associated with amyloid-beta precursor protein processing and amyloid-beta protein clearance. "J Nat Prod." 73. 7 (2010). 1196-202.
- PAVIA, D. L., LAMPMAN, G. M., KRIZ, G. S., VYVYAN, J. R. (2013)- Introduction to spectroscopy. Cengage Learning, (2013). Chapter Available
- PETTERSSON, M.[et. al.] (2016) - Quantitative Assessment of the Impact of Fluorine Substitution on P-Glycoprotein (P-gp) Mediated Efflux, Permeability, Lipophilicity, and Metabolic Stability. "J Med Chem." 59. 11 (2016). 5284-96.
- POSTINA, R.[et. al.] (2004) - A disintegrin-metalloproteinase prevents amyloid plaque formation and hippocampal defects in an Alzheimer disease mouse model. "J Clin Invest." 113. 10 (2004). 1456-64.
- PRILLER, C.[et. al.] (2006) - Synapse formation and function is modulated by the amyloid precursor protein. "J Neurosci." 26. 27 (2006). 7212-21.
- RAJAPAKSHA, T. W.[et. al.] (2011) - The Alzheimer's beta-secretase enzyme BACE1 is required for accurate axon guidance of olfactory sensory neurons and normal glomerulus formation in the olfactory bulb. "Mol Neurodegener." 6. (2011). 88.
- RAMACHANDRAN, V.[et. al.] (2013) - Efficacy of asiatic acid, a pentacyclic triterpene on attenuating the key enzymes activities of carbohydrate metabolism in streptozotocin-induced diabetic rats. "Phytomedicine." 20. 3-4 (2013). 230-6.
- READ, J. [et. al.] (2013)- Dropping the BACE: Beta Secretase (BACE1) as an Alzheimer's Disease Intervention Target, Neurodegenerative Diseases. 2013).

- READ, J., SUPHIOGLU, C. (2013)- Dropping the BACE: Beta Secretase (BACE1) as an Alzheimer's Disease Intervention Target. 2013). Chapter Available
- REFOLO, L. M.[et. al.] (2001) - A cholesterol-lowering drug reduces beta-amyloid pathology in a transgenic mouse model of Alzheimer's disease. "Neurobiol Dis." 8. 5 (2001). 890-9.
- RIVKIN, A.[et. al.] (2002) - On the introduction of a trifluoromethyl substituent in the epothilone setting: chemical issues related to ring forming olefin metathesis and earliest biological findings. "Org Lett." 4. 23 (2002). 4081-4.
- ROCHIN, L.[et. al.] (2013) - BACE2 processes PMEL to form the melanosome amyloid matrix in pigment cells. "Proc Natl Acad Sci U S A." 110. 26 (2013). 10658-63.
- Salvador, J. A. R., Leal, A. S., Alho, D. P. S., Gonçalves, B. M. F., Valdeira, A. S., Mendes, V. I. S., Jing, Y. - Highlights of Pentacyclic Triterpenoids in the Cancer Settings. Em (B.V., E.) Studies in Natural Products Chemistry. 2014.
- SATHYA, M.[et. al.] (2012) - BACE1 in Alzheimer's disease. "Clin Chim Acta." 414. (2012). 171-8.
- SAVONENKO, A. V.[et. al.] (2008) - Alteration of BACE1-dependent NRG1/ErbB4 signaling and schizophrenia-like phenotypes in BACE1-null mice. "Proc Natl Acad Sci U S A." 105. 14 (2008). 5585-90.
- SELKOE, D. J. (2002) - Alzheimer's disease is a synaptic failure. "Science." 298. 5594 (2002). 789-91.
- SEUBERT, P.[et. al.] (1993) - Secretion of beta-amyloid precursor protein cleaved at the amino terminus of the beta-amyloid peptide. "Nature." 361. 6409 (1993). 260-3.
- SHAH, P.[et. al.] (2007) - The role of fluorine in medicinal chemistry. "J Enzyme Inhib Med Chem." 22. 5 (2007). 527-40.
- SIGMA-ALDRICH (2013)- Fluorination Chemistry. 2013). Chapter Available from: WWW: <<http://www.sigmaaldrich.com/content/dam/sigma-aldrich/docs/Sigma-Aldrich/Brochure/1/fluorination-chemistry.pdf>>.
- SILVESTRI, R. (2009) - Boom in the development of non-peptidic beta-secretase (BACE1) inhibitors for the treatment of Alzheimer's disease. "Med Res Rev." 29. 2 (2009). 295-338.
- SMART, BRUCE E. (2001) - Fluorine substituent effects (on bioactivity). "J. Fluorine Chem." 109 (2001). 3-11.
- SOLOSHONOK, VADIM A. (2005)- Fluorine - Containing Synthons. 2005). Chapter Available

- SONEIRA, C. F.[et. al.] (1996) - Severe cardiovascular disease and Alzheimer's disease: senile plaque formation in cortical areas. "Clin Anat." 9. 2 (1996). 118-27.
- SOSCIA, S. J.[et. al.] (2010) - The Alzheimer's disease-associated amyloid beta-protein is an antimicrobial peptide. "PLoS One." 5. 3 (2010). e9505.
- STEPHENSON, K. A.[et. al.] (2007) - Fluoro-pegylated (FPEG) imaging agents targeting Abeta aggregates. "Bioconjug Chem." 18. 1 (2007). 238-46.
- STOCKLEY, J. H.[et. al.] (2008) - Understanding BACE1: essential protease for amyloid-beta production in Alzheimer's disease. "Cell Mol Life Sci." 65. 20 (2008). 3265-89.
- SUN, X.[et. al.] (2005) - Distinct transcriptional regulation and function of the human BACE2 and BACE1 genes. "FASEB J." 19. 7 (2005). 739-49.
- SWAHN, B. M.[et. al.] (2012) - Design and synthesis of beta-site amyloid precursor protein cleaving enzyme (BACE1) inhibitors with in vivo brain reduction of beta-amyloid peptides. "J Med Chem." 55. 21 (2012). 9346-61.
- SWALLOW, S. (2015) - Fluorine in medicinal chemistry. "Prog Med Chem." 54. (2015). 65-133.
- TABATON, M.[et. al.] (2010) - Signaling effect of amyloid-beta(42) on the processing of AbetaPP. "Exp Neurol." 221. 1 (2010). 18-25.
- TAPIOLA, T.[et. al.] (2009) - Cerebrospinal fluid {beta}-amyloid 42 and tau proteins as biomarkers of Alzheimer-type pathologic changes in the brain. "Arch Neurol." 66. 3 (2009). 382-9.
- TSAO, S. M.[et. al.] (2015) - Antioxidative and antiinflammatory activities of asiatic acid, glycyrrhizic acid, and oleanolic acid in human bronchial epithelial cells. "J Agric Food Chem." 63. 12 (2015). 3196-204.
- TURNER, P. R.[et. al.] (2003) - Roles of amyloid precursor protein and its fragments in regulating neural activity, plasticity and memory. "Prog Neurobiol." 70. 1 (2003). 1-32.
- VAN DE WATERBEEMD, H.[et. al.] (2001) - Property-based design: optimization of drug absorption and pharmacokinetics. "J Med Chem." 44. 9 (2001). 1313-33.
- VANDENBERG, J. I.[et. al.] (2012) - hERG K(+) channels: structure, function, and clinical significance. "Physiol Rev." 92. 3 (2012). 1393-478.
- VASSAR, R. (2014) - BACE1 inhibitor drugs in clinical trials for Alzheimer's disease. "Alzheimers Res Ther." 6. 9 (2014). 89.
- VASSAR, R.[et. al.] (1999) - Beta-secretase cleavage of Alzheimer's amyloid precursor protein by the transmembrane aspartic protease BACE. "Science." 286. 5440 (1999). 735-41.

Bibliographic references

- VASSAR, R.[et. al.] (2014) - Function, therapeutic potential and cell biology of BACE proteases: current status and future prospects. "J Neurochem." 130. 1 (2014). 4-28.
- WANG, H.[et. al.] (2008) - BACE1 knock-outs display deficits in activity-dependent potentiation of synaptic transmission at mossy fiber to CA3 synapses in the hippocampus. "J Neurosci." 28. 35 (2008). 8677-81.
- WANG, P.[et. al.] (2005) - Defective neuromuscular synapses in mice lacking amyloid precursor protein (APP) and APP-Like protein 2. "J Neurosci." 25. 5 (2005). 1219-25.
- WANG, Y. J.[et. al.] (2006) - Clearance of amyloid-beta in Alzheimer's disease: progress, problems and perspectives. "Drug Discov Today." 11. 19-20 (2006). 931-8.
- WILLEM, M.[et. al.] (2006) - Control of peripheral nerve myelination by the beta-secretase BACE1. "Science." 314. 5799 (2006). 664-6.
- WISEMAN, F. K.[et. al.] (2015) - A genetic cause of Alzheimer disease: mechanistic insights from Down syndrome. "Nat Rev Neurosci." 16. 9 (2015). 564-74.
- WOLFE, M. S. (2007) - When loss is gain: reduced presenilin proteolytic function leads to increased Abeta42/Abeta40. Talking Point on the role of presenilin mutations in Alzheimer disease. "EMBO Rep." 8. 2 (2007). 136-40.
- YAN, R.[et. al.] (1999) - Membrane-anchored aspartyl protease with Alzheimer's disease beta-secretase activity. "Nature." 402. 6761 (1999). 533-7.
- YAN, S. L.[et. al.] (2014) - Asiatic acid ameliorates hepatic lipid accumulation and insulin resistance in mice consuming a high-fat diet. "J Agric Food Chem." 62. 20 (2014). 4625-31.
- ZAINOL, N. A., VOO, S. C., SARMIDI, M. R., AZIZ, R. A. (2008) - Profiling of Centella Asiatica (L.) Urban extract. "The Malaysian Journal of Analytical Sciences." 12. 2 (2008). 322-327.
- ZHANG, W.[et. al.] (2005) - F-18 Polyethyleneglycol stilbenes as PET imaging agents targeting Abeta aggregates in the brain. "Nucl Med Biol." 32. 8 (2005). 799-809.
- ZHAO, J.[et. al.] (1996) - Beta-secretase processing of the beta-amyloid precursor protein in transgenic mice is efficient in neurons but inefficient in astrocytes. "J Biol Chem." 271. 49 (1996). 31407-11.